

Dissertation zur Erlangung des Doktorgrades  
der Fakultät für Chemie und Pharmazie  
der Ludwig-Maximilians-Universität München

**Analysis of TF interactions with ribosome-nascent chain complexes  
-photocrosslinking and fluorescence spectroscopic approaches**

Sathish Kumar Lakshmiopathy

aus

Cuddalore, Tamilnadu

India

2009

## **Erklärung**

Diese Dissertation wurde im Sinne von § 13 Abs. 3 der Promotionsordnung vom 29. Januar 1998 von Herrn Professor Dr. F. Ulrich Hartl betreut.

## **Ehrenwörtliche Versicherung**

Diese Dissertation wurde selbständig, ohne unerlaubte Hilfen erarbeitet.

München, am ....26-03-2009.....

.....  
Sathish Kumar Lakshmipathy

Dissertation eingereicht am 26-03-2009

1. Gutachter: Professor Dr. F. Ulrich Hartl

2. Gutachter: Professor Dr. Roland Beckmann

Mündliche Prüfung am 19-05-2009

## **Acknowledgements**

I would like to thank Prof. F. Ulrich Hartl for providing me the opportunity to work under his guidance and introducing me to the fascinating field of Chaperone mediated protein folding. His constant support, encouragement, ideas and often stimulating discussions were important for the fruitful completion of this work. I also take this opportunity to thank Dr. Manajit Hayer-Hartl for her advice and discussions during the course of the work.

I would like to thank Prof. Dr. Roland Beckmann for being a co-referee of my thesis committee.

My special thanks to Dr. Stephanie Etchells for her supervision of my work throughout the last five years. Her guidance, suggestions and support during this whole period forms the basis of my work. I would like to thank her and Dr. Alex Hastie for their help in my thesis corrections.

I would like to thank Dr. Kausik Chakraborty and Dr. Hung-Chun Chang for their expert and valuable suggestions. I would also like to thank Dr. Sladjana Tomic, Florian Ruessmann, Florian Brandt and Dr. Raluca Antonoae for engaging in regular weekly discussions.

My thanks to Andrea for all her help during my entire stay. I would like to thank all the members of the Department of Cellular Biochemistry for providing a congenial atmosphere during my stay.

My thanks to Rashmi not only for her loving support and patience but also for standing by me during the ups and downs.

Last but not the least; I would like to thank my parents and sisters in India for their tireless support without which this work would not have been possible.

## Contents

I Summary.....	1
II Introduction .....	4
II.1 Translation and protein folding .....	4
II.1.1 Levels and determinants of protein structure .....	4
II.1.2 Protein folding <i>in vitro</i> .....	6
II.1.3 Protein folding in the cell .....	8
II.2 Molecular chaperones .....	9
II.2.1 The DnaK chaperone system and it's interaction with nascent chains .....	11
II.2.2 Chaperonins.....	14
II.2.2.1 Group I chaperonins .....	14
II.2.2.2 Group II chaperonins.....	15
II.2.3 Other chaperone systems.....	16
II.2.4 Ribosome associated chaperones .....	17
II.2.4.1 Eukaryotic ribosome associated chaperones .....	17
II.2.4.2 Prokaryotic ribosome associated chaperones.....	17
II.2.4.2.1 The Signal Recognition Particle and Trigger Factor.....	18
II.3 Trigger Factor.....	19
II.3.1 TF-ribosome interactions .....	20
II.3.2 Structure of TF and explanation for nascent chain interactions.....	21
II.3.3 TF-substrate interactions .....	26
II.4 Aim of the study .....	29
III Materials and Methods.....	30
III.1 Chemicals.....	30
III.2 Materials and Instrumentation .....	31
III.3 Media and buffers .....	32
III.3.1 Media .....	32
III.3.2 Buffers.....	32
III.4 DNA manipulations .....	33
III.4.1 General molecular biology methods .....	33
III.4.2 Cloning of <i>E. coli</i> TF in pBAD vector.....	36
III.4.3 Cloning of <i>E. coli</i> S7 in pET 22b vector.....	37
III.4.4 Site directed mutagenesis.....	37
III.4.5 Other constructs used in this study .....	38
III.4.6 Preparation of linear template DNA for <i>in vitro</i> translation in the PURE system .....	38
III.5 Protein preparative methods .....	38
III.5.1 Expression of TF proteins in the presence of the <i>pBpa</i> .....	38
III.5.2 Purification of <i>pBpa</i> labeled TF.....	39
III.5.3 Purification of TF.....	40
III.5.4 <i>In vitro</i> translation in the PURE system .....	40
III.5.5 Photocrosslinking of <i>pBpa</i> -TF to RNCs.....	40

III.5.6 Separation of ribosome-nascent chain complexes (RNCs).....	41
III.5.7 RNase A Digestion .....	41
III.5.8 Site specific labeling of single cysteine TF proteins .....	41
III.6 Protein analytical methods.....	42
III.6.1 Sodium Dodecyl Sulfate-Polyacrylamide Gel Electrophoresis (SDS-PAGE) .....	42
III.6.2 Autoradiography .....	43
III.6.3 Western blotting.....	43
III.6.4 Immunoprecipitation.....	44
III.6.5 Quantification of proteins .....	44
III.6.6 <i>In vivo</i> functionality test for TF single site mutants .....	44
III.6.7 Luciferase activity measurements.....	45
III.7 Fluorescence measurements.....	45
III.7.1 Overview.....	45
III.7.2 RCM-RNase T1 refolding.....	45
III.7.3 Equilibrium fluorescence measurements .....	46
III.7.4 Kinetic fluorescence measurements.....	46
III.7.5 Competition experiments.....	47
III.7.6 Evaluation of the kinetic data .....	47
<b>IV Results.....</b>	<b>48</b>
IV.1 <i>In vitro</i> translation in the PURE system and site-specific photocrosslinking experiments with <i>pBpa</i> -TF .....	48
IV.1.1 Incorporation of <i>pBpa</i> into TF and characterization of <i>pBpa</i> -TF .....	49
IV.1.1.1 Expression of <i>pBpa</i> -labeled TF .....	51
IV.1.1.2 <i>In vivo</i> complementation of the synthetic lethal phenotype of $\Delta$ <i>tig</i> $\Delta$ <i>dnaK</i> by <i>pBpa</i> -TF .....	52
IV.1.1.3 Tryptophan fluorescence of <i>pBpa</i> -TF.....	55
IV.1.2 Photocrosslinking of <i>pBpa</i> -TF to RNCs.....	56
IV.1.2.1 Photocrosslinking of <i>pBpa</i> -TF to Luc-RNCs .....	57
IV.1.2.2 Crosslinking of the N-terminal domain of TF to Luc-RNCs.....	61
IV.1.2.3 Crosslinking of the C-terminal domain of TF to Luc-RNCs.....	62
IV.1.2.4 Crosslinking of the PPIase domain of TF to Luc-RNCs .....	64
IV.1.2.5 TF crosslinking to $\alpha$ -Synuclein-RNCs .....	66
IV.1.2.6 Nature of PPIase domain-nascent chain interactions.....	69
IV.1.3 Identification of the TF dimer interface by photocrosslinking.....	70
IV.2 Trigger factor-nascent chain interactions monitored by real-time fluorescence measurements.....	73
IV.2.1 TF interactions with RNCs .....	74
IV.2.1.1 Characterization of TF labeled with NBD .....	74
IV.2.1.2 Recruitment of TF to RNCs.....	77
IV.2.1.3 Recruitment of additional TF molecules towards elongating nascent chains .....	83
IV.2.2 Kinetics of TF dissociation from RNCs .....	85
<b>V Discussion.....</b>	<b>97</b>
V.1 Interaction of the domains of TF with nascent chains .....	98

V.2 Differential interaction of TF with nascent chains.....	100
V.3 Dimerization interface of TF.....	100
V.4 TF-nascent chain interactions monitored by real-time fluorescence experiments	101
V.5 Kinetic characterization of TF dissociation from nascent chains .....	103
V.6 Overview of TF-nascent chain interactions .....	105
<b>VI References.....</b>	<b>108</b>
<b>VII Appendices .....</b>	<b>119</b>
VII.1 Abbreviations .....	119
VII.2 Curriculum vitae.....	122

# I Summary

Nascent chains emerge from ribosomes in a vectorial fashion and are prone to aggregation in the highly crowded environment of the cell. Ribosome associated chaperones, which are present in all kingdoms of life, bind to and prevent aggregation of the elongating nascent chains during translation. Trigger Factor (TF) is such a eubacterial chaperone, which interacts with the ribosome associated nascent chains. It is a 48 kDa protein with three domains, an N-terminal domain responsible for ribosome binding, a middle domain with PPIase function and a C-terminal domain with chaperone activity. Ribosome binding is essential for TF's interactions with nascent chains. TF is not regulated by nucleotides or chaperones and cooperates with the downstream DnaK/J chaperone system in chaperoning nascent chains.

In this study the interactions of TF with nascent chains have been investigated *in vitro* in a coupled transcription/translation system (PURE system) reconstituted from purified components. In the first part of the study, a site-specific photocrosslinking technique was employed to identify the regions of TF that were in close proximity to the nascent chains during translation. In the second part, TF-nascent chain interactions have been monitored in real-time using fluorescence technology.

Photocrosslinking experiments revealed that all of the domains of TF were adjacent to luciferase nascent chains during translation. The PPIase domain interacted with nascent chains in a length dependent manner. Less hydrophobic nascent chains such as those of  $\alpha$ -Synuclein displayed much weaker crosslinking to the PPIase domain compared to the other regions of TF. The above data is consistent with the previous observation that the PPIase domain acts as a secondary binding site for nascent chains (Kaiser et al., 2006; Tomic et al., 2006). In addition, the interaction of the PPIase domain with nascent chains was found to be independent of its PPIase activity. TF forms dimers in solution but only the monomeric form interacts with the ribosomes (Patzelt et al., 2002). Photocrosslinking of the labeled TF proteins revealed that the substrate-binding site of a monomer is within the dimer interface, thus explaining the inability of the dimeric form to interact with the ribosome-nascent chain complexes (RNCs).

TF-ribosome interactions in real time has previously been documented by our laboratory (Kaiser et al., 2006) and TF was found to dissociate from the ribosomes with a half-time ( $t_{1/2}$  value) of  $\sim 10$ - $12$  s. The  $t_{1/2}$  value of TF dissociation from the ribosome was independent of the translation status of the ribosomes. However, TF underwent a conformational change upon ribosome binding and the  $t_{1/2}$  value of this conformation was found to be higher than that of ribosome dissociation, depending on the nascent chain's hydrophobicity. This was thought to be the  $t_{1/2}$  value of TF dissociation from the nascent chains (Kaiser et al., 2006).

In the second part of this study, experiments were performed to directly measure TF-nascent chain interactions in real time. TF was labeled with an environmentally sensitive fluorophore (NBD) at regions that were in close proximity to the nascent chain based on photocrosslinking experiments. The interactions of labeled TF were found to be dependent on hydrophobic segments in the nascent chains. The dissociation of TF from nascent chains was then documented. During dissociation from the nascent chains, TF labeled with NBD at the C-terminal domain had two reaction phases, a fast phase and a slow phase. These two phases varied dependent on the nascent chains tested. The presence of two phases may reflect the existence of multiple conformations of the C-terminal domain of TF in solution (Yao et al., 2008).

TF labeled with NBD at the interface between the C-terminal and PPIase domains was utilized to accurately monitor its dissociation from the nascent chains as it was found to be mono-phasic. In this case the dissociation from Luc- and GatD-RNCs occurred with a  $t_{1/2}$  value of  $111 \pm 7$  s and  $25 \pm 2$ , respectively. In both the cases, the  $t_{1/2}$  values of TF dissociation from the nascent chains were longer than the  $t_{1/2}$  value of TF dissociation from the ribosomes translating the respective nascent chains. This confirms that TF remains associated with the nascent chains for an additional time even after its ribosome dissociation, depending on the hydrophobicity of the nascent chains.

These studies have revealed the role of different domains of TF in nascent chain interactions and facilitated the observation of these interactions in real time during translation. Results of this work contribute towards our understanding of the interplay of chaperones with ribosomes and provide insight into the coupling of translation and chaperone-assisted protein folding. The techniques developed here to investigate TF-



nascent chain interaction may prove useful in the analysis of other factors that act early in the folding process, such as the signal recognition particle and the DnaK (Hsp70) chaperone systems.

## II Introduction

### II.1 Translation and protein folding

Protein synthesis, or translation, is the process in which the genetic information contained in the form of mRNA is converted into a polypeptide chain. In all kingdoms of life translation occurs in specialized complexes called ribosomes, which are made of RNA and protein. Ribosomes catalyze the assembly of individual amino acids to yield polypeptide chains. Numerous additional essential factors, including tRNA synthetases, initiation, elongation and termination factors, etc, function in concert with the ribosomes in this process. The energetic requirements for translation are met by the hydrolysis of GTP. Once the polypeptide chain is synthesized on the ribosome, it has to reach its unique three-dimensional (3-D) conformation to be able to perform its destined biological function. The process by which the linear polypeptide chains are transformed into their proper conformation is called “protein folding”. *In vitro* the final active structure can be attained by the polypeptide alone, referred to as spontaneous folding. *In vivo*, folding in many cases is accomplished with the aid of a class of proteins known as molecular chaperones. Both of these processes will be discussed below.

#### II.1.1 Levels and determinants of protein structure

The primary structure of proteins is the linear sequence of amino acids in the polypeptide chain that is specified by the genetic information. Secondary structure is the ordered arrangement or conformation of amino acids in localized regions of the polypeptide chain. Hydrogen bonding plays an important role in stabilizing these folding patterns. The two main forms of secondary structure are the  $\alpha$ -helix and the  $\beta$ -pleated sheet.

The tertiary structure of a polypeptide or protein is the arrangement of secondary structural elements in three-dimensional space. The term quaternary structure is used to describe the assembly of two or more folded protein molecules (subunits or monomers) into complexes. Such complexes may be homo- or hetero oligomeric.

In a polypeptide chain, the N-C $_{\alpha}$  and C $_{\alpha}$ -C bonds are free to rotate and are represented by the torsion angles Phi ( $\phi$ ) and Psi ( $\psi$ ) respectively (Figure 1). No rotation occurs around the axis formed by the peptide bond (represented by omega ( $\omega$ ), not shown in Figure 1) due to the planar nature of the peptide bonds.

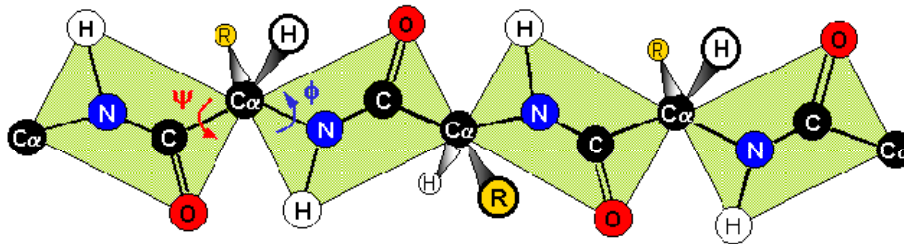


**Figure 1: Torsion angles in a fully extended polypeptide chain**

Each amino acid in a polypeptide chain contributes three bonds to its backbone. The peptide bond is planar. The N-C $_{\alpha}$  and the C $_{\alpha}$ -C bonds represented by  $\phi$  and  $\psi$  allow rotation of the backbone.

These two torsion angles ( $\phi$ ,  $\psi$ ) define the conformation of the polypeptide backbone and a graphical representation of these two angles gives rise to the “Ramachandran Plot”. Calculating the energy contained in various pairs of  $\phi$  and  $\psi$  angles led to the identification of the two most stable conformations known as the  $\alpha$  and  $\beta$  conformations (Ramachandran and Sasisekharan, 1968).

An initial introduction to protein folding dynamics often begins with the understanding of Levinthal’s paradox. Each bond connecting amino acids can have several (e.g., 3) possible conformational states, so that a protein of, say, 100 amino acids could exist in  $3^{100}$  or  $5 \times 10^{47}$  configurations. Even if a folding protein were able to sample this conformational space at a rate of  $10^{13}$  per second, or  $3 \times 10^{20}$  per year, it would take  $10^{27}$  years to try them all (Levinthal et al., 1962; Zwanzig et al., 1992). Since proteins fold in a biologically relevant time scale, this suggests that a random conformational search cannot be the basis of the folding process. Rather, folding is likely to proceed via transient folding intermediates. These intermediates, often involving local folded elements are stabilized and dictate further downstream folding by reducing the large number of theoretically possible conformations.

### II.1.2 Protein folding *in vitro*

Spontaneous re-folding *in vitro* was demonstrated in pioneering experiments by Christian Anfinsen with denatured ribonuclease A upon dilution into a non-denaturing buffer (Anfinsen, 1972, 1973; Taniuchi and Anfinsen, 1969). These experiments established the central dogma that the amino acid sequence contains sufficient information to specify the 3-D structure of the protein.

Several models have been proposed to describe the protein folding process. The hydrophobic collapse model is one of the models which explain the mechanism of protein folding (Figure 2). This model can be partitioned into three different stages; the first stage involves a specific or non-specific collapse of the polypeptide chain. The second stage is the formation of secondary and tertiary structures. This could be due to local and nonlocal, native and non-native interactions. The third stage is the desolvation of the protein chain as it folds to lower energy conformations (Ferguson and Fersht, 2003). The hydrophobic collapse model is supported by the view that hydrophobic driving forces provided by the expulsion of water (desolvation) from the burial of non-polar surfaces is enough to induce collapse (Kauzmann, 1959). The hydrophobic collapse model also led to the idea of molten globule formation, proposing that secondary structures are formed in the process of collapse.

Another model proposed for explaining protein folding is the “Framework model” (Figure 2). Support for this model came from studies on small, relatively stable helical peptides. This model suggests that secondary structures fold first followed by docking of these structures to yield native, folded protein (Kim and Baldwin, 1982, 1990).

The hydrophobic collapse model and the framework model converged to give a unified mechanism for folding called the “Nucleation-condensation” mechanism (Figure 2). This mechanism explains that some proteins could fold by simple two-state kinetics, without the accumulation of folding intermediates. It proposes that the formation of both long range and native hydrophobic interactions in the transition state during folding stabilize the inherent weak secondary structures. (Daggett and Fersht, 2003).

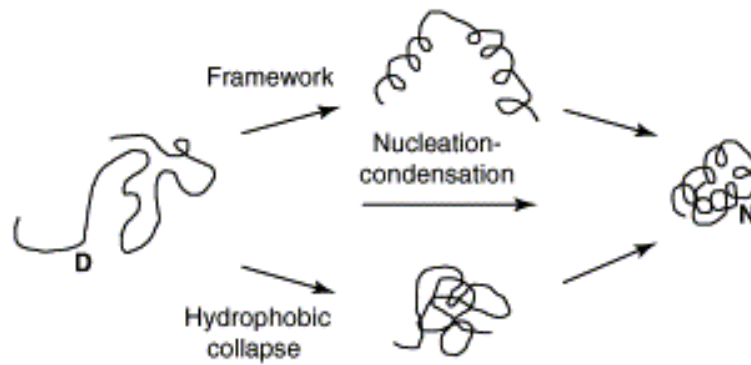


**Figure 2: Models for protein folding**

The hydrophobic collapse and the framework models. The nucleation-condensation model unites features from both of the two models, as it invokes the formation of both long range interactions and other native hydrophobic interactions. D and N denote the denatured and native state respectively. Adapted from Daggett and Fersht, 2003.

A “folding funnel” cartoon represents the theoretical formulation of protein folding in an energy landscape perspective (Clark, 2004) (Figure 3). This describes the *in vitro* progression of an isolated polypeptide chain from an ensemble of random conformations to the native structure at the global energy minimum. As a protein chain folds to lower energy conformations it might populate intermediate states ( $I_A$  and  $I_B$ ) i.e. local energy minimum in folding landscape known also as kinetic traps. The number and depth of the kinetic traps on the landscape represent the degree of frustration of the polypeptide sequence (Onuchic, 1997). During the folding process, if a polypeptide chain becomes trapped in a local minimum, it may eventually aggregate. Current folding funnels however cannot explain this off-pathway behavior, which is particularly important in explaining protein folding *in vivo*. This is mainly due to the fact that collisions between partially folded structures, an intrinsic feature of the actual folding process are not explained in the folding funnel hypothesis. To control the problem of aggregation, cells have evolved a machinery of molecular chaperones.

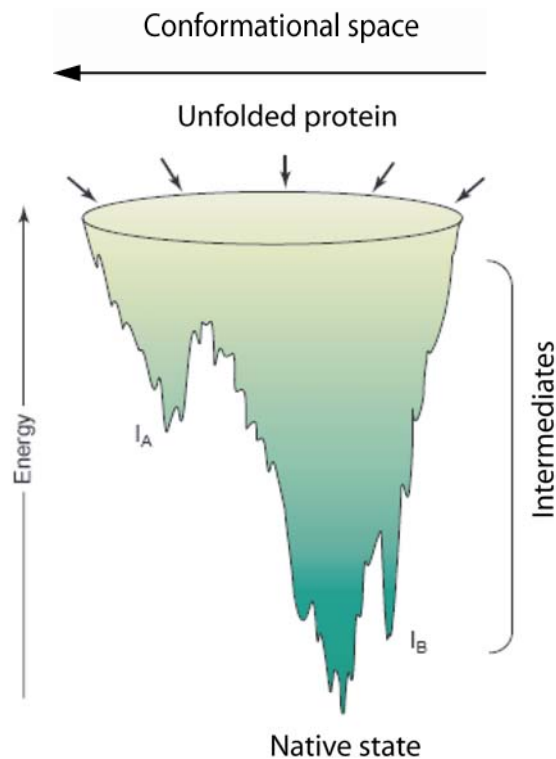


**Figure 3: Protein folding funnel diagram**

Unfolded proteins populating a wide range of conformations enter the top of the funnel. During their travel down the funnel towards the native conformation, they might populate intermediates with local energy minima represented as  $I_A$  and  $I_B$ . If the polypeptide escapes the local minima it would attain the native structure with the lowest possible energy. Depending on the depth of the kinetic trap protein molecules might get trapped irreversibly or eventually aggregate. Adapted from Clark, 2004.

### II.1.3 Protein folding in the cell

The central dogma of molecular biology is the flow of genetic information from DNA to RNA and subsequent decoding of the message from RNA to protein. Although linear polypeptides are formed as a result of translation, to attain their biologically active structure they have to be folded properly. When folding *in vivo*, a protein is confronted with various additional problems compared to the situation of *in vitro* folding. Nascent polypeptides synthesized on the ribosomes expose hydrophobic patches during their synthesis. The whole sequence of the protein is not available for folding into its complete 3-D structure before its synthesis is completed. This problem is compounded in bacteria

because of a fast translation speed of 4-20 residues per second compared to ~ 5 residues per second in eukaryotes (Mathews 2000). This poses a high risk of aggregation to the incomplete polypeptide chains, which are in a highly crowded environment, in contrast to the dilute milieu used in refolding *in vitro*. For a majority of proteins this environment would hinder productive folding. Complications due to aberrant protein folding and aggregation can result in severe cellular dysfunctions leading to a number of human diseases (Barral et al., 2004).

Cells have evolved mechanisms to prevent unproductive interactions between nascent and newly synthesized polypeptide chains with the aid of specialized proteins called molecular chaperones. Molecular chaperones generally bind to the folding intermediates of polypeptides, thereby preventing their aggregation (Young et al., 2004). In addition they assist the folding of certain proteins by repeated cycles of binding and release. Interestingly, different types of chaperones form a network to chaperone polypeptides at different stages of folding (Figure 4). Chaperones also play a role in preventing cellular toxicity that is due to the formation of protein aggregates observed in several neurodegenerative diseases (Barral et al., 2004; Behrends et al., 2006; Chan et al., 2000; Schaffar et al., 2004; Warrick et al., 1999).

## **II.2 Molecular chaperones**

Molecular chaperones prevent aggregation of nonnative proteins both during *de novo* folding and also during stress. Figure 4 presents a model of the chaperone pathways in the cytosol in the three kingdoms of life. Although most of the chaperones are constitutively expressed in cells, many of them are also known as heat shock or stress proteins, as their expression is increased under stress, such as heat stress. These proteins are called as heat shock proteins (Hsps). Chaperones can be broadly classified into four groups: ribosome-associated chaperones, Hsps70s, chaperonins and small Hsps. Some of them act on substrate proteins through repeated binding and release cycles until the native structure is attained. On many occasions they are regulated by their ATPase activity and also by their respective cofactors, so called co-chaperones.

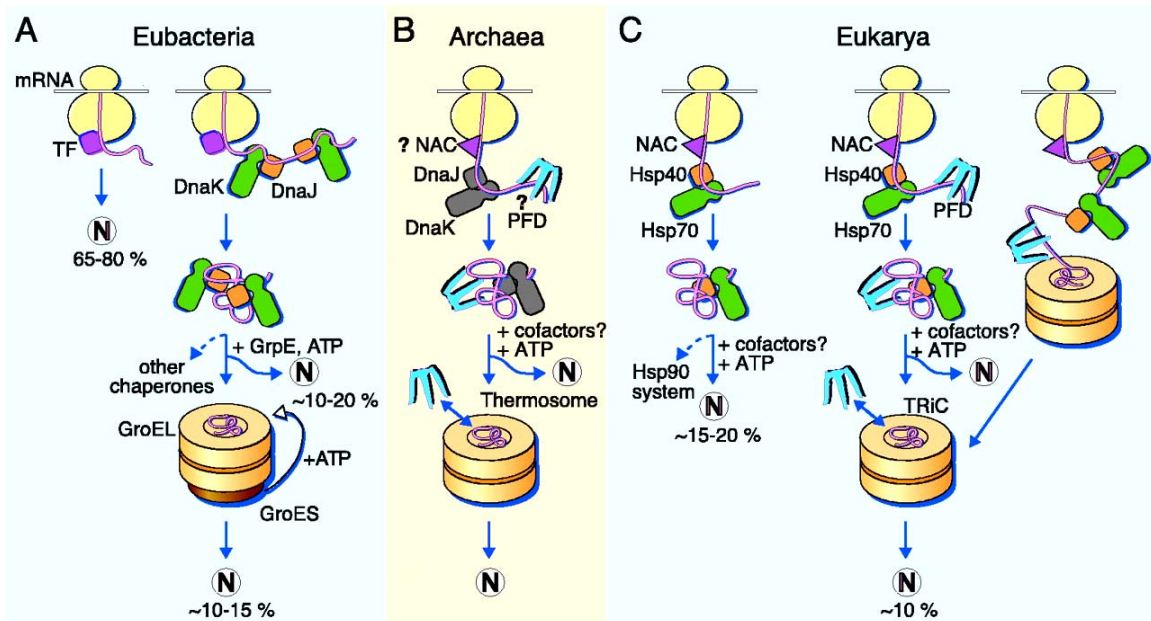


**Figure 4: Models for chaperone-assisted protein folding in the cytosol**

Native protein is denoted as N. (A) Chaperone systems in Eubacteria. Trigger Factor (TF) is the first chaperone to interact with the majority of nascent polypeptides. ~ 65-80% proteins attain their native structure without further assistance. Nascent chains would then interact with the DnaK chaperone system. About 10 to 15% of chains interact with the GroEL and GroES chaperonin system. GroEL does not interact with nascent chains directly and a fraction of substrates once they exit the DnaK system rely on GroEL for further assistance. (B) Archaea. The DnaK chaperone system does not exist in all the archaeal members. The presence of the ribosome-bound NAC homolog and the interaction of nascent chains with Prefoldin (PFD) have not yet been confirmed. (C) Eukarya. Like TF in bacteria, NAC plays a major role in chaperoning nascent chains in eukarya. A majority of small nascent chains may fold upon release from the ribosomes without further assistance. At least 15-20% of chains reach their native states by Hsp70 and Hsp40 action and a fraction of them are transferred to Hsp90 for further folding. About 10% of chains are then co- or post-translationally transferred to the chaperonin TRiC with the assistance of PFD. Adapted from Hartl and Hayer-Hartl, 2002.

Chaperones act sequentially along the folding pathway. There are chaperones that act on protein substrates at specific stages of their biogenesis. For example, there are ribosome-associated chaperones in all kingdoms of life, which act on nascent polypeptides immediately after translation. Trigger Factor (TF) and the signal recognition



particle (SRP) in *E. coli*, NAC, RAC and Zuotin in eukaryotes are some examples of ribosome-associated chaperones. Hsp70s are another class of chaperones found to be associated with the nascent chains. Chaperonins are the third class of chaperones, which generally act at the later stages of protein folding. There are other chaperone systems found in all kingdoms of life, for instance, Hsp90 and Prefoldin which have a variety of roles other than folding, including the maturation and conformational activation of substrates, and the transfer of substrates to other chaperone systems.

The remainder of this section will briefly describe the structure and function of these various chaperones and focus in more detail on Trigger Factor (TF), a bacterial ribosome associated chaperone.

### **II.2.1 The DnaK chaperone system and its interaction with nascent chains**

Members of the Hsp70 family exist in eubacteria, eukaryotes and some archaea, as well as in eukaryotic organelles, mitochondria and the endoplasmic reticulum. The Hsp70 homolog in eubacteria is known as DnaK and is well characterized. DnaK acts along with its co-chaperones DnaJ (Hsp40 homolog) and GrpE, its nucleotide exchange factor (NEF). It consists of two domains, an N-terminal ATPase domain, and a C-terminal substrate-binding domain (SBD). The ATP bound state of DnaK has low affinity for substrates (Pierpaoli et al., 1997; Theyssen et al., 1996). DnaJ stimulates the ATPase activity of DnaK, generating the ADP-bound state of DnaK, which has high affinity for its substrates. GrpE releases the bound nucleotide from DnaK (Harrison et al., 1997) and rebinding of ATP by DnaK promotes substrate release from DnaK, thereby completing the cycle (Figure 5).

DnaJ has an N-terminal “J” domain characteristic of all Hsp40s, that stimulates the ATPase activity of DnaK (Pellecchia et al., 2000). The C-terminal domain of DnaJ functions in substrate binding and there is evidence that DnaJ targets substrates to DnaK through its SBD in addition to stimulating its ATPase activity (Langer et al., 1992; Rudiger et al., 2001; Sha et al., 2000). GrpE is a homodimer that interacts with the N-terminal domain of DnaK. The dimer interface of GrpE encompasses two long paired N-

terminal  $\alpha$ -helices (Harrison et al., 1997). GrpE stimulates nucleotide exchange by stabilizing the open conformation of the ATPase domain of DnaK and, as a result, triggers substrate release from DnaK (Harrison, 2003; Harrison et al., 1997). In addition to nucleotide exchange, GrpE also plays a role in the release of tightly bound substrates from DnaK independent of the nucleotide bound status of DnaK (Brehmer et al., 2004; Harrison et al., 1997). This is accomplished by the interaction of its long N-terminal domain with the substrate domain of DnaK. But the *in vivo* significance of this function remains to be investigated.

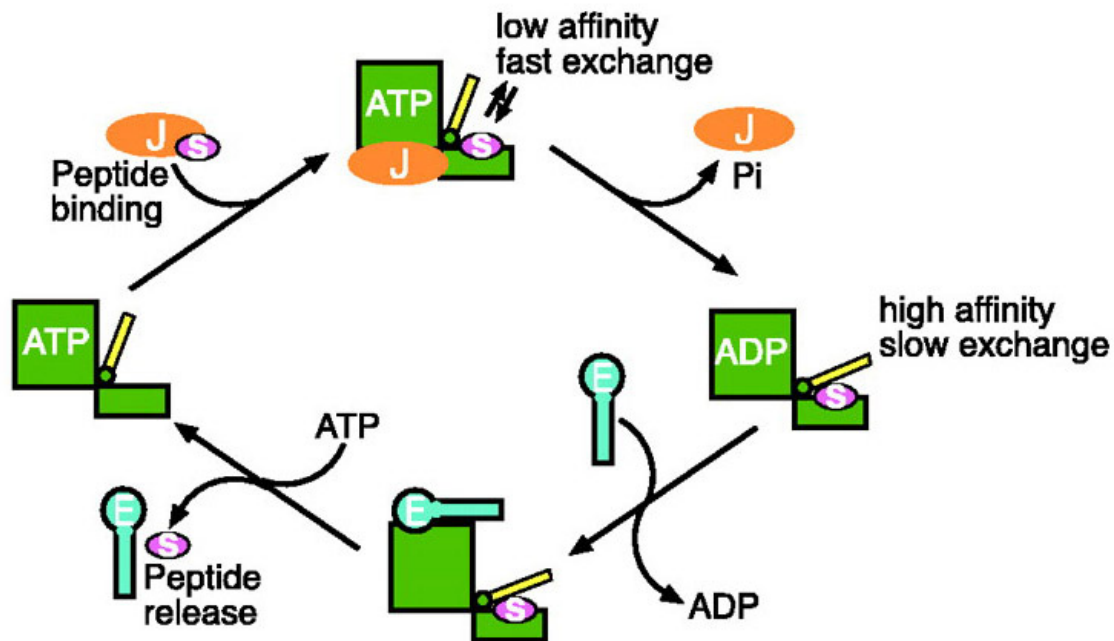


**Figure 5: Reaction cycle of the DnaK system**

J, E and S denote DnaJ (orange), GrpE (light blue) and substrate peptide (purple), respectively. DnaK is shown in green. Rapid peptide binding and dissociation occurs in the ATP-bound state of DnaK. The N-terminal J domain of DnaJ accelerates ATP hydrolysis by DnaK. Stable substrate binding by DnaK is achieved in its ADP-bound state. The C-terminal domain of DnaJ recognizes hydrophobic surfaces on nascent chains and targets them to DnaK. GrpE induces ADP release from DnaK and upon ATP rebinding by DnaK, substrate dissociates from DnaK, completing the reaction cycle. Adapted from Hartl and Hayer-Hartl, 2002.

DnaK was shown to interact with newly synthesized polypeptides although it was never shown to interact directly with the ribosomal exit site during translation (Teter et al., 1999). Studies from immobilized peptides have shown that DnaK recognizes a hydrophobic core of four to five residues flanked by approximately four basic residues (Rudiger et al., 1997). This explains the ability of DnaK to bind to hydrophobic polypeptide segments, which is a common feature in nascent chains and unfolded proteins. The DnaK system cooperates with TF in delaying the folding of certain multidomain proteins with respect to translation, thereby increasing their yield (Agashe et al., 2004). Although *dnaK* deletion strains ( $\Delta dnaK$ ) do not have any observable growth defects at temperatures of 30 °C- 37 °C, the combined knockout of both *tig* and *dnaK* is lethal to cells at the same temperatures but not at lower temperatures (Genevaux et al., 2004). This implies the role of DnaK in chaperoning nascent chains and its functional cooperation with TF. Indeed, the combined deletion of both *tig* and *dnaK* ( $\Delta tig \Delta dnaK$ ) reduced the folding efficiency of a model protein, Luciferase, and also resulted in the aggregation of at least 40 cytosolic proteins and a 2.5-fold increase in aggregation of preexisting proteins *in vivo* (Deuerling et al., 1999).

Pulse chase experiments in intact spheroplasts have demonstrated that DnaK interacts with nascent chains of 30-75 kDa with a specific preference between 45-66 kDa (Teter et al., 1999). The interaction of DnaK with the nascent chains was modulated by TF. Similar pulse chase experiments performed in  $\Delta tig$  strains have revealed that DnaK was able to interact with shorter lengths of nascent chains, below 22 kDa (Teter et al., 1999). Alternatively chemical crosslinking experiments in *in vitro* translation systems have suggested that both TF and DnaK compete with each other for substrate binding (Deuerling et al., 2003). However, in the above experiments TF was found to interact with the nascent chains under physiological concentrations while addition of at least a 10-fold excess of DnaK was necessary to observe its interaction with the nascent chains. This confirms that TF has an advantage over DnaK in binding to the nascent chains by virtue of its ribosome binding ability.

## II.2.2 Chaperonins

Chaperonins are cylindrical double-ringed multimeric complexes encompassing a central cavity in each ring. There are two classes of chaperonins: Group I chaperonins, also known as Hsp60s, exist in eubacteria, mitochondria and chloroplasts whereas group II chaperonins are found in archaea and the eukaryotic cytosol. The Group I chaperonins consist of two ring structures stacked back-to-back, each ring containing seven subunits. They cooperate along with their Hsp10 co-chaperones during the folding cycle. The Group II chaperonins contain 8-9 subunits per ring and are independent of a Hsp10 co-chaperone. Both groups of chaperonins are regulated by ATP binding and hydrolysis. The central hydrophobic cavity within them provides space for the substrate protein to undergo multiple rounds of binding and dissociation until its native conformation is attained.

### II.2.2.1 Group I chaperonins

GroEL, an essential protein in eubacteria, along with its co-chaperone GroES binds to non-native polypeptide substrates and releases them into the central cavity where the substrate's native structure can be attained (Figure 6). GroEL and GroES, collectively called GroE prevent aggregation in the cell by encapsulating individual polypeptide chains and allowing their folding to occur in isolation from other proteins (Brinker et al., 2001; Mayhew et al., 1996; Weissman et al., 1996). This action of the GroE chaperone is accomplished by ATP binding and hydrolysis. At physiological concentrations, ATP binds within the seven sites of one ring. Binding of GroES is dependent on the presence of ATP as it binds to the ring that is occupied by ATP. ATP binding induces an allosteric movement in the polypeptide binding apical domains and provide competency for GroES binding to the ATP bound ring (Ranson et al., 2001). A large body movement in the apical domain, due to GroES binding, drives the release of the polypeptide into the now hydrophilic, encapsulated cavity called the *cis*-cavity, where folding commences (Mayhew et al., 1996; Ranson et al., 2006; Weissman et al., 1995; Xu et al., 1997). ATP hydrolysis in the *cis*-cavity weakens the affinity of GroEL for GroES and allows the binding of ATP in the opposite ring, the so-called *trans*-cavity (Rye et al., 1997). Binding

of ATP in the *trans* ring creates an allosteric signal allowing the release of GroES, substrate polypeptide and ADP from this *cis* ring. The substrate from the *cis* ring at this point will be folded or in a partially folded state. ATP binding to the *trans* ring begins the cycle anew, whereby the former *trans* ring becomes the new *cis* ring. Thus, the two rings switch back and forth as *cis* and *trans* forms triggered by ATP binding, facilitating substrate release and capture by the rings until its native structure is attained. If the chain has internalized its hydrophobic residues or regions as a result of folding, it finally remains free in the cytosol.

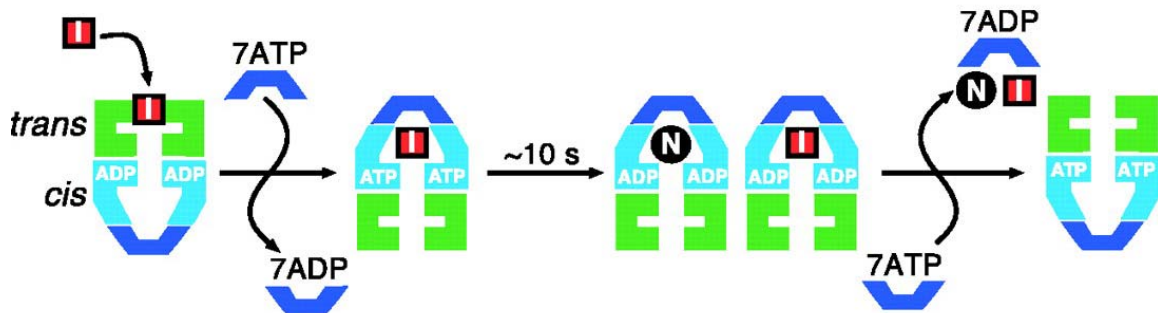


**Figure 6: Protein folding reaction in the GroEL-GroES cage**

The folding intermediate bound by GroEL is denoted by I and native protein folded inside the cage by N. Folding occurs with the help of ATP hydrolysis. Multiple rounds of chaperonin action are needed for some substrates to achieve the N state. Both I and the N state accumulate after each round of binding and release. The substrate, upon achieving the N state, leaves the cage but the I state is rebound by GroEL and the chaperonin cycle might continue until the N state is attained. Adapted from Hartl and Hayer-Hartl, 2002.

### II.2.2.2 Group II chaperonins

Group II chaperonins are oligomeric, high molecular weight chaperones found in archaea and the eukaryotic cytosol. The Group II chaperonin TCP-1 ring complex (TRiC, also called as CCT for Chaperone Containing TCP1, (t-complex peptide 1)) is present in the eukaryotic cytosol. Thermosome is another Group II chaperonin, which is found in archaea. Unlike GroEL, the Group II chaperonins function without any known cofactors.

The crystal structure of the thermosome, an archaeal version of TRiC, indicates that substrates of up to 50 kDa can be encapsulated in the central cavity (Ditzel et al., 1998).

The essential role of TRiC is highlighted by its absolute requirement for folding a subset of essential proteins. Although initially thought of as a chaperonin known to fold only actin and tubulin, later proteomic studies have identified many non-cytoskeletal proteins as additional substrates. A substantial fraction of these contain tryptophan-aspartic acid (WD40) repeat domains (Ho et al., 2002). TRiC recognizes a variety of substrates that exceed the size of its central cavity. One possible explanation is that TRiC sequentially binds to and folds individual domains of these large substrates. A commonality of TRiC substrates is that most of them function only as oligomeric complexes (e.g., actin polymerization, VHL and CDC20) (Camasses et al., 2003; Feldman et al., 1999). As in the case of GroEL, ATP binding and hydrolysis-driven conformational changes mediate the folding of the substrate by TRiC action.

### **II.2.3 Other chaperone systems**

Hsp90 belong to a class of ATP dependent chaperones, which play an essential role in maintaining the activity of numerous signaling proteins, steroid hormone receptors, transcription factors and kinases. They generally do not act at the early stages of protein folding, rather at the late folding stages of substrates that require activation by other factors (Jakob et al., 1995; Nathan et al., 1997). The bacterial homolog of Hsp90 is called HtpG and does not require any co-chaperones for its action. Eukaryotic Hsp90 cooperates with a variety of co-chaperones, which regulate the function of both Hsp90 and Hsp70. These co-chaperones bind to Hsp90 via a domain containing a 34 amino acid, helix-turn-helix tetratricopeptide repeat (TPR) motif. The TPR domains have been identified to be fused to other TPR domains recognizing Hsp70. Hop, one such co-chaperone with a TPR domain (Scheufler et al., 2000), transfers the substrate polypeptides from Hsp70 to Hsp90 (Prodromou et al., 1999) leading to the maturation of substrates.

Prefoldin or GimC (for genes involved in microtubule biogenesis complex) is thought to stabilize and deliver polypeptide nascent chains to TRiC for their folding. It is a heterohexameric protein found in archaea and eukaryotes (Leroux et al., 1999;

Vainberg et al., 1998). The loss of GimC is not lethal in yeast but causes a reduced efficiency in actin and tubulin folding (Vainberg et al., 1998).

## **II.2.4 Ribosome associated chaperones**

### **II.2.4.1 Eukaryotic ribosome associated chaperones**

Eukaryotes possess ribosome-associated chaperones that are unrelated to bacterial Trigger factor (TF). One such chaperone family is the NAC (Nascent chain Associated Complex). Like TF, NAC also associates with ribosomes in a 1:1 stoichiometry (Rospert et al., 2002). It is a highly conserved protein complex in eukaryotes and consists of two subunits,  $\alpha$  NAC (33kDa) and the  $\beta$  NAC (22kDa). Although both the subunits interact with the nascent chains, only  $\beta$  NAC interacts with the ribosomes (Wegrzyn et al., 2006). With prokaryotic ribosomes, it was shown that NAC occupies the same location on the ribosomes as TF and SRP, suggesting a common strategy utilized by the ribosome-associated chaperones to interact with the nascent chains (Ferbitz et al., 2004; Pool et al., 2002; Spreter et al., 2005; Wegrzyn et al., 2006).

Two ribosome-associated Hsp70 homologs are present in the yeast *Saccharomyces cerevisiae*, Ssb1 and Ssb2 (Pfund et al., 1998). They exist as a complex with Ssz1p and Zuotin. This complex has also been called RAC (Ribosome Associated Complex) (Gautschi et al., 2001). These components form a functional chaperone triad for the nascent chains emerging from the ribosome. RAC plays a role in recruiting Ssb to the nascent polypeptides and the J domain of Zuotin is essential for this function (Gautschi et al., 2002). There are speculations that Ssz1p might modulate the ability of Zuotin to interact with Ssb1/2p (Gautschi et al., 2002).

### **II.2.4.2 Prokaryotic ribosome associated chaperones**

In prokaryotes there are two major ribosome associated factors, TF and the SRP (Signal Recognition Particle). Both interact with nascent chains during translation. The following section summarizes what is known about the interplay of SRP and TF at the ribosomal exit tunnel.

#### **II.2.4.2.1 The Signal Recognition Particle and Trigger Factor**

The SRP pathway is required for the targeting of IMPs (inner membrane proteins) to the plasma membrane (de Gier et al., 1996; Macfarlane and Muller, 1995; Seluanov and Bibi, 1997). It is present as a ribonucleoprotein complex in all organisms but with varied composition of protein to RNA (Figure 7). In eubacteria it contains a protein called Ffh (54 homolog) and a 4.5S RNA. Ffh has three domains, N, G and the M domain. The M domain binds both the 4.5S RNA and the emerging signal peptide of the nascent chain. By mutational studies it was found that SRP binding to the nascent chains is dependent on the hydrophobicity of the signal peptide (Valent et al., 1997).

Recent structural studies have shown that TF and SRP both bind to L23 on the 50S ribosomal subunit (Ferbitz et al., 2004; Schlunzen et al., 2005; Halic et al., 2006). TF interacts with a large fraction of nascent chains while SRP was thought to interact more specifically with the IMPs. The question arises about how these chaperones select their substrates. Crosslinking studies to address this question have suggested that SRP is the major interacting partner with nascent IMPs whereas TF has a low affinity for IMPs during the early stages of synthesis (Beck et al., 2000). SRP and TF might selectively bind their substrates by competing for binding to the ribosome and SRP exerting an advantage over TF in binding to IMPs because of its high affinity for the signal sequence (Ullers et al., 2003). Alternatively, SRP and TF may co-exist on the ribosome and TF is released from the ribosomes once FtsY (SRP receptor) binds to the SRP-RNCs (Buskiewicz et al., 2004; Schlunzen et al., 2005). Hence, the exact mechanism of nascent chain sorting by TF and SRP during the early stages of synthesis is unclear and remains to be investigated.



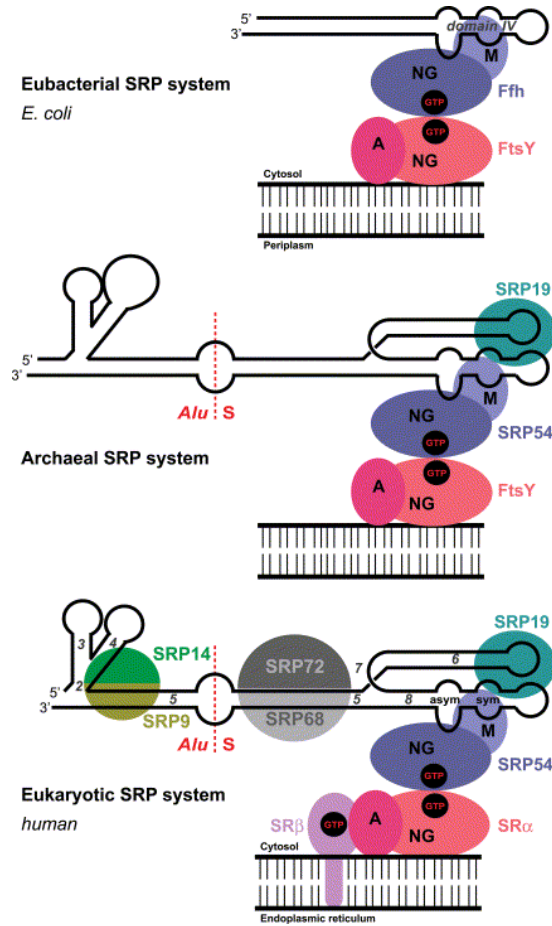


**Figure 7: Schematic representation of SRP and SR components in the three kingdoms of life**

Eubacteria on the top, Archaea in the middle and Eukaryotes on the bottom. The colour code is blue (Ffh/SRP54; NG domain in dark blue, M domain in light blue), cyan (SRP19), grey (SRP68/72), green (SRP9/14), black (RNA). The SRP receptor is shown in pink (FtsY, SR $\alpha$ ; NG domain in light pink, A domain in dark pink) and violet (SR $\beta$ ). Adapted from Luirink and Sinning, 2004.

## II.3 Trigger Factor

As TF is the major focus of this dissertation, we shall begin with a brief overview of its function and discovery. In later sections each aspect of TF's structure and function will be discussed in detail. In eubacteria, the ribosome associated Trigger Factor (TF) encoded by the *tig* gene is the first chaperone to interact with nascent chains and is absent in eukaryotes. Originally, TF was identified as a protein involved in the secretion of

secretory proteins (Crooke et al., 1988a; Crooke et al., 1988b; Crooke and Wickner, 1987). Later it was found to be a peptidyl prolyl isomerase (PPIase) associated with ribosomes (Stoller et al., 1995). It was then shown to possess PPIase activity towards small chromogenic substrates and to improve the refolding of model substrates whose peptidyl prolyl isomerisation was rate limiting (Hesterkamp and Bukau, 1996). TF associates with ribosomes with a 1:1 stoichiometry through the ribosomal protein L23 close to the exit tunnel (Kramer et al., 2002). The concentration of TF (40-50  $\mu\text{M}$ ) is in excess over ribosomes (30  $\mu\text{M}$ ), hence there exists an equilibrium between the ribosome-bound and non-ribosome bound TF. TF is a modular protein with three domains, an N-terminal ribosome binding domain, middle PPIase domain and a C-terminal domain proposed to be the substrate-binding domain (Ferbitz et al., 2004). PPIase activity is dispensable for TF function as TF binding to substrate proteins is independent of proline residues (Kramer et al., 2004a).

Structures of TF and co-crystals of the ribosome-binding domain of TF along with the 50S ribosomal subunit led to predictions about TF-nascent chain interactions (Baram et al., 2005; Ferbitz et al., 2004; Schlunzen et al., 2005). TF has also been shown to protect nascent polypeptides from proteolytic degradation *in vitro* (Hoffmann et al., 2006; Tomic et al., 2006). A real-time observation of TF interaction with translating ribosomes has been reported from our laboratory (Kaiser et al., 2006).

### **II.3.1 TF-ribosome interactions**

It was initially shown that the N-terminal domain of TF interacts with the 50S subunit of the ribosome (Hesterkamp et al., 1997). Later, the exact region on the ribosome where TF binds was identified as proteins L23 and L29, with L23 playing the major role in TF binding (Kramer et al., 2002). Aligning the N-terminal domains of several TF homologues identified a sequence of 17 amino acids called the “TF signature” sequence, which is a highly conserved yet unstructured region. Three residues in this exposed region F44, R45, K46, were shown to mediate TF-ribosome binding. The mutant protein, TF FRK/AAA, did not yield observable crosslinks to the ribosomal protein L23 or to ribosome-bound nascent chains. Mutations in the L23 protein of residues V16, S17 and E18 to alanine, yielding L23 VSE/AAA, prevented TF binding to the ribosome. In

particular the involvement of residue E18 in binding, which is located at the rim of the polypeptide exit tunnel, indicates that TF is optimally positioned to interact with the nascent chains exiting the ribosomal tunnel (Kramer et al., 2002).

Maier and colleagues performed the initial experiments addressing the kinetics of the TF-ribosome interaction (Maier et al., 2003). From binding and displacement reactions using fluorescently labeled TF and non-translating ribosomes they showed that the affinity of the TF-ribosome interaction is  $\sim 1 \mu\text{M}$  and the lifetime of the complex was  $\sim 30 \text{ s}$  at  $20 \text{ }^\circ\text{C}$ . Using these measurements and also the displacement kinetics of TF with unfolded substrate proteins, which is in the range of  $100 \text{ ms}$  (Maier et al., 2001), they modeled that TF binds and releases from nascent chains staying bound to the ribosomes, thereby preventing their aggregation. This model of TF-ribosome-nascent chain interactions was built based on the weak affinity TF exerts towards unfolded substrates in solution. However, this may not reflect the properties of TF's interaction with nascent chains, because TF attains a more open conformation upon ribosome binding (Kaiser et al., 2006). The affinity of this activated TF towards nascent chains might be different than the affinity of TF towards unfolded substrates in solution.

### **II.3.2 Structure of TF and explanation for nascent chain interactions**

The X-ray crystal structure of *Vibrio cholerae* TF (VCTF), which is 70% homologous to *E. coli* TF, was solved at  $2.5 \text{ \AA}$  resolution (Ludlam et al., 2004) and shortly thereafter *E. coli* TF was solved at  $2.7 \text{ \AA}$  resolution (Ferbitz et al., 2004). The structure folds into a unique extended shape much longer than expected for a 48 kDa protein. The N-terminal domain is solely responsible for ribosome binding, as reported earlier, the middle PPIase domain is located at the opposite end of the molecule and the C-terminal domain contributes the back and two arms to the molecule (Figure 8). The PPIase domain is connected to the N-terminal domain by means of a “linker” extending along the back of the TF. The C-terminal domain adds two extended “arms” to the core of the protein and it is structurally similar to the chaperone domain of SurA (Ferbitz et al., 2004). The characteristic “signature motif” is located between the two helices  $\alpha 1$  and  $\alpha 2$  containing the ribosome-binding region. It was calculated that at least  $3500 \text{ \AA}^2$  of

surface area is buried through intertwining of the “arms” and inner portion of the N-terminal domain.

The co-crystals of *Haloarcula marismortui* 50S ribosomal subunit along with the N-terminal domain of *E. coli* TF (H50S-EcTFa) were solved to 3.5 Å resolution and this structure allowed the whole chaperone to be modeled on to the 50S ribosome through the ribosome-binding domain (Figure 8). Based on this model, it was proposed that the nascent chains interact with a “crevice” of TF that is formed by helices from the N-terminal domain and the “arms” of the C-terminal domain. This crevice exposes its hydrophobic inner surface towards the polypeptide exit tunnel. The PPIase domain might interact with the nascent chains during their late stages of synthesis. The same study also proposed that the affinity of TF for the ribosome could be stabilized with the presence of a nascent chain due to hydrophobic interactions between TF and the nascent chain. The “folding space” formed between the ribosome and TF was calculated to be large enough to accommodate a domain size of at least 14 kDa (Ferbitz et al., 2004).

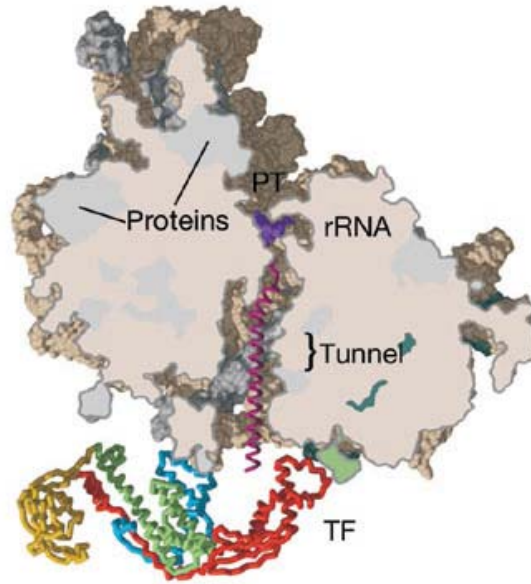


**Figure 8: Overview of the TF-50S complex**

Full-length TF positioned by superimposition onto the ribosome-bound fragment (residues 1-144) is shown as C $\alpha$ -trace together with a slice of 50S along the peptide exit with a modelled nascent chain (magenta), extending from the peptidyl transferase centre (PTC). Coloring, ribosome binding domain in red, PPlase domain in yellow, arm 1 and arm 2 in green and blue respectively. Colouring of the ribosomal proteins L29 in turquoise, L23 in green and L19 in bluish green. Adapted from Ferbitz et al., 2004.

The details derived from the co-crystal structures in this study may not provide an entirely accurate view of TF-ribosome interactions for two major reasons, first, only one third of the N-terminal domain (35 residues) was used to assign the structural details and second, TF does not exist in archaea, which was the source of the 50S subunit.

The co-crystal structure of a homologous complex of *Deinococcus radiodurans* 50S ribosomal subunit along with the ribosome-binding domain of TF were solved with the aim of providing a clearer picture (Baram et al., 2005; Schlunzen et al., 2005). In the study by Schlunzen and colleagues, a contact between helix  $\alpha 2$  in the TF-BD (TF-ribosome binding domain) with the 30 Å long extension of L24, was observed. This extension is specific to bacteria and is missing in the *H. marismortui* ribosome (Figure 9). This extension would significantly occupy the proposed “molecular cradle” of TF, making any folding events in this space less likely. Interaction of the tip of L24 with the

TF-BD could shift the position of helix  $\alpha 2$  by  $40^\circ$  in the ribosome-bound form relatively to the unbound form. This conformational change in  $\alpha 2$  opens up a channel from the exit tunnel to the end of the TF body (Schlunzen et al., 2005).

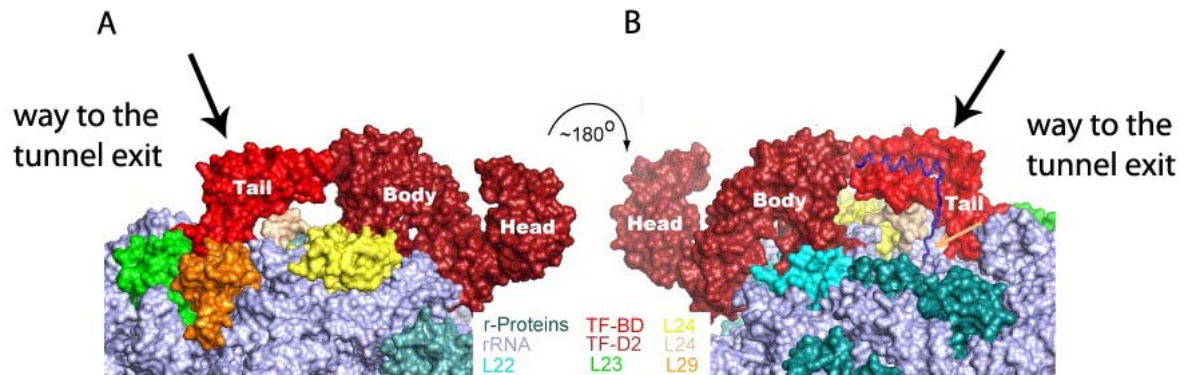


**Figure 9: The molecular cradle is envisaged by the extension of L24**

(A) Model of the full-length TF (dark red) with the ribosome binding domain (red) on the 50S subunit, with ribosomal proteins L23 (green), L29 (orange), the globular domain of L24 (yellow) and the extension of L24 (gold). (B) The path of the nascent chain. Model of the nascent polypeptide chain (dark blue) exiting the tunnel (black arrow), passing the tip of extension of L24 and entering into the hydrophobic crevice in the binding domain of the TF. The molecular cradle is severely restricted by the extension of L24 (gold) between the ribosome binding domain and the arm 1 of TF. Adapted from Schlunzen et al., 2005.

In the study by Baram et al., analysis of the co-crystal structures revealed that the ribosome-bound form of TF has an altered conformation compared to the unbound form. Superimposing the unbound form on the location of the bound form shows that in the unbound form, helix  $\alpha 2$  is too far away to interact with both L23 and L29 and this conformational change might play a role in TF docking onto the 50S subunit (Figure 10). The altered conformational change also forces helices  $\alpha 1$  and  $\alpha 3$  to move away from each other, thereby separating helix  $\alpha 3$  from the  $\beta$ -sheets exposing a hydrophobic pocket near the opening of the ribosomal exit tunnel. This hydrophobic environment may be essential in providing binding sites for the growing nascent chain. Furthermore, it was found that the elongated loop of L23 that is specific to eubacteria extends into the tunnel opening and is predicted to interact with the nascent chains in the tunnel, which was not observed in the H50S-EcTFa structure. An interaction of TF with the regions of this loop was

observed in this structure, which may enable efficient TF interaction with the nascent chains.

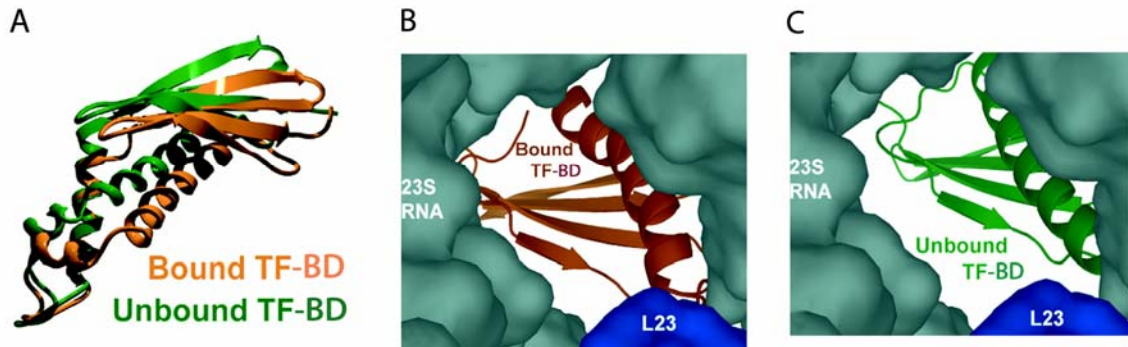


**Figure 10: Conformational rearrangements in TF ribosome binding domain (TF-BD) upon association with the ribosome**

TF-BD (ribosome binding domain of TF) is represented by its main chain, whereas the ribosomal components are shown in space-filling representation. Ribosome bound TF-BD, orange; ribosome unbound TF-BD (green), L23 (blue), 23S rRNA (light gray). (A). Superposition of the folds of unbound and bound TF-BD. To obtain this image, loop L1 and helix  $\alpha 1$  of the unbound TF-BD were aligned with those of the bound TF-BD. (B). A view from the ribosomal exit tunnel into the exposed hydrophobic pocket, created by the bound conformation of TF-BD. (C). A hypothetical view of the structure formed by TF-BD binding at its unbound conformation. This indicates that the bound conformation could create a folding pocket because of the separation of helix  $\alpha 1$  and helix  $\alpha 3$  interactions and with the  $\beta$ -sheet which exposes hydrophobic regions facing the exit tunnel. Adapted from Baram et al., 2005.

These studies initially suggested that there is a conformational change in TF upon binding to the ribosome that exposes a hydrophobic pocket, which could be necessary for TF function in binding aggregation-prone hydrophobic sequences in growing nascent chains.

*In vivo*, TF is present in a 2-3 fold molar excess over ribosomes and associates with the ribosomes in a 1:1 stoichiometry. Therefore the majority of TF is free in the cytosol, suggesting equilibrium between these two forms. Analytical ultracentrifugation experiments indicated that there exists an equilibrium between the monomeric and dimeric forms of TF with a dissociation constant of 18  $\mu\text{M}$  (Patzelt et al., 2002) and 1.8

$\mu\text{M}$  (Maier et al., 2003). The N- and the C-terminal domains were thought to contribute towards dimer formation in isolation or in combination with other domains, as shown by glutaraldehyde crosslinking (Patzelt et al., 2002). Experiments from the same group also suggested that only monomers associate with the ribosomes.

C-terminal deletions of TF failed to dimerize and also displayed reduced chaperone activity *in vitro* (Zeng et al., 2006). Inter-molecular FRET experiments and model building suggested that the substrate-binding domain might be occluded in the dimer (Kaiser et al., 2006). This might explain the inability of dimeric TF to bind to ribosome-nascent chain complexes. Taking all-previous experiments together, the C-terminal domain is likely to form part of the dimer interface.

Interestingly, *in vitro* studies by Liu and colleagues have shown that dimeric TF has the ability to hold folding intermediates and prevent them from aggregating, suggesting other possible extra-ribosomal functions of TF (Liu et al., 2005) and hinting at some chaperone functions of the dimeric TF

### II.3.3 TF-substrate interactions

The chaperone role of TF was identified when it was found to promote the folding of denatured GAPDH (Huang et al., 2000). By analyzing peptide arrays from several protein structures revealed that most TF binding sites were buried in the hydrophobic interior of the molecules (Patzelt et al., 2001). The catalysis of RNase T1 refolding was efficient only with the full length TF and not by the isolated PPIase domain although catalysis is actually carried out by the PPIase domain (Scholz et al., 1997). This indicated that the other domains cooperate with the PPIase domain to enhance its activity.

Independent studies were then carried out to identify the role of different domains in TF function (Genevaux et al., 2004; Kramer et al., 2004b). Genevaux and colleagues showed that substitutions known to abolish ribosome binding or deletion of the TF “signature motif” had only mild a effect in *in vivo* complementation assays compared to the complete deletion of the N-terminal domain. Based on this, it was reasoned that those specific mutations did not completely abolish ribosome binding *in vivo* (Kramer et al., 2002). In contrast, Kramer and colleagues have shown that the N-terminal domain alone was enough to function in the *in vivo* complementation assay, although this was not



observed by Genevoux and colleagues. In both the studies, a TF mutant containing the N- and C-terminal domains without the PPIase domain (NC TF) complemented the loss of *tig* and *dnaK* at 37 °C suggesting the C-terminal domain contributes to the major chaperone activity of TF.

Other experiments were done to address the chaperone role of the C-terminal domain of TF (Hoffmann et al., 2006; Merz et al., 2006; Tomic et al., 2006). In the studies by Tomic et al. and Hoffmann et al., protease protection experiments were employed to emphasize that TF protects nascent chains on the ribosome from protease digestion. Protease protection experiments by Hoffmann and colleagues suggested that TF protects nascent chains of length which would fit the proposed cradle of TF. Tomic and colleagues have shown that the TF protects nascent chains from protease digestion which exceed the size of the putative cradle. The lack of protease protection of longer nascent chains as observed in Hoffmann et al could be due to the nature of the chosen model substrate. Hence the protection mediated by TF might be a result of the hydrophobic interactions between nascent chains and TF and is not due to TF forming a shielded folding environment around the ribosomal exit tunnel. Both the studies implied that the NC TF provided a more or less similar level of protection as compared to full-length TF and the presence of the PPIase domain played only a minor role. In the study by Merz and colleagues, deletion of the C-terminal 53 residues of TF completely abolished the *in vitro* chaperone activity. Since this deletion would destabilize the entire C-terminal domain (Merz et al., 2006), the loss of chaperone function might be attributed globally to the entire C-terminal domain rather than specifically to those 53 residues.

Real time experiments from our laboratory using fluorescently labeled TF have shown that TF dissociates from either translating or non-translating ribosomes with a  $t_{1/2}$  value of ~ 10-12 s at 30 °C. This indicates that the presence of a nascent chain does not strongly influence the duration of TF interactions with the ribosome. FRET experiments showed that TF attains a more open conformation upon binding to the ribosome, which is stabilized during binding to translating ribosomes (Kaiser et al., 2006). Interestingly, this conformational change persisted depending on the nascent chain being translated and was found to decay with a  $t_{1/2}$  value of as long as ~ 35 s. The  $t_{1/2}$  value of this conformational change varied between nascent chains relative to the extent of their hydrophobic motifs.

These findings suggested that TF dissociates from the ribosome but can remain associated with the nascent chain for an additional length of time, with multiple TF molecules being involved in preventing nascent chain aggregation. Similar FRET experiments demonstrated that the PPIase domain offers an additional binding site on TF but the nature of this interaction with the nascent chain remain to be investigated.

## II.4 Aim of the study

TF is a ribosome-associated chaperone that initially interacts with nascent chains during their translation. Alone or together with the downstream DnaK chaperone system, TF plays an important role in the transformation of nascent polypeptides into functional proteins (Agashe et al., 2004; Deuerling et al., 1999; Teter et al., 1999). The structure of TF is modular, consisting of an N-terminal ribosome binding domain, middle PPIase domain and a C-terminal domain. The regions of TF that interact with the nascent chains during translation remain poorly understood. Identifying and characterizing these regions forms the primary aim of this study.

Cell free transcription/translation in a system consisting exclusively of purified components (PURE system) was employed to investigate the interactions between nascent chains and added TF or its mutant versions. Photocrosslinking experiments with site specifically labeled TF (*p*Bpa-TF) were performed to identify the regions of TF adjacent to the nascent chains. The multi-domain model protein Firefly luciferase (Luc) was used as a substrate for TF. The interaction of TF with nascent chains less hydrophobic than Luc was also analyzed. The relationship of TF sites involved in nascent chain interactions and dimerization was also investigated.

A second aim of this study was to develop an experimental system to monitor the interaction of TF with nascent chains directly and in real time during translation. This was achieved by incorporating an environmentally sensitive fluorophore, NBD, at the sites of TF that are in close contact with the nascent polypeptides. Using this system the kinetics of TF binding and release from various nascent chains was measured and compared with the kinetics of TF binding and dissociation from the ribosome. Together these studies provided detailed insights in the function of TF in protecting nascent and newly-synthesized proteins during the initial phase of folding.

## III Materials and Methods

### III.1 Chemicals

Unless specified, chemicals used in this work were of *pro analysi* grade and purchased from Fluka (Deisenhofen, Germany), Calbiochem (Bad Soden, Germany), Merck (Darmstadt, Germany), Sigma-Aldrich (Steinheim, Germany), Roth (Karlsruhe, Germany) or Roche (Mannheim, Germany).

**Amersham Pharmacia Biotech** (Freiburg, Germany): ECL plus detection kit, Protein A Sepharose

**Bachem** (Weil am Rhein, Germany): *p*-benzoyl-L-phenylalanine

**BioMol** (Hamburg, Germany): IPTG

**BioRad** (Munich, Germany): Ethidium Bromide, Bradford Assay

**Difco** (Heidelberg, Germany): Bacto tryptone, Bacto yeast extract, Bacto agar

**Fermentas** (St. Leon-Rot, Germany): GeneRuler 1kb DNA Ladder, GeneRuler 100bp DNA Ladder

**Invitrogen** (Karlsruhe, Germany): BADAN, IANBD ester, Protein markers for SDS-PAGE

**Merck** (Darmstadt, Germany): Ampicillin

**New England Biolabs** (Frankfurt a. Main, Germany): Restriction endonucleases, T4 DNA Ligase, Calf Intestinal Alkaline Phosphatase (CIAP)

**Post Genome Institute** (Tokyo, Japan): PURE system II classic translation system

**Qiagen** (Hilden, Germany): Ni-NTA Agarose

**Roche** (Basel, Switzerland): RNase A, Benzonase, EDTA free Complete Protease Inhibitor

**Schleicher & Schuell** (Dassel, Germany): Protran Nitrocellulose Transfer Membrane

**Stratagene** (Amsterdam, Netherlands): Herculase DNA polymerase

## III.2 Materials and Instrumentation

**Abimed** (Langenfeld, Germany): Gilson Pipetman 2, 10, 20, 100, 200 and 1000  $\mu$ l

**Amersham Pharmacia Biotech** (Freiburg, Germany): ÄKTA Explorer 100 chromatography system, chromatography columns: HiTrap-Q, HiTrap chelating column, HiPrep desalting column, NAP-5, NAP-10, NAP-25 desalting columns, EPS 300 electrophoresis power supply

**Amicon** (Beverly, MA, USA): Concentration devices (Centricon)

**Avestin** (Mannheim, Germany): EmulsiFlex C5 homogenizer

**Applied biosystems** (Darmstadt, Germany): GeneAmp PCR system 2400

**Beckman** (Munich, Germany): DU 640 UV/VIS Spectrophotometer, Avanti J-25 centrifuge with rotors JLA 10.500 and JA 25.50, Optima LE 80k ultracentrifuge with TLA rotor

**Berthold** (Bad-Wildbad, Germany): Luminometer Lumat LB 9507

**BioRad** (Munich, Germany): MiniProtean 2 electrophoresis chamber, Tank blot system, Gene Pulser Xcell electroporation device, Gene Pulser electroporation cuvettes

**Eppendorf** (Hamburg, Germany): 5415C and 5417R centrifuges, Thermomixer Comfort

**Fisher Scientific** (Schwerte, Germany): Accumet Basic pH meter

**Fuji** (Tokyo, Japan): FLA 2000 Phosphorimager, ImageReader LAS-3000

**LOT-Oriel** (Darmstadt, Germany): Mercury arc lamp (500 W)

**Mettler Toledo** (Gießen, Germany): AG285 and PB602 balances

**Millipore** (Eschborn, Germany): Millex SV Filter Units, pore size 0.22  $\mu$ M, Steritop GP Filter Units, pore size 0.22  $\mu$ M, MilliQ plus deionization system

**MWG BiotechAG** (Göttingen, Germany): Gel documentation system BioCapt

**New Brunswick Scientific** (Nürtingen, Germany): Innova 4430 incubator

**Raytest** (Straubenhardt, Germany): AIDA version 2.31 gel imaging software

**SA-Instruments** (New Jersey, USA): fluorescence spectrometer Fluorolog-3

**Savant** (Strasbourg, France): SGD 2000 slab gel dryer

**WTW** (Weilheim, Germany): pH-Meter pH538

### **III.3 Media and buffers**

#### **III.3.1 Media**

##### **LB medium**

10 g/l bacto tryptone, 5 g/l bacto yeast extract, 10 g/l NaCl, pH adjusted to 7.0 with NaOH

##### **LB agar**

16 g/l Bacto agar dissolved in LB medium

#### **III.3.2 Buffers**

##### **4x SDS sample buffer**

240 mM Tris (pH 6.8), 8% SDS (w/v), 40% glycerol, 1.4 M  $\beta$ -Mercaptoethanol, 0.02% bromphenol blue

##### **10x DNA loading buffer**

2 g/l Orange G, 2 g/l Bromophenol Blue, 2 g/l Xylene cyanol FF, 0.37 g/l EDTA disodium salt di-hydrate, 500 g/l sucrose

##### **PBS (Phosphate buffered saline)**

137 mM NaCl, 2.68 mM KCl, 10.1 mM  $\text{Na}_2\text{HPO}_4$ , 1.76 mM  $\text{NaH}_2\text{PO}_4$ , pH adjusted to 7.4 with HCl

##### **SDS-PAGE electrophoresis buffer**

50 mM Tris-HCl pH 8.3, 380 mM glycine, 0.1% (w/v) SDS

##### **TAE-buffer**

242 g/l Tris base, 57.1 ml/l acetic acid, 50 mM EDTA

##### **TBS (Tris buffered saline)**

25 mM Tris-HCl, pH 7.2, 150 mM NaCl

##### **TBST (TBS + Tween 20)**

0.1% Tween 20 in TBS

##### **0.5 M Sucrose cushion**

0.5 M Sucrose, 15 mM  $\text{MgCl}_2$ , 100 mM KoAc, 20 mM HEPES (pH 7.5)

**Luciferase dilution buffer**

25 mM Tris-phosphate pH 7.8, 2 mM DTT, 2 mM CDTA, 10% glycerol, 1% Triton X-100, 1 mg/ml BSA (w/v)

**Transfer buffer for Western blotting**

25 mM Tris, 192 mM glycine, 20% methanol (v/v), pH 8.4

**RIPA buffer**

20 mM HEPES (pH 7.5), 140 mM KCL, 1% (w/v) sodium deoxycholate, 1% (v/v) NP40, 0.1% (w/v) SDS

## III.4 DNA manipulations

### III.4.1 General molecular biology methods

All routine molecular biology methods (e.g. agarose gel electrophoresis, DNA quantification, competent cell preparation and transformation of bacterial cells, etc.) were performed according to “Molecular Cloning” (Sambrook 1989) unless otherwise stated. Plasmid DNA was purified from *E. coli* DH5 $\alpha$  cells using QIAprep kits (Qiagen) according to the manufacturer’s protocol. Primers for cloning were purchased from Metabion (Martinsried, Germany); DNA sequencing was performed by Medigenomix (Martinsried, Germany), the sequencing facility (Core facility, MPI Biochemistry, Martinsried, Germany) or Sequiserve (Vaterstetten, Germany). PCR and gel purification of DNA were done with Wizard SV Gel and PCR Clean-Up System (Promega).

For all the PCR reactions, Herculase DNA polymerase (Stratagene) along with its buffer supplied by the manufacturer was utilized. Typically a 50  $\mu$ l PCR reaction was set up with 20 ng template DNA, 20 pmol of each of the primers, 200  $\mu$ M of each of the dNTPs, 1X enzyme buffer (containing Mg<sup>2+</sup> ions) and 1 unit of the enzyme. Denaturation was set at 94 °C for 1 min, annealing at 52 °C for 30 s and extension at 72 °C depending on the length of the insert to be amplified. After an initial denaturation of 2 min, the above-mentioned steps were performed for 25 cycles. When performing colony PCR, a single bacterial colony was picked with a sterile pipette and utilized as a source of DNA instead of purified DNA.

**Oligonucleotides for cloning**

Primer	Sequence
TF FOR	5' GGA GGA ATT AAC <b>CAT</b> GGA AGT TTC AGT TGA AAC CAC 3'
TF REV	5' TTT TTG TTC <b>GGG CCC</b> CGC CTG CTG GTT CAT CAG CTC 3'
S7 FOR	5' GAT ATA <b>CAT ATG</b> CCA CGT CGT CGC GTC ATT GG 3'
S7 REV	5' CCG <b>CTC GAG</b> TCA ATT TAA GTA GCC CAA AGCG 3'

The TF FOR and TF REV primers were used for cloning in pBAD vector and the S7 FOR and S7 REV primers were used for cloning in pET 22b vector. The restriction endonuclease sites introduced for cloning are highlighted in red.

**Oligonucleotides for site-directed mutagenesis**

Primer	Sequence
TF 14 FOR	5' CTT GGC CGC <b>TAG</b> GTA ACG ATT 3'
TF 14 REV	5' AAT CGT TAC <b>CTA</b> GCG GCC AAG 3'
TF 34 FOR	5' GAG CTG GTC <b>TAG</b> GTT GCG AAA 3'
TF 34 REV	5' TTT CGC AAC <b>CTA</b> GAC CAG CTC 3'
TF 73 FOR	5' CTG ATG AGC <b>TAG</b> AAC TTC ATT 3'
TF 73 REV	5' AAT GAA GTT <b>CTA</b> GCT CAT CAG 3'
TF 88 FOR	5' AAT CCG GCT <b>TAG</b> GCA CCG ACT 3'
TF 88 REV	5' AGT CGG TGC <b>CTA</b> AGC CGG ATT 3'
TF 118 FOR	5' GAA GTT GAA CTG <b>TAG</b> GGT CTG GAA GCG 3'
TF 118 REV	5' CGC TTC CAG ACC <b>CTA</b> CAG TTC AAC TTC 3'
TF 168 FOR	5' GTA ACC ATC GAC <b>TAG</b> ACC GGT TCT 3'
TF 168 REV	5' AGA ACC GGT <b>CTA</b> GTC GAT GGT TAC 3'
TF 177 FOR	5' GAC GGC GAA GAG <b>TAG</b> GAA GGC GGT 3'
TF 177 REV	5' ACC GCC TTC <b>CTA</b> CTC TTC GCC GTC 3'
TF 185 FOR	5' AAA GCG TCT GAT <b>TAG</b> GTA CTG GCG 3'
TF 185 REV	5' CGC CAG TAC <b>CTA</b> ATC AGA CGC TTT 3'
TF 198 FOR	5' ATG ATC CCG GGC <b>TAG</b> GAA GAC GGT 3'



<b>TF 198 REV</b>	5' ACC GTC TTC <b>CTA</b> GCC CGG GAT CAT 3'
<b>TF 233 FOR</b>	5' AAA GCA GCG AAA <b>TAG</b> GCT ATC AAC 3'
<b>TF 233 REV</b>	5' GTT GAT AGC <b>CTA</b> TTT CGC TGC TTT 3'
<b>TF 320 FOR</b>	5' CGC CAG GCT GCA <b>TAG</b> CGT TTC GGT 3'
<b>TF 320 REV</b>	5' ACC GAA ACG <b>CTA</b> TGC AGC CTG GCG 3'
<b>TF 322 FOR</b>	5' GCT GCA CAG CGT <b>TAG</b> GGT GGC AAC 3'
<b>TF 322 REV</b>	5' GTT GCC ACC <b>CTA</b> ACG CTG TGC AGC 3'
<b>TF 373 FOR</b>	5' GGC CTG ATC GAA <b>TAG</b> ATG GCT TCT GCG 3'
<b>TF 373 REV</b>	5' CGC AGA AGC CAT <b>CTA</b> TTC GAT CAG GCC 3'
<b>TF 377 FOR</b>	5' GAG ATG GCT TCT <b>TAG</b> TAC GAA GAT 3'
<b>TF 377 REV</b>	5' ATC TTC GTA <b>CTA</b> AGA AGC CAT CTC 3'
<b>TF 378 FOR</b>	5' ATG GCT TCT GCG <b>TAG</b> GAA GAT CCG 3'
<b>TF 378 REV</b>	5' CGG ATC TTC <b>CTA</b> CGC AGA AGC CAT 3'
<b>TF 387 FOR</b>	5' GAA GTT ATC GAG <b>TAG</b> TAC AGC AAA 3'
<b>TF 387 REV</b>	5' TTT GCT GTA <b>CTA</b> CTC GAT AAC TTC 3'
<b>TF 419 FOR</b>	5' GCG AAA GTG ACT <b>TAG</b> AAA GAA ACC 3'
<b>TF 419 REV</b>	5' GGT TTC TTT <b>CTA</b> AGT CAC TTT CGC 3'

Stop codons contained within the primers are highlighted in red.

Trigger Factor (TF) constructs used in this study

<b>Plasmid</b>	<b>Description</b>
<b>pBAD TF</b>	wild type trigger factor (TF)
<b>pBAD TF FRK/AAA</b>	Ribosome binding deficient TF
<b>pBAD TF 14</b>	R14TAG mutation
<b>pBAD TF 34</b>	N34TAG mutation
<b>pBAD TF 73</b>	R73TAG mutation
<b>pBAD TF 88</b>	G88TAG mutation
<b>pBAD TF 118</b>	Q118TAG mutation
<b>pBAD TF 168</b>	F168TAG mutation
<b>pBAD TF 177</b>	F177TAG mutation
<b>pBAD TF 185</b>	F185TAG mutation

<b>pBAD TF 198</b>	F198TAG mutation
<b>pBAD TF 233</b>	F233TAG mutation
<b>pBAD TF 320</b>	Q320TAG mutation
<b>pBAD TF 320 FRK/AAA</b>	Q320TAG mutation in the ribosome binding deficient mutant
<b>pBAD TF 322</b>	Q322TAG mutation
<b>pBAD TF 373</b>	E373TAG mutation
<b>pBAD TF 377</b>	A377TAG mutation
<b>pBAD TF 378</b>	Y378TAG mutation
<b>pBAD TF 387</b>	F387TAG mutation
<b>pBAD TF 419</b>	E419TAG mutation
<b>pPROEX TF</b>	wild type TF
<b>pPROEX TF FRK/AAA</b>	Ribosome binding deficient TF
<b>pPROEX TF14</b>	R14C mutation
<b>pPROEX TF150</b>	T150C mutation
<b>pPROEX TF326</b>	E326C mutation
<b>pPROEX TF326 FRK/AAA</b>	E326C mutation in the ribosome binding deficient mutant
<b>pPROEX TF376</b>	S376C mutation

### III.4.2 Cloning of *E. coli* TF in pBAD vector

The ORF of TF was amplified by colony PCR from *E. coli* MC4100 cells using primers TF FOR and TF REV which were designed to incorporate *Nco* I and *Apa* I sites, respectively. The DNA fragments generated after colony PCR were eluted from agarose gel and stored in nuclease free (NF) water. The purified DNA was digested with *Nco* I and *Apa* I restriction endonucleases, subjected to PCR clean up and eluted with NF water. The plasmid backbone (pBAD) was also digested with *Nco* I and *Apa* I enzymes and subsequently dephosphorylated with calf intestinal alkaline phosphatase (CIAP). The vector backbone was purified and eluted with NF water. For the ligation reaction, both the purified vector and insert were incubated with 400 units of T4 DNA ligase at 16 °C for 16 h. In a control reaction NF water was added instead of the insert.

The whole ligation reaction was transformed into chemically competent DH5 $\alpha$  cells and plated on LB<sup>Tet</sup> plates and incubated overnight at 37 °C. Single colonies were inoculated in LB<sup>Tet</sup> for overnight cultures. Cultures were harvested and plasmids were prepared. The presence of the insert was confirmed by restriction digestion with *Nco* I and *Apa* I enzymes. Positive clones were confirmed additionally by sequencing the DNA.

### III.4.3 Cloning of *E. coli* S7 in pET 22b vector

The ORF for the *E. coli* small ribosomal protein S7 was amplified using primers S7 FOR and S7 REV by colony PCR from *E. coli* MC4100 cells. S7 FOR and S7 REV primers were designed to include *Nde* I and *Xho* I sites, respectively. The insert was amplified and digested with *Nde* I and *Xho* I. The pET 22b vector (Invitrogen) was cut with the same enzymes and the insert was ligated with the linear vector as mentioned above. Positive clones were confirmed by restriction digestion and sequencing.

### III.4.4 Site directed mutagenesis

Site directed mutagenesis was employed to introduce TAG-amber (Amb) codons in the ORF of TF. Primers were designed such that they incorporate the mutations in the middle of their sequence and they were complementary to each other. 20 ng of the template DNA per 50  $\mu$ l PCR reaction was mixed with 20 pmol of each of the primers, 200  $\mu$ M dNTPs, 1X enzyme buffer and 1 unit of Herculase DNA polymerase. Elongation was performed at 72 °C for 6 min. The PCR products were digested with 1  $\mu$ l of *Dpn* I for an hour at 37 °C to cleave the parental DNA. 20  $\mu$ l of the PCR reaction was used to transform chemically competent DH5 $\alpha$  cells and plated on LB<sup>Tet</sup> plates. The plates were incubated overnight at 37 °C. Cells were harvested and plasmids were prepared. The presence of mutations was confirmed by DNA sequencing.

The pBAD TF vectors were constructed in this study and were designed for incorporation of *pBpa*. The pPROEX cysteine mutants were from our laboratory collection and utilized for labeling with fluorescent dyes.

### III.4.5 Other constructs used in this study

Plasmid	Description	Reference
pET 3a Luc	Firefly luciferase for expression in the PURE system	Kaiser 2006
pET 15b Luc	Firefly luciferase for expression in the PURE system	Tomic 2006
$\alpha$ -Syn	Mouse $\alpha$ -Synuclein for expression in the PURE system	Tomic 2006
pET 22b S7	<i>E. coli</i> small ribosomal protein S7 for expression in the PURE system	This study
pET 22b GatD	<i>E. coli</i> GatD for expression in the PURE system	Kaiser 2006

### III.4.6 Preparation of linear template DNA for *in vitro* translation in the PURE system

Linear DNA templates for protein production in the PURE system were amplified from their respective plasmids using Herculase DNA polymerase. The DNA templates were amplified to have all the regulatory components for *in vitro* translation such as the promoter for T7 RNA polymerase and the ribosomal binding site. Subsequent to PCR amplification, template DNA was subjected to PCR clean-up, eluted and stored in NF water. pET 15b Luc was used for preparing Luc DNA templates involving photocrosslinking experiments and pET 3a Luc was used for the same reason in fluorescence experiments.

## III.5 Protein preparative methods

### III.5.1 Expression of TF proteins in the presence of the pBpa

*E. coli* MG1655 electro competent cells were transformed with ~ 100 ng of pBAD WT TF or TF amber mutants along with pBk pBpa plasmids and were plated at 37 °C for overnight in LB<sup>KanTet</sup> plates. Single colonies were inoculated in LB<sup>KanTet</sup> media and grown

overnight at 37 °C. Secondary cultures were inoculated from the overnight cultures and grown in the presence of either 0.2% arabinose or 1 mM *pBpa* or in the presence or absence of both with shaking at 37 °C. Equal amounts of cells from all the cultures were pelleted and resuspended in SDS sample loading buffer. The samples were heated at 95 °C, loaded onto a 12% SDS gel, transferred to nitrocellulose membrane and blotted against anti-TF antibodies as primary and anti-IgG as secondary antibodies. The expression levels of the TF amber mutants compared to endogenous TF were determined.

### III.5.2 Purification of *pBpa* labeled TF

BL21 (DE3) chemically competent cells were transformed with pBAD vectors harboring WT TF or TF amber mutants along with pBK *pBpa*. The cells were grown in LB<sup>KanTet</sup> plates and overnight cultures were inoculated with the single colonies obtained. The overnight culture was diluted into 3 l of LB<sup>KanTet</sup> and grown till  $A_{600\text{nm}}$  0.6. Cultures were induced with 0.2% arabinose, 1 mM *pBpa*, 50 ml of 1 M K<sub>2</sub>HPO<sub>4</sub> and 20 ml of 1 M KH<sub>2</sub>PO<sub>4</sub> and cells were grown for 8 h after induction. Cells were harvested by centrifugation, resuspended in PBS and flash frozen in liquid nitrogen. The cell resuspension was thawed at 37 °C, incubated with a tablet of EDTA free Complete Protease Inhibitor (CPI), 10 U/ml benzonase and 0.5 mg/ml lysozyme for 30 min on ice. Cells were passed at least three times through the Emulsiflex C5 Homogenizer to ensure complete lysis. The lysate was centrifuged and cleared by centrifugation at 50,000 g, for 60 min at 4 °C.

The cleared lysate was passed over 1 ml of Ni<sup>2+</sup>-NTA agarose in a BioRad econo column pre-equilibrated with PBS. The flow through (FT) was passed over Ni-NTA for three additional times to ensure efficient binding of the protein. The matrix was subsequently washed with 10 mM and 25 mM imidazole in PBS. The bound His<sub>6</sub> tagged protein was eluted with 250 mM imidazole in PBS. The purified protein was pooled and dialyzed against 20 mM Tris-HCl pH 7.0 and passed over a Resource Q anion exchange column pre-equilibrated in the same buffer. The column was subjected to an increasing linear gradient of 1 M NaCl in 20 mM Tris-HCl pH 7.0. The bound protein eluted around

150 mM NaCl. Fractions of purified protein were pooled, dialyzed against 20 mM Tris-HCl pH 7.0, concentrated using centricon and stored in amber colored tubes at  $-80^{\circ}\text{C}$ .

### III.5.3 Purification of TF

BL21 (DE3) chemically competent cells were transformed with pPROEX-HTa plasmids encoding TF or TF mutants and plated on LB<sup>Amp</sup> plates. Secondary cultures in 3 l LB<sup>Amp</sup> were grown until an  $A_{600\text{nm}}$  0.6 was reached, induced with 1 mM IPTG and grown for 4 h post induction. Cells were harvested, washed, resuspended in PBS, lysed and the lysate was cleared in the same manner as described in the above section. Cleared lysate was passed over a HiTrap chelating column charged with  $\text{Ni}^{2+}$  and pre-equilibrated with PBS. The column was washed with 10 mM and 25 mM imidazole in PBS and the bound protein was eluted with 250 mM imidazole in PBS. Fractions of purified protein were pooled, desalted in a HiPrep desalting column to remove imidazole.

Purified TF in PBS was subjected to TEV protease digestion in the presence of 2 mM DTT for removal of the N-terminal His<sub>6</sub> sequence. The reaction mix was passed onto the HiTrap chelating column charged with  $\text{Ni}^{2+}$  to remove the uncleaved protein and the His<sub>6</sub> tagged TEV protease, which would bind to the column by virtue of its His<sub>6</sub> tag. Purified protein without the His<sub>6</sub> tag was collected in the flowthrough, pooled, concentrated and aliquoted in small fractions and stored at  $-80^{\circ}\text{C}$ .

### III.5.4 *In vitro* translation in the PURE system

*In vitro* translations were performed in the PURE system (Shimizu 2001). Template DNA [10 ng/ $\mu\text{l}$ ] was added to the reconstituted PURE system along with other additional components (1  $\mu\text{M}$  pBpa labeled TF, 0.8  $\mu\text{Ci}/\mu\text{l}$  <sup>35</sup>S-methioine) and incubated at 30  $^{\circ}\text{C}$  for  $\sim$  50 min. Translation was arrested by the addition of 0.2  $\mu\text{l}$  of chloramphenicol from a 34 mg/ml stock and incubated on ice for 5 min.

### III.5.5 Photocrosslinking of pBpa-TF to RNCs

Translation reactions were performed as mentioned above. Typically 25  $\mu\text{l}$  of the translation reactions were transferred to a 1.5 ml Eppendorf tube and placed in a metal

tube holder on ice. The samples were placed under a 500 W mercury arc lamp at a distance of ~ 12 cm from the lamp. A filter combination that provides a 300-400 nm bandpass was used. Negative control reactions for light dependency were wrapped in aluminum foil and placed on ice in the same room. A small aliquot was withdrawn from the tubes to serve as a “total” sample prior to separation of the ribosome-nascent chain complexes and the supernatant.

### **III.5.6 Separation of ribosome-nascent chain complexes (RNCs)**

Typically a 25  $\mu$ l reaction of the translated product was layered over a 100  $\mu$ l sucrose cushion and centrifuged at 100,000 rpm for 20 min at 4 °C in Optima TLX ultracentrifuge. The supernatant was aspirated from pellet by gentle pipetting. The pellet was air-dried and subjected to RNase A digestion (see below). The total protein in the supernatant was precipitated by the addition of an equal volume of 50% trichloroacetic acid (TCA) (v/v) followed by centrifugation at 14,000 rpm for 15 min. The supernatant was gently aspirated with vacuum and the pellet was washed with 1 ml of 100% acetone. The supernatant was again gently aspirated, the pellet was air dried and resuspended in SDS loading buffer.

### **III.5.7 RNase A Digestion**

To digest the terminal peptidyl-tRNA (p-tRNA) associated with the ribosome-nascent chains, RNase A digestion was performed. The ribosomal pellet fraction obtained after centrifugation in the ultracentrifuge (see above section) was air dried and resuspended in 100  $\mu$ l of NF water. Protease free RNase A and EDTA were added to a final concentration of 100  $\mu$ g/ml and 10 mM respectively, resuspended thoroughly and incubated at 37 °C for 10 min. The samples were TCA precipitated and resuspended in SDS loading buffer.

### **III.5.8 Site specific labeling of single cysteine TF proteins**

Dyes for site-specific labeling utilized in this study were 6-bromoacetyl-2-dimethyl-aminonaphthalene (BADAN) and *N*-((2-(iodoacetoxy)ethyl)-*N*-methyl)amino-

7-nitrobenz-2-oxa-1,3-diazole (IANBD ester). Desalting steps in the course of site-specific labeling procedures were performed using Sephadex G-25 desalting columns (Nap-5 columns).

Typically, ~ 75 nmol of TF single cysteine mutant protein was incubated with 150 nmol tris-(2-carboxyethyl) phosphine (TCEP) in 150  $\mu$ l PBS for 10 min at 25 °C to completely reduce cysteine thiol groups. A 4-fold molar excess of the fluorescent dye and 400  $\mu$ l of 20 mM Tris-HCl, pH 7.5 were added. The reaction was allowed to proceed for 90 min at 25 °C in the dark.  $\beta$ -mercapto-ethanol ( $\beta$ -ME) was added to a final concentration of 10 mM to quench the reaction. Excess dye and  $\beta$ -ME were removed by desalting the protein into PBS. The eluate was concentrated to ~ 500  $\mu$ l in centricon tubes and desalted into PBS again. The eluate was again concentrated 2- to 3-fold and small aliquots of the labeled protein were flash-frozen in liquid nitrogen and stored at -80 °C in the dark.

The extent of labeling was calculated based on the molar absorptivity coefficient of 23000  $M^{-1} cm^{-1}$  for NBD and 21000  $M^{-1} cm^{-1}$  for BADAN. The concentration of the total protein was calculated by the Bradford method (Bradford 1976). The ratio of the amount of the labeled protein to the total protein will yield the labeling efficiency. For example the extent of the NBD labeling is calculated by,

$$\text{Moles dye per mole protein} = A_{472} * \text{dilution factor} / 23,000 * \text{protein concentration (M)}$$

where 23,000 and 21,000 are the approximate molar extinction coefficients of NBD and BADAN at 472 nm and 397 nm respectively.

## **III.6 Protein analytical methods**

### **III.6.1 Sodium Dodecyl Sulfate-Polyacrylamide Gel Electrophoresis (SDS-PAGE)**

SDS-PAGE was performed using a discontinuous buffer system under denaturing and reducing conditions (Laemmli, 1970). Typically, gels were poured with a 5%



polyacrylamide (v/v) stacking gel on top of a 9-15% polyacrylamide separating gel, depending on the required resolution. SDS loading buffer was added to the protein samples to a 1x concentration. Prior to loading, samples were heated at 95 °C for 5 min. Electrophoresis was carried out at a constant current of 30 mA/gel in running buffer.

**Stacking gel:** 5% acrylamide/bisacrylamide (30:0.8), 130 mM Tris pH 6.8, 0.1% SDS, 0.1% TEMED, 0.1% ammonium persulfate

**Separating gel:** 9-15% acrylamide/bisacrylamide (30:0.8), 0.75 M Tris pH 8.8, 0.1% SDS, 0.1% TEMED, 0.05% ammonium persulfate

**4x SDS sample buffer:** 240 mM Tris pH 6.8, 8% SDS, 40% glycerol, 1.4 M  $\beta$ -Mercaptoethanol, 0.02% bromphenol blue

**Running buffer:** 50 mM Tris-Base, 380 mM glycine, 0.1% SDS

**Coomassie stain:** 0.1% Coomassie Brilliant Blue R250, 30% methanol, 10% acetic acid

**Destain solution:** 30% methanol, 10% acetic acid

### III.6.2 Autoradiography

Samples containing radiolabeled proteins were subjected to SDS-PAGE. After electrophoresis, gels were fixed in 50% methanol, 12% acetic acid, briefly rinsed in water and dried on Whatman paper in a Slab Gel Dryer SGD 2000 for 50 min at 76 °C. Dried gels were exposed to a phospho-imaging plate (Fuji) overnight. The imaging plate was analyzed using an FLA 200 imaging system (Raytest). Band intensities were quantified using the AIDA software version 2.31 (Raytest).

### III.6.3 Western blotting

Western blotting was carried out in a semi-dry blotting unit. After separation by SDS-PAGE, proteins were transferred onto a nitrocellulose membrane by applying a constant current of  $\sim 1 \text{ mA/cm}^2$  gel size in transfer buffer for 1 h.

Blocking was carried out with 5% skimmed milk powder in TBST for 1 h. The membranes were then incubated with primary antibody (diluted in 5% milk-TBST) for 1 h at room temperature or overnight at 4 °C, followed by the incubation with HRP-conjugated secondary antibody (diluted 1:2000 in 5% milk-TBST) for 1 h at room

temperature. Extensive washing between the incubation steps was performed with TBST. Immunodetection was carried out with the ECL system (Amersham Pharmacia) and developed with ImageReader (Fuji LAS-3000).

### III.6.4 Immunoprecipitation

Typically 25  $\mu$ l of the crosslinked samples were added to 650  $\mu$ l of RIPA buffer and 30  $\mu$ l of TF-antiserum and rocked overnight at 4 °C. The samples were spun at top speed in a Beckmann tabletop centrifuge to remove any particulate aggregates. The supernatant was transferred to a new Eppendorf tube and 40  $\mu$ l of Protein A sepharose (1:1 w/v) and 15% BSA (w/v) delipidated in RIPA buffer were added. The samples were then rocked for 2 h at 4 °C. The beads were washed 3 times with 750  $\mu$ l of RIPA buffer. The bound protein was eluted from the beads with 40  $\mu$ l SDS loading buffer. The samples were heated at 95 °C and loaded on SDS-PAGE. The dried gels were exposed to the autoradiographic screens and scanned.

### III.6.5 Quantification of proteins

Purified, unmodified proteins were quantified by absorbance spectroscopy at 280 nm in 6 M Guanidine-HCl, 20 mM Na<sub>2</sub>PO<sub>4</sub>, pH 6.5 using calculated extinction coefficients (Gill and von Hippel, 1989). Extinction coefficient of TF ( $\epsilon_{280 \text{ nm}}$ ) = 15,930 M<sup>-1</sup>cm<sup>-1</sup>. Fluorescently labeled proteins were quantified in a colorimetric assay (Bio-Rad Protein Assay, BioRad) based on the method developed by Bradford (Bradford, 1976). As a reference, a calibration curve with the respective unmodified protein was prepared.

### III.6.6 *In vivo* functionality test for TF single site mutants

*E. coli* MG1655  $\Delta$ *tig* $\Delta$ *dnaK* cells were transformed with pBAD WT TF, TF FRK/AAA or TF amber mutants along with pBk *pBpa* and grown at 23 °C for 36 h in LB<sup>KanTet</sup> plates. Single colonies were inoculated in LB<sup>KanTet</sup> and grown overnight at 23 °C. Cells were serially diluted in LB<sup>KanTet</sup> plates in the presence of either 0.2% arabinose or 1 mM *pBpa* or in the presence or absence of both and incubated at 23 °C, 30 °C, 34 °C and 37 °C overnight.

### III.6.7 Luciferase activity measurements

pET 3a vector encoding the Firefly Luciferase (*Pyrococcus pyralis*) gene was translated in the PURE system in the presence of either 5  $\mu\text{M}$  WT TF or other TF variants and 0.8  $\mu\text{Ci}/\mu\text{l}$   $^{35}\text{S}$ -methionine for  $\sim 50$  min at 30  $^{\circ}\text{C}$ . In a control reaction, translation was performed in the absence of TF. To measure enzymatic activity 2  $\mu\text{l}$  aliquots were diluted into 200  $\mu\text{l}$  of Luciferase dilution buffer. 2  $\mu\text{l}$  of the above mixture was added to 48  $\mu\text{l}$  of Luciferase assay buffer (Promega) and firefly luminescence was measured in the luminometer. Simultaneously a fraction of the translation reactions was loaded on SDS-PAGE and the amount of Luciferase protein synthesized was calculated by autoradiography. Specific activity of Luciferase was calculated by dividing the enzymatic activity with the amount of protein synthesized.

## III.7 Fluorescence measurements

### III.7.1 Overview

All buffers used in spectroscopic measurements were filtered and degassed. Spectra and kinetic traces were collected on a Fluorolog 3 fluorometer (Jobin Yvon) at the indicated temperatures. The bandwidth of the excitation and emission light was adjusted to yield a maximum of  $\sim 10^6$  counts per second (cps). To correct for the fluctuations in the excitation light source, the reference signal (R) was recorded along with the actual signal (S) in the course of all the measurements. S/R was used for data evaluation.

### III.7.2 RCM-RNase T1 refolding

Reduction, carboxymethylation and refolding of RNase T1 were done according to the previously published protocol (Mucke and Schmid, 1992). Typically, 0.24 pmol of RNase T1 was dissolved in 275  $\mu\text{l}$  of 0.2 M Tris/HCl, pH 8.7, containing 7.0 M GdmCl and 2 mM EDTA. The protein was reduced by adding 30  $\mu\text{l}$  of a 0.2 M DTT solution (in 0.2 M Tris/HCl, pH 8.7, 7.0 M GdmCl, and 2 mM EDTA) to give a final concentration

of 20 mM DTT and incubated at 25 °C for 2 h. The reduced protein was subsequently carboxymethylated by adding 60  $\mu$ l of 0.6 M iodoacetate solution in 0.2 M Tris/HCl, pH 7.5 and incubated for 5 min in the dark. The reaction was stopped by adding 100  $\mu$ l of 0.5 M reduced glutathione in 0.2 M Tris/HCl, pH 7.5. The modified protein (RCM-RNase T1) was immediately separated from the reagents by gel filtration over a NAP-5 column, equilibrated with 0.1 M sodium acetate, pH 5.0. The protein was stored in solution at 4 °C.

Folding kinetics was initiated by a  $\sim$  30-fold dilution of unfolded RCM-RNase T1 in the buffer containing 2.0 M NaCl. The kinetics was followed by the change in fluorescence at 320 nm after excitation at 268 nm. All kinetic experiments were carried out in 0.1 M Tris/HCl, pH 8.0 at 15 °C.

### **III.7.3 Equilibrium fluorescence measurements**

Emission spectra were obtained with increments in excitation wavelength of 1 nm and an integration time of 0.25 s per data point. Measurements were recorded in triplicate and averaged. Measurements with TFB and TFNBD were performed with the final concentration of labeled protein of 250 nM. TFB was excited at 387 nm and emission spectra were collected from 410 nm to 600 nm. TFNBD was excited at 472 nm and emission spectra were collected at 500 nm to 650 nm. For monitoring TF-ribosome binding, 1  $\mu$ M of the labeled TF was incubated with 1  $\mu$ M purified ribosomes.

### **III.7.4 Kinetic fluorescence measurements**

For monitoring changes in TF fluorescence during translation, 250 nM of labeled TF was added to the PURE system in the absence of the template DNA. The reactions were transferred to a cuvette prewarmed to 30 °C. Once a steady signal was reached,  $\sim$  after 3 min from the start of measurement, translation was initiated upon addition of DNA at a final concentration of 10 ng/ $\mu$ l. The change in fluorescence was monitored as translation proceeded.

For the kinetic analysis of TF binding to ribosomes, 250 nM of TF labeled with BADAN at position 14 was used. For analysis of TF binding to nascent chains, 250 nM of TF labeled with NBD at the indicated positions was utilized.

### III.7.5 Competition experiments

For displacement of labeled TF with the unlabeled TF during translation, excess unlabeled WT TF (competitor) at a final concentration of 20  $\mu$ M was added to the translation reaction. The competitor was generally added once the fluorescence of the labeled TF has reached steady state.

### III.7.6 Evaluation of the kinetic data

Data from the competition experiments were analyzed using a three parameter single exponential function or a five parameter double exponential function depending on the best fit.

Data for a single exponential function were analyzed using the equation 1,

$$y = y_0 + ae^{-bx} \quad (\text{Eq. 1})$$

and data for a double exponential function were analyzed using the equation 2,

$$y = y_0 + ae^{-bx} + ce^{-dx} \quad (\text{Eq. 2})$$

where  $y_0$  is the initial value,  $a$  and  $c$  represent the amplitudes,  $b$  and  $d$  represent the time constants. The time constant  $b$  is used to calculate the half-time in the single exponential reactions and time constants  $b$  and  $d$  are used to calculate both the half-times in a double exponential reaction by the equations

$$t_{1/2} = \ln(2)/b \quad (\text{Eq. 3})$$

and  $t_{1/2} = \ln(2)/d \quad (\text{Eq. 4})$

## IV Results

### IV.1 *In vitro* translation in the PURE system and site-specific photocrosslinking experiments with *pBpa*-TF

The goal of this part of the study was to investigate nascent chain interacting sites on TF. To achieve this, a photocrosslinking approach was utilized. TF, labeled site-specifically with a photoactivable crosslinker was employed for this purpose. Translation reactions for examining TF-nascent chain interactions were carried out in the PURE system. The PURE system is a reconstituted translation reaction consisting of purified components from *E. coli*, namely 32 translation factors, purified ribosomes, 46 tRNAs, the 20 amino acids and factors required for the energy regeneration (Shimizu et al., 2001). The PURE system is superior to conventional translation systems is that it lacks contaminating proteases and nucleases.

There are two major advantages of employing the PURE system in nascent chain-chaperone interaction studies, the first being the absence of chaperone components, which are present in considerable amounts in crude bacterial translation lysates. As a result, the role of specific chaperones and the exact concentrations required in exerting chaperone action can be examined by adding defined quantities of the respective factors (Shimizu et al., 2005). As a second advantage, the PURE system facilitates the production of ribosome-stalled nascent chains. PCR fragments of DNA as templates can be used to initialize transcription-translation. When the stop codons in the DNA template are omitted, the translated nascent polypeptides will be stalled at the P site of the peptidyl transferase center and is not released from the ribosome (Kaiser et al., 2006; Tomic et al., 2006). The stalled nascent chains produced in this manner are stable over a long period of time (Matsuura et al., 2007) due to the absence of the SsrA system in the PURE system, which has a role in disrupting ribosome-stalled nascent chain complexes (Keiler et al., 1996). The PURE system is also suitable for fluorescence experiments because it is devoid of contaminants that might contribute to background fluorescence.

To identify the regions of TF interacting with the nascent chains during translation, a UV inducible site-specific photocrosslinking approach was utilized. *para-*

Benzoyl-L-phenylalanine (*p*Bpa), an unnatural amino acid-benzophenone derivative (Dorman and Prestwich, 1994) was used as the photoreactive probe throughout all the photocrosslinking experiments (Chin et al., 2002). *p*Bpa is not sensitive to ambient light but is excited at  $\sim 320$  nm. It specifically reacts with C-H bonds even in the presence of solvent water (Dorman and Prestwich, 1994). The reversible excitation of benzophenone facilitates repeated excitation of *p*Bpa to the triplet-excited state, which results in improved crosslinking yields (Kauer et al., 1986). The reactive moiety of the benzophenone is centered at the ketone oxygen with a radius of 3.1 Å and hence regions of nascent chains that are within this distance from the reactive site of *p*Bpa, can form covalent bonds with the *p*Bpa labeled residue upon exposure to UV light (Dorman and Prestwich, 1994). *p*Bpa was incorporated into TF in a site-specific manner. Thus, photocrosslinking allowed the identification of specific regions in TF that interact with nascent chains.

#### **IV.1.1 Incorporation of *p*Bpa into TF and characterization of *p*Bpa-TF**

To investigate the interaction of TF with nascent chains, surface-exposed sites in TF were chosen for the incorporation of *p*Bpa (Figure 12). These sites were distributed over all three domains of TF. When ribosome-bound, TF is predicted to expose a hydrophobic crevice, formed by the N- and the C-terminal domains, towards the ribosomal exit tunnel, for association with nascent chains (Ferbitz et al., 2004). As negative controls for nascent chain interactions, several sites exposed on the back of the molecule facing away from ribosome exit site were investigated. These sites were mutated to amber stop codons (TAG) for *p*Bpa incorporation. Site-specific incorporation of *p*Bpa into TF mutants was carried out *in vivo* using an orthogonal pair of *Methanococcus janaschii* tyrosyl tRNA<sup>amb</sup> and tyrosyl tRNA synthetase with the addition of 1 mM *p*Bpa to the growth media (Figure 11). The *M. janaschii* tyrosyl tRNA synthetase specifically aminoacylates its orthogonal tRNA pair with *p*Bpa which in turn incorporates *p*Bpa at an amber codon, but is not aminoacylated by the endogenous tRNA synthetases (Chin et al., 2002; Chin and Schultz, 2002). In the absence of suppression by the *p*Bpa-tRNA, *p*Bpa is not incorporated during TF expression. As a result, only

truncated TF molecules are synthesized which will not contribute towards photoadduct formation.

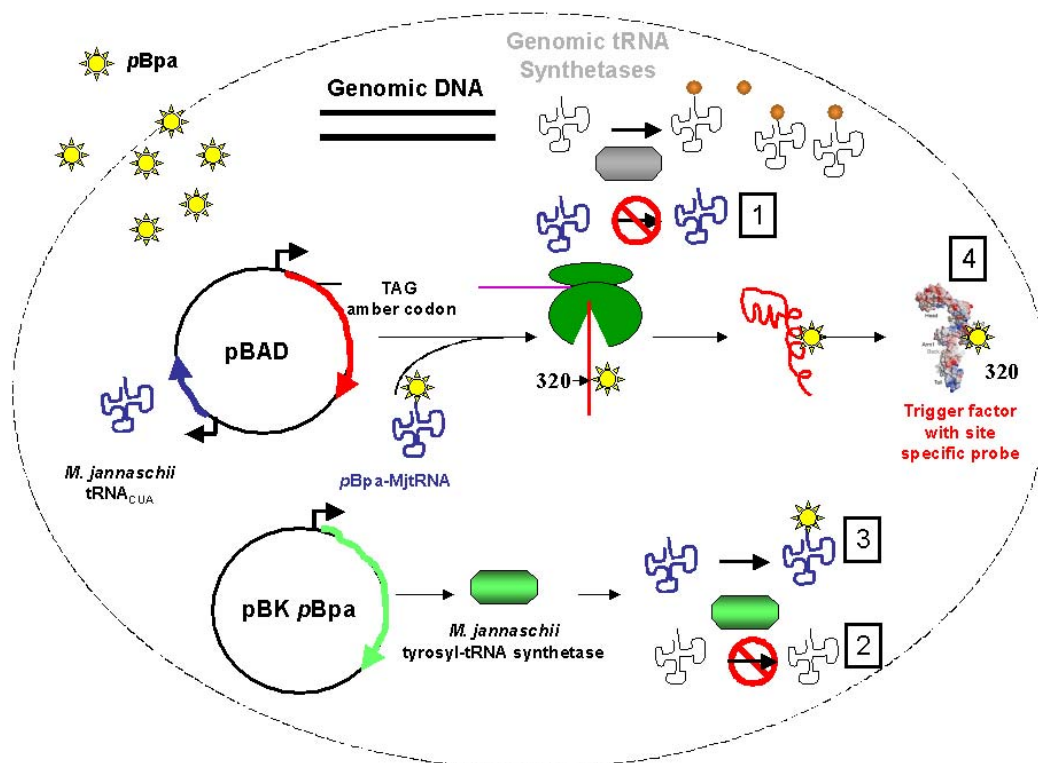


**Figure 11: Incorporation of pBpa in vivo**

*E. coli* cells were transformed with plasmids pBK pBpa that encodes a mutant *M. jannaschii* tyrosyl-tRNA synthetase (green) and a pBAD vector that encodes a mutant *M. jannaschii* tyrosyl tRNA<sup>amb</sup>. The mutant tyrosyl-tRNA synthetase specifically aminoacylates pBpa (stars) onto the mutant tyrosyl tRNA<sup>amb</sup> (3). The pBAD vector also encodes TF with an inframe amber codon (TAG) at a specific position (for example at position 320 as shown in the figure) under an arabinose promoter (red). The aminoacylated *M. jannaschii* tyrosyl tRNA<sup>amb</sup> incorporates pBpa in response to the amber codon during translation (4) resulting in TF labeled with pBpa at a specific position. The mutant tRNA synthetase does not aminoacylate endogenous tRNA with pBpa (2) and the mutant tRNA is not aminoacylated with the endogenous tRNA synthetases (1).

Positions R14, N34, R73 and G88 in the N-terminal domain of TF were chosen as possible nascent chain interaction sites. F168, F177, F185, F198 and F233 were selected in the PPIase domain, while Q320 and F322 were chosen in arm 1 and E373, A377, Y378 and F387 in arm 2 of the C-terminal domain. Positions Q118 and E419 on the back of the



proposed substrate-binding crevice served as negative controls. The mutation at position Q320 was also introduced in the FRK/AAA TF background to serve as a negative control for ribosome-dependent TF interactions with the nascent chains (Figure 12).

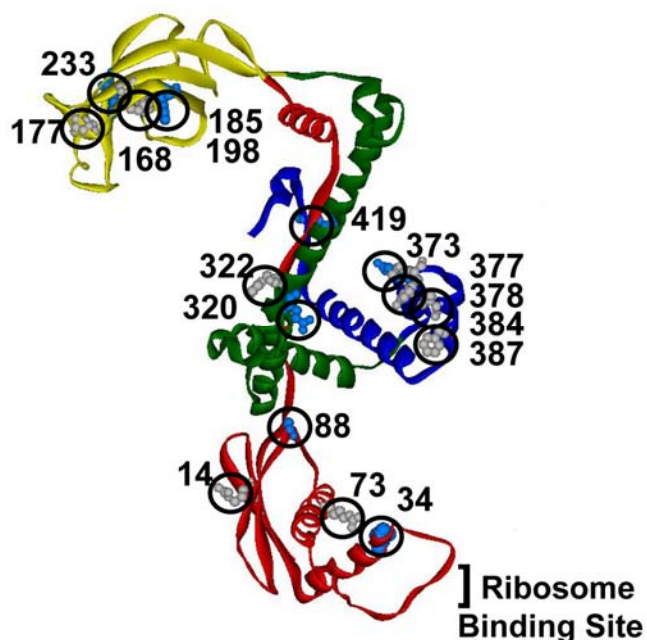


**Figure 12: The crystal structure of *E. coli* TF (pdb-code 1w26)**

The three domains of TF are shown in different colors: N-terminal domain in red, PPlase domain in yellow, arm 1 and arm 2 of C-terminal domain in green and blue, respectively. The numbers denote the residues chosen for *pBpa* incorporation.

#### IV.1.1.1 Expression of *pBpa*-labeled TF

Expression of TF amber mutants was performed in *E. coli* MG1655 cells in the presence of 0.2% arabinose and 1 mM *pBpa*. The expression levels were analyzed by Western blotting with anti-TF antibodies. WT TF was expressed to substantially higher levels compared than *pBpa*-TF because its expression is independent of the incorporation of *pBpa* (Figure 13, lane 1). *pBpa*-TF was expressed at levels comparable to endogenous TF. Truncated TF proteins were observed with TF labeled at positions 373, 377, 378, 384, and 387 resulted from incomplete suppression by *pBpa*-tRNA at the amber codons (Figure 13, lanes 3, 4, 5, 6 and 7).

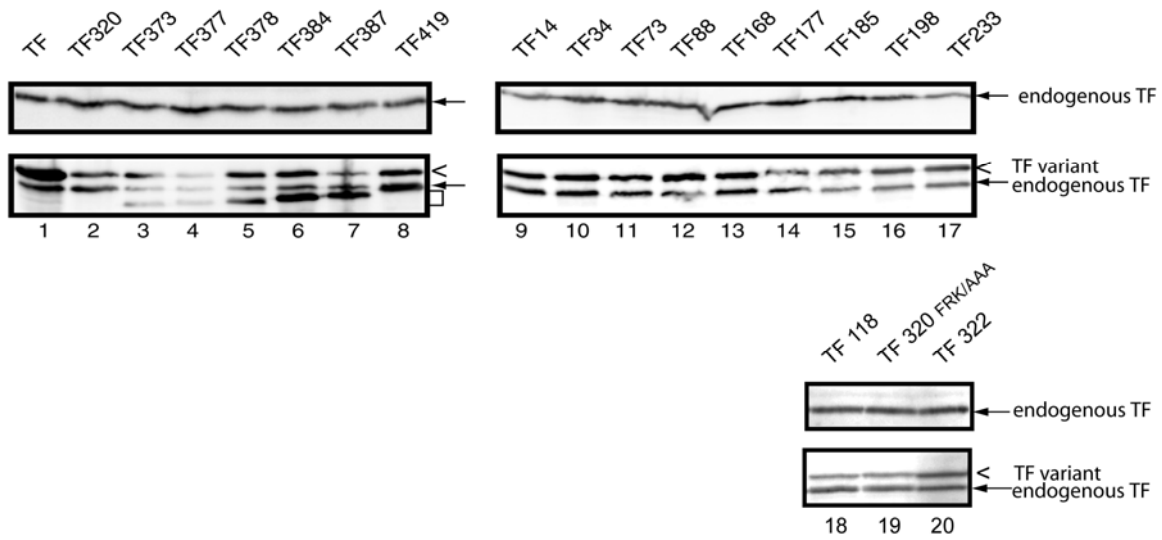


**Figure 13: Expression of the *pBpa*-TF variants *in vivo***

*E. coli* MG1655 cells transformed with pBK *pBpa* along with plasmids encoding either of pBAD TF mutants were grown in LB<sup>KanTet</sup>. The cultures were induced with 1 mM *pBpa* in the absence of arabinose (Upper panel), or induced with 0.2% arabinose and 1 mM *pBpa* (Lower panel) at an  $A_{600nm}$  0.6 and grown for 4 h post induction. Cells were pelleted, lysed in SDS sample buffer, separated on SDS-PAGE and blotted against anti-TF antibodies.

#### IV.1.1.2 *In vivo* complementation of the synthetic lethal phenotype of $\Delta$ *tig* $\Delta$ *dnaK* by *pBpa*-TF

Modifying TF with *pBpa in vivo* offered the advantage of screening for the functionality of *pBpa*-labeled TF. *E. coli* cells lacking both TF and DnaK exhibit synthetic lethality (in this case, inability to grow above 30 °C) due to defective protein folding (Deuerling et al., 1999; Teter et al., 1999). Cultures of *E. coli* MG1655  $\Delta$ *tig* $\Delta$ *dnaK* cells transformed with the corresponding arabinose-regulated pBAD TF mutants and pBK *pBpa* were grown overnight at 16 °C. Cultures were serially diluted on LB<sup>KanTet</sup> plates containing both arabinose and *pBpa* and incubated at 37 °C (Figure 14 A). Since all the mutant proteins were expressed as a result of suppression by *pBpa* at the amber codons (Figure 13), the ability of the mutants to rescue the phenotype was taken as a measure of their functionality *in vivo*. Failure to rescue this phenotype might be due to

the lack of chaperone function of the TF mutants, structural alterations or misfolding introduced as a consequence of the presence of *pBpa*.

As a control, cells were also spotted on plates lacking *pBpa*. This allowed the expression of the proteins in the presence of arabinose, but full-length proteins were not synthesized because of the absence of *pBpa* and hence no rescue would be observed (Figure 14 B). Overexpression of TF is toxic to cells due to impairment of cell division processes (Guthrie and Wickner, 1990), and in the absence of DnaK and DnaJ this toxicity is further intensified (Genevaux et al., 2004). Since the overexpression of WT TF from the pBAD vector was toxic to the cells due to its high expression levels (Figure 13 lane 1), WT TF was cloned downstream of an IPTG inducible promoter in the pOFX vector and used for controlled expression at lower levels.

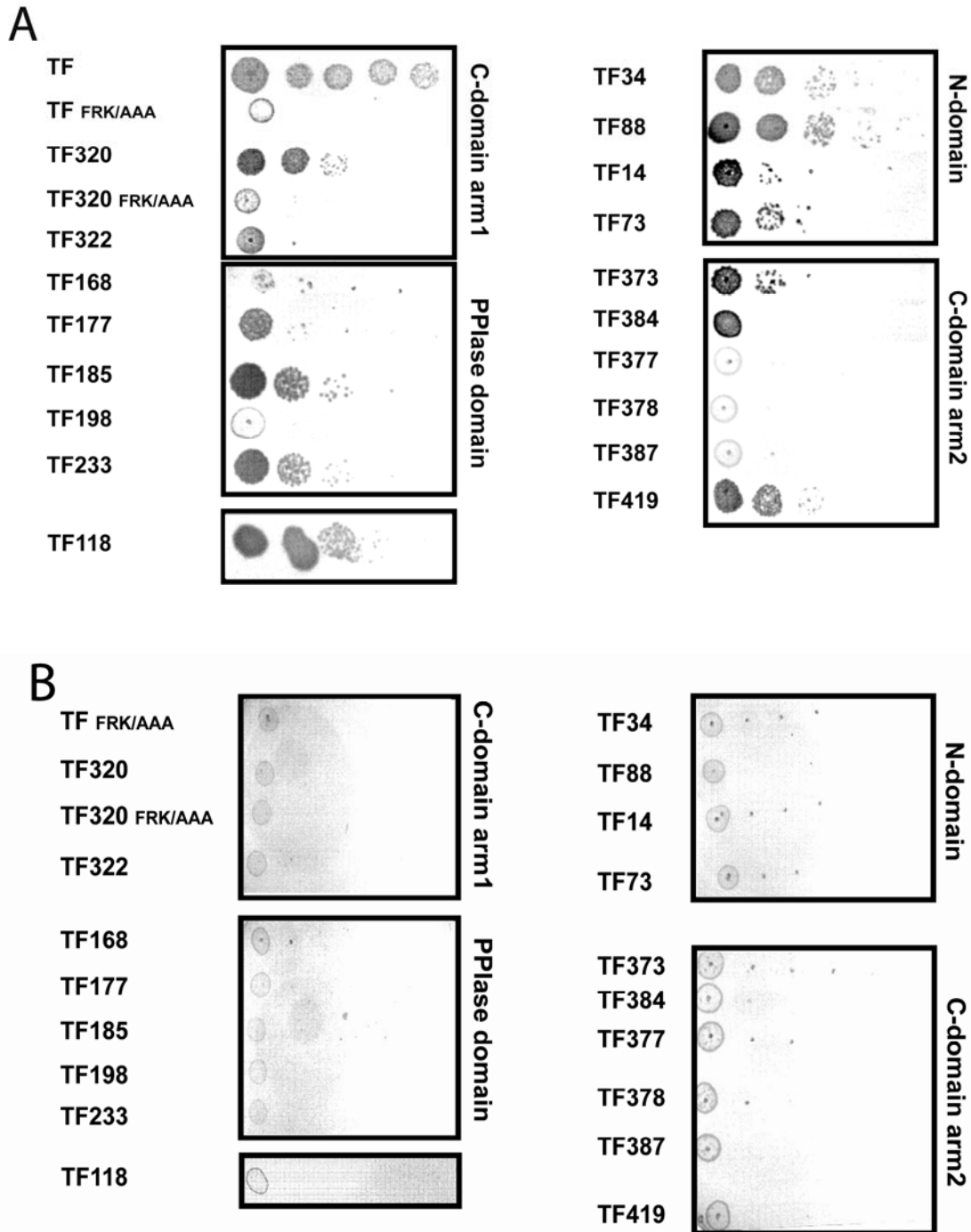


**Figure 14: In vivo activity of pBpa-TF variants**

(A). Serial dilutions of *E. coli* MG1655  $\Delta tig\Delta dnaK$  overnight cultures harboring plasmids pBK pBpa and the corresponding pBAD TF mutants in LB<sup>KanTet</sup> plates supplemented with 0.2% arabinose and 1 mM pBpa. The plates were incubated at 37 °C overnight. WT TF was cloned in the IPTG-controlled pOFX vector and grown in the presence of 250 mM IPTG. (B). Cells were spotted on plates lacking pBpa.

TF-mutants labeled with *pBpa* at positions 34, 88, 118, 185, 233, 320, 373 and 419 partially rescued the synthetically lethal phenotype (Figure 14 A) and were therefore used in subsequent crosslinking experiments. TF FRK/AAA 320 did not complement the phenotype, consistent with ribosome-binding being essential for *in vivo* function (Kramer et al., 2004b). The rest of the positions 14, 73, 168, 177, 198, 322, 377, 378 and 387 did not rescue the phenotype and were not chosen for further experiments.

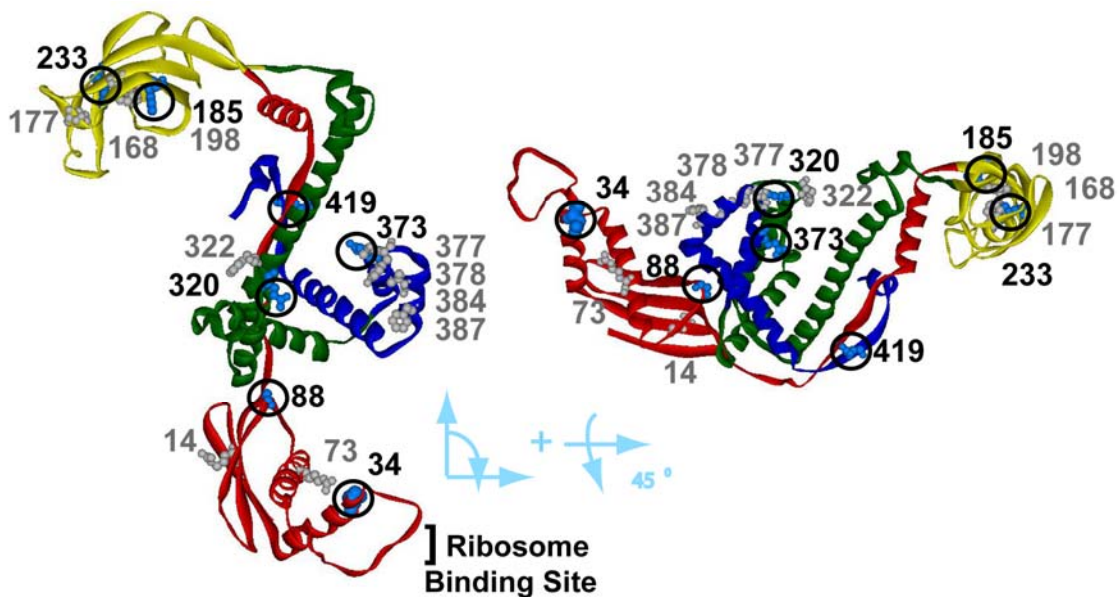


**Figure 15: *pBpa*-TF positions that rescued the  $\Delta$ *tig* $\Delta$ *dnaK* synthetic lethal phenotype**

The three domains of TF are shown in color as in Figure 12. Positions highlighted in gray are mutants that did not rescue the  $\Delta$ *tig* $\Delta$ *dnaK* phenotype. Positions shown in black are mutants that rescued the  $\Delta$ *tig* $\Delta$ *dnaK* phenotype and were utilized for further crosslinking experiments.

#### IV.1.1.3 Tryptophan fluorescence of *pBpa*-TF

The intrinsic tryptophan fluorescence of proteins can be used as a measure of their conformational properties (Lakowicz 1999). To verify the structural integrity of *pBpa*-TF; fluorescence emission of the single tryptophan residue in TF (W151) was analyzed.

Fluorescence emission of *pBpa*-TF were recorded after excitation at 295 nm and normalized. The emission maxima (345 nm) of all the *pBpa*-TF were similar to WT TF suggesting that the global conformation of *pBpa*-TF were not affected by the presence of *pBpa* (Figure 16). The fluorescence emission maxima at 360 nm when TF was denatured in 6 M Guanidium Hydrochloride serves as reference spectra for the unfolded protein.

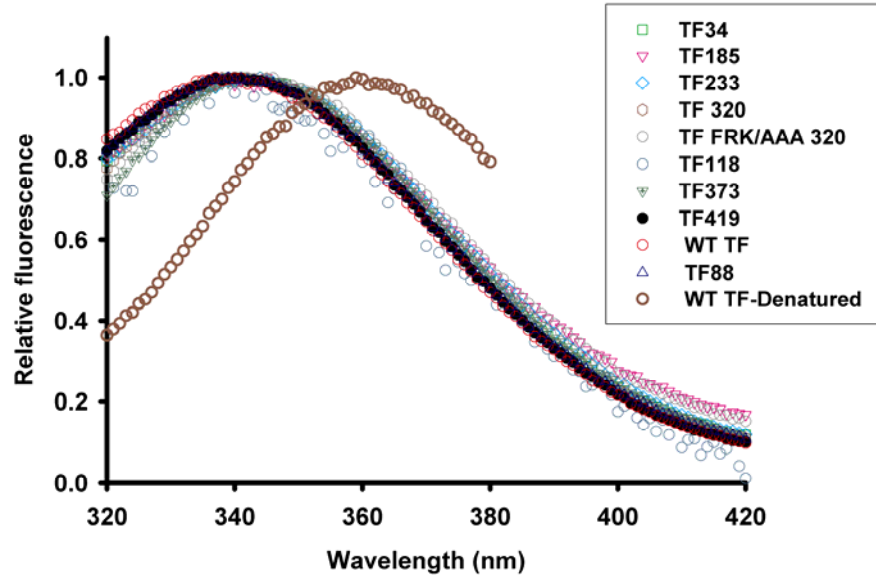


**Figure 16: Tryptophan fluorescence of *pBpa*-TF**

Fluorescence emission scans of WT TF and *pBpa*-TF were recorded after excitation at 295 nm and normalized to unity. The fluorescence maxima of all *pBpa*-TF were similar to WT TF, suggesting that *pBpa* incorporation did not alter their global conformation. Measurements were performed with 2  $\mu$ M TF in 20 mM Tris-HCl, pH 7.0.

#### IV.1.2 Photocrosslinking of *pBpa*-TF to RNCs

The inability of the rest of the sites (14, 73, 168, 177, 198, 322, 377, 378 and 387) to rescue the phenotype could be due to either the alterations introduced to TF's structure or misfolding by *pBpa*. These possibilities were not investigated further. Based on the *in vivo* complementation assay (Figure 14), *pBpa*-TF variants that rescued the synthetic lethal phenotype of  $\Delta$ *tig* $\Delta$ *dnaK* were purified and used in crosslinking experiments.

Firefly luciferase (Luc) was chosen as the translated model substrate throughout the crosslinking experiments because earlier studies had shown that the specific activity

of luciferase increased in the presence of TF (Agashe et al., 2004). Moreover, TF was shown to interact directly with Luc nascent chains upon *in vitro* translation and photocrosslinking with the reactive probes incorporated in the nascent chain (Tomic et al., 2006).

For all the crosslinking experiments, stalled nascent chains of Luc 60, 77, 125 and 164 residues in length (Luc 60mer, Luc 77mer, Luc 125mer and Luc 164mer respectively) were used. The ribosomal exit tunnel can accommodate at least 28-40 residues as based on proteolysis experiments (Blobel and Sabatini, 1970; Malkin and Rich, 1967; Sabatini and Blobel, 1970). Nascent chains are thought to remain largely unfolded in the hydrophilic exit tunnel (Nissen et al., 2000). However, some degree of  $\alpha$ -helix formation was observed with the hydrophobic segments of trans-membrane proteins (Woolhead et al., 2004). Luc 60mer was the shortest nascent chain used and considering the aforementioned observations the  $\sim$  20-30 N-terminal residues would be expected to be exposed outside the polypeptide exit tunnel. Likewise, in the Luc 77mer  $\sim$  35-45 residues, in the Luc 125mer  $\sim$  85-95 residues and in the Luc 164mer  $\sim$  125-135 residues would be exposed outside the ribosomal tunnel.

Translations were performed in the PURE system in the presence of 1  $\mu$ M *pBpa*-TF and  $^{35}$ S-methionine for  $\sim$  50 min and nascent chains were stabilized with the addition of 230  $\mu$ g/ml chloramphenicol. Subsequent to translation, photocrosslinking was performed as described (see Materials and Methods). The ribosome associated nascent chains were then separated by ultracentrifugation on a sucrose cushion. RNase A digestion was performed on the ribosome associated pellet fractions to digest the peptidyl-tRNA. Samples were resolved on SDS-PAGE, followed by autoradiography and shown in all the experiments below. Authenticity of the crosslinks were confirmed by their light and probe dependency as no crosslinks were observed with WT TF and in the absence of UV light. Immunoprecipitations were carried out with anti-TF antibodies to confirm the identity of the crosslink products.

#### **IV.1.2.1 Photocrosslinking of *pBpa*-TF to Luc-RNCs**

To obtain initial insights into TF-nascent chain interactions by photocrosslinking with *pBpa*-TF, Luc nascent chains 77 and 164mers were utilized. *pBpa*-TF labeled at

position 320 (TF320) in the tip of arm 1 of the C-terminal domain was used because nascent chains were predicted to interact with the hydrophobic crevice formed by the C-terminal domain (Ferbitz et al., 2004; Ludlam et al., 2004). Labeling at positions 233 and 185 (TF233, TF185) in the PPIase domain was used to probe nascent chain interactions because these residues were identified to form a hydrophobic surface for substrate interaction based on homology modeling with the *S. cerevisiae* PPIase, FKBP12, as a template (Patzelt et al., 2001). Position 419 (TF419) was employed to test whether nascent chains also interact with the back of the TF molecule.

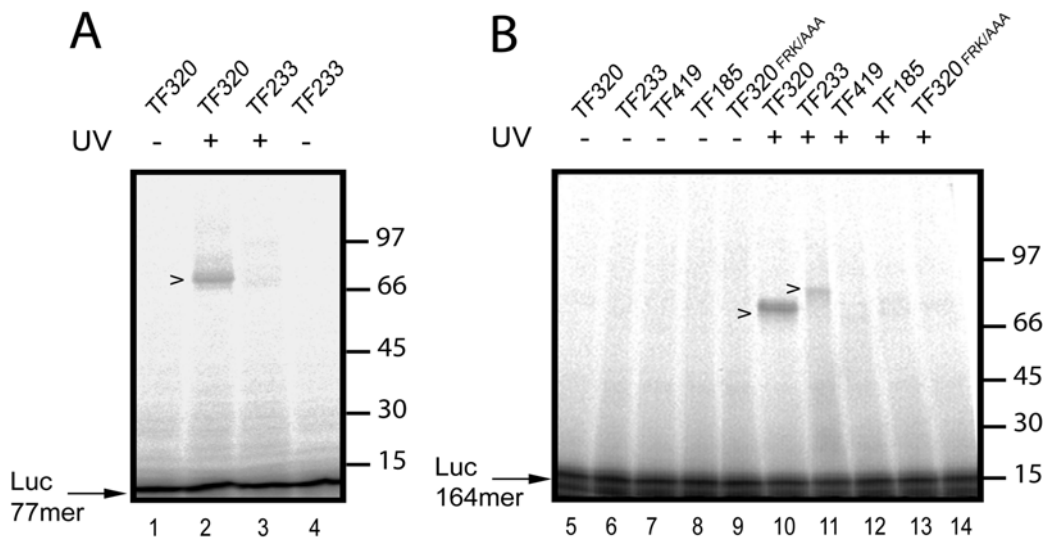


### Figure 17: Photocrosslinking of pBpa-TF to Luc-RNCs

*In vitro* translations were performed in the PURE system to generate  $^{35}\text{S}$ -methionine labeled Luc 77mer or 164mer nascent chains (A and B, respectively) in the presence of 1  $\mu\text{M}$  pBpa-TF. The samples were crosslinked under UV light for 60 min for reactions in (A) and 2 min for reactions in (B). Samples not irradiated are indicated on top of the gel. (A). TF320 and TF233 crosslinked to Luc 77mer (lanes 2 and 3). (B). TF320, TF233, TF419, TF185 and TF320 FRK/AAA crosslinked to Luc 164mer (lanes 10 to 14). Black arrows indicate hydrolyzed nascent chains and open arrows indicate crosslinked nascent chains.

TF320 crosslinked to Luc 77mer (Figure 17, lane 2) but TF233 did not crosslink to this nascent chain (Figure 17, lane 3). TF320 and TF233 both crosslinked to Luc 164mer (Figure 17, lanes 10 and 11). TF 320 FRK/AAA did not crosslink to Luc 164mer confirming that the interaction of TF320 with nascent chains requires binding to the



ribosome (Figure 17, lane 14). TF185 also failed to crosslink to Luc 164mer (Figure 17, lane 13). The absence of photoadducts with TF419 confirmed that the nascent chains interact with the inner hydrophobic crevice as they elongate and do not interact with the back of the molecule (Figure 17, lane 12). A prolonged crosslinking time of 60 min was used to produce efficient crosslinking with Luc 77mer. Prolonged crosslinking also served to demonstrate the complete absence of TF233-Luc 77mer crosslinking. As will be discussed the absence of crosslinking could be due to the inability of the short Luc 77mer to reach position 233 in the PPIase domain.

To confirm the authenticity of the photoadducts, immunoprecipitations (IPs) of the <sup>35</sup>S-methionine labeled crosslinked samples were performed with anti-TF antibodies (see Materials and Methods). Figure 18 shows a representative IPs of TF320 crosslinking to Luc 77mer and Luc 164mer (Figure 18, lanes 1 and 2). As seen in lanes 1 and 2, the photoadducts obtained with Luc 77mer and Luc 164mer were immunoprecipitated with anti-TF antibodies, confirming that the photoadducts contain both TF and the nascent chain. The ribosome binding deficient TF-mutant, TF320 FRK/AAA, yielded substantially weaker crosslinks with the nascent chains tested (Figure 18, lanes 3 and 4).

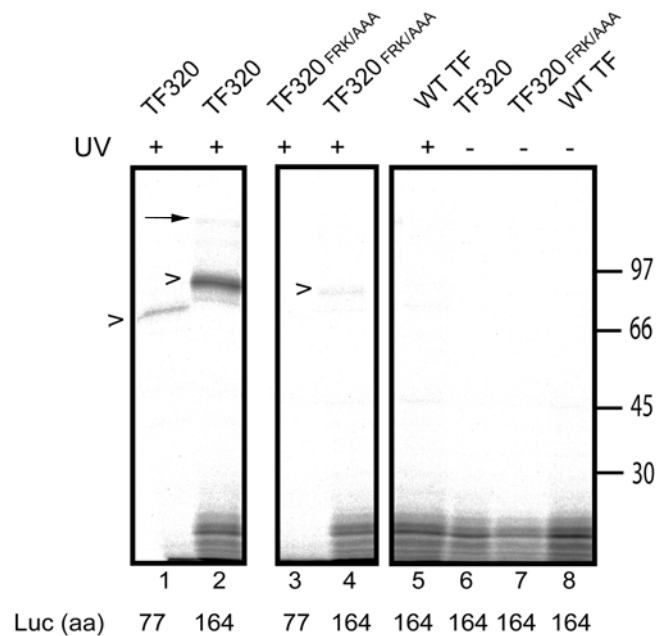


**Figure 18: Immunoprecipitation of pBpa-TF-nascent chain photoadducts with anti-TF antibodies**

Luc 77mer and Luc 164mer was generated in the PURE system (as indicated in the Fig) in the presence of  $^{35}\text{S}$ -methionine and 1  $\mu\text{M}$  TF320 or TF320 FRK/AAA or WT TF (as shown in the top of the gel) and crosslinked with UV for 15 min. Samples not irradiated with UV were indicated on the top of the gel. The photoadducts obtained with Luc 77mer and Luc 164mer in the presence of TF320 were immunoprecipitated with anti-TF antibodies confirming the presence of TF in the photoadducts (lanes 1 and 2). Open arrows indicate crosslinked nascent chains. The black arrow (lane 2) indicates p-tRNA of the TF320-Luc164mer photoadduct.

The above experiment demonstrated that TF-nascent chain interactions can be followed by photocrosslinking. The nascent chains were in close proximity to both the C-terminal domain and the PPIase domain in a length-dependent manner but not with the back of the molecule. Photoadduct formation was also dependent on ribosome binding as TF320 FRK/AAA yielded photoadducts with strongly reduced efficiency. A fraction of Luc 164mer nascent chains were immunoprecipitated with anti-TF antibodies probably due to non-specific interaction of Luc 164mer with the antibodies or with the Protein A sepharose. These initial results provided the basis for a systematic study of the role of the three domains of TF in nascent chain binding.

#### **IV.1.2.2 Crosslinking of the N-terminal domain of TF to Luc-RNCs**

The N-terminal domain of TF binds to the ribosome close to the exit tunnel and is positioned to interact with the nascent chains during translation (Ferbitz et al., 2004; Kramer et al., 2002). In complex with the ribosome, residues 34 and 88 of TF are both surface exposed but residue 34 is in close vicinity of the flexible loop carrying the “signature motif” sequence ( $_{43}\text{GFRxGxxP}_{50}$ ) that is responsible for ribosome-binding. Residue 88 is located in the interior of the N-terminal domain, at least 50 Å from the “signature motif” sequence (Figure 12) (Ferbitz et al., 2004). TF34 crosslinked to Luc nascent chains 60, 77 and 164 mers in a light-dependent manner (Figure 19, lanes 5, 11 and 17). This confirms that the nascent chains emerging from the ribosome interact with the region of TF close to the polypeptide exit tunnel. None of the nascent chain lengths tested showed detectable crosslinks to TF88 (Figure 19, lanes 6, 12 and 18), suggesting that this residue is not in close proximity to the nascent chain.

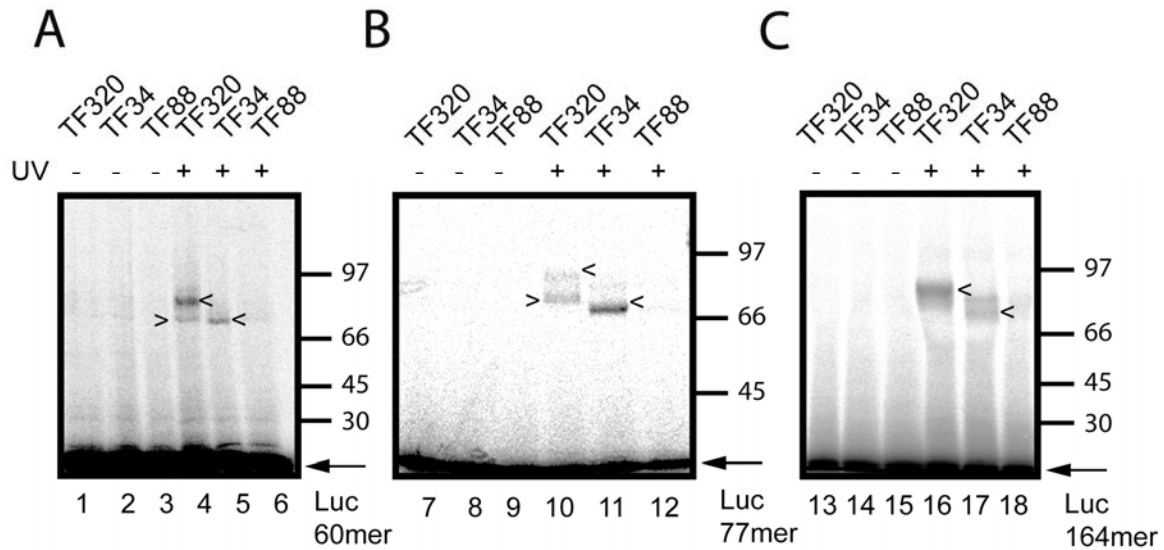


**Figure 19: Photocrosslinking of TF N-terminal domain variants to Luc-RNCs**

*In vitro* translations were performed in the PURE system to generate  $^{35}\text{S}$ -methionine labeled Luc 60mer, 77mer or 164mer nascent chains (A, B and C, respectively) in the presence of 1  $\mu\text{M}$  pBpa-TF. Reactions were crosslinked under UV light for 15 min for reactions in (A) and (B). Samples were crosslinked for 2 min for reactions in (C). (A). TF34 and TF88 crosslinked to Luc 60mer (lanes 5 and 6). (B). TF34 and TF88 crosslinked to Luc 77mer (lanes 11 and 12). (C). TF34 and TF88 crosslinked to Luc 164mer (lanes 17 and 18). TF320 was utilized as a positive control throughout all the experiments. Black arrows indicate hydrolyzed nascent chains and open arrows indicate crosslinked nascent chains.

#### IV.1.2.3 Crosslinking of the C-terminal domain of TF to Luc-RNCs

The C-terminal domain forms the crevice of the TF molecule and has two arm-like projections from its main body, called arm 1 and arm 2 (Figure 12). Residues 320 and 373 were chosen to represent arm 1 and arm 2 respectively, to investigate nascent chain interactions with the C-terminal domain. On exit from the ribosome, nascent chains are predicted to interact with the inner surface of TF that contain exposed hydrophobic residues (Ferbitz et al., 2004; Ludlam et al., 2004). Sites 118 and 419 on the back of the molecule were chosen as controls (Figure 12).

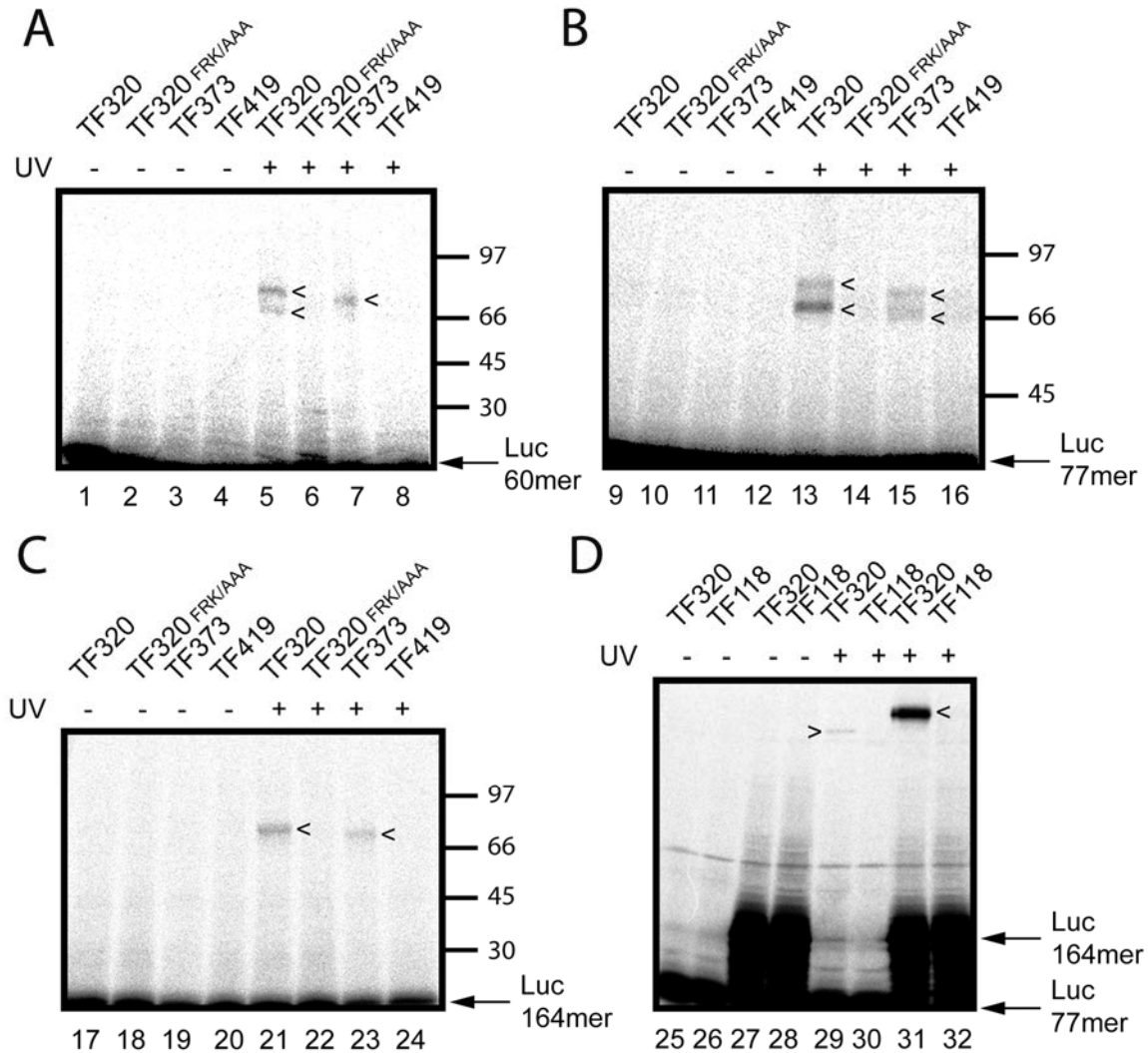


**Figure 20: Photocrosslinking of TF C-terminal domain variants to Luc-RNCs**

*In vitro* translations were performed in the PURE system to generate  $^{35}\text{S}$ -methionine labeled Luc 60mer, 77mer or 164mer nascent chains (A, B and C, respectively) in the presence of  $1\ \mu\text{M}$  pBpa-TF. The samples were crosslinked under UV light for 15 min for reactions in (A), (B) and (D). Samples were crosslinked for 2 min for reactions in (C). (A). TF320, TF320 FRK/AAA, TF373 and TF419 crosslinked to Luc 60mer (lanes 5 to 8). (B). TF320, TF320 FRK/AAA, TF373 and TF419 crosslinked to Luc 77mer (lanes 13 to 16). (C). TF320, TF320 FRK/AAA, TF373 and TF419 crosslinked to Luc 164mer (lanes 21 to 24). (D). TF118 crosslinked to Luc 77mer or Luc 164mer (lanes 30 and 32). Black arrows indicate hydrolyzed nascent chains and open arrows indicate crosslinked nascent chains.

TF320 and TF373 crosslinked to Luc nascent chains 60, 77 and 164 mers (Figure 20, lanes 5, 7, 13, 15, 21 and 23) in a light dependent manner. None of the nascent chains tested crosslinked to TF320 FRK/AAA (Figure 20, lanes 6, 14 and 22), TF118 (Figure 20, lanes 30 and 32) or TF419 (Figure 20, lanes 8, 16 and 24). The lack of crosslinking with TF118 and TF419 suggests that nascent chains interact with the inner hydrophobic crevice of TF as they elongate and not with the back of the molecule.

#### **IV.1.2.4 Crosslinking of the PPIase domain of TF to Luc-RNCs**

In the 3-D structure of TF, the N-terminal domain and the PPIase domains are positioned at opposite ends. The PPIase domain is connected to the N-terminal domain via a long linker that extends across the back of the molecule (Ferbitz et al., 2004; Ludlam et al., 2004). Although the PPIase domain was shown to catalyze the refolding substrates that rely on prolyl isomerisation (Scholz et al., 1997), its importance in nascent chain binding if any remained to be addressed. Importantly in this context, the PPIase domain is dispensable for TF function *in vivo* (Genevaux et al., 2004; Kramer et al., 2004). Residues 185 and 233 were chosen in the PPIase domain for *pBpa* incorporation and subsequent crosslinking experiments.

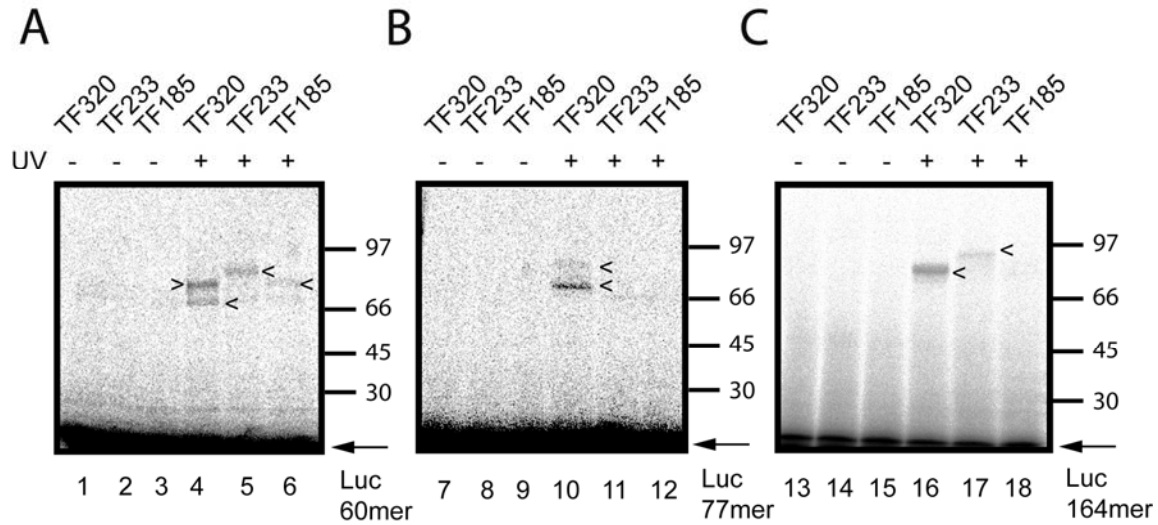


**Figure 21: Photocrosslinking of the TF PPIase domain variants to Luc-RNCs**

*In vitro* translations were performed in the PURE system to generate  $^{35}\text{S}$ -methionine labeled Luc 60mer, 77mer or 164mer nascent chains (A, B and C, respectively) in the presence of 1  $\mu\text{M}$  pBpa-TF. The samples were crosslinked under UV light for 15 min for reactions in (A) and (B) and for 2 min in (C). (A). TF233 and TF185 crosslinked to Luc 60mer (lanes 5 and 6). B. TF233 and TF185 crosslinked to Luc 77mer (lanes 11 and 12). (C). TF233 and TF185 crosslinked to Luc 164mer (lanes 17 and 18). Black arrows indicate hydrolyzed nascent chains and open arrows indicate crosslinked nascent chains.

Interestingly, the crosslinking of nascent chains to the PPIase domain displayed clear length-dependence. TF233 and TF185 both crosslinked to Luc 60mer (Figure 21, lanes 5 and 6) but neither of them crosslinked to Luc 77mer (Figure 21, lanes 11 and 12). TF233 crosslinked to Luc 164mer but TF185 did not crosslink to Luc 164mer (Figure 21, lanes 17 and 18). The length of the ribosomal exit tunnel is  $\sim 100$  Å (Ban et al., 2000) and the calculated distance between TF34, close to the exit tunnel, and TF233 is 87 Å. Based on calculations as mentioned earlier (Section IV.1.2), the Luc 60mer nascent chains must be in rather extended conformation (210 Å) to reach the probe at position 185 or 233, far from the ribosomal exit tunnel. Crosslinking of these probe sites to the Luc 60mer indicates that at least a portion of the nascent chain is maintained in an extended conformation by TF. This might also explain the loss of interaction of TF88 with nascent chains, as this residue is in the interior of the molecule as mentioned above (Figure 19). Neither TF185 nor TF233 crosslinked to the Luc 77mer. On the other hand,

only TF233 crosslinked to the Luc 164mer. This suggests that different portions of Luc nascent chains are adjacent to the probe position at 233 as the chain elongates from 60 to 164 amino acids. Thus, it appears that the nascent chains can move relative to TF during translation.

#### **IV.1.2.5 TF crosslinking to $\alpha$ -Synuclein-RNCs**

Luc nascent chains interacted with all three major domains of TF during translation. The interactions of the domains of TF with other nascent chains were examined next.  $\alpha$ -Synuclein ( $\alpha$ -Syn) was chosen as a natively unfolded model protein. Previous experiments had shown that  $\alpha$ -Syn is in close proximity to TF by photocrosslinking experiments with crosslinker incorporated in the nascent chains (Tomic et al., 2006). Although in this study  $\alpha$ -Syn nascent chains crosslinked to TF, they were not protected from protease digestion by TF, suggesting the absence of stable complex formation.  $\alpha$ -Syn has no substantial hydrophobic regions compared to Luc, as judged by hydrophobicity plots (Kaiser et al., 2006) (Figure 22 B and C).  $\alpha$ -Syn 140mer nascent chains were generated in the PURE system and crosslinking was performed with all the *pBpa*-TF variants. TF34, TF320, TF373 and TF233 crosslinked to  $\alpha$ -Syn 140mer nascent chains (Figure 22 A, lanes 1, 3, 5 and 7), although the crosslinking efficiency was weaker with TF233. Crosslinks were not detectable with both TF88 and TF185 (Figure 22 A, lanes 2 and 8).



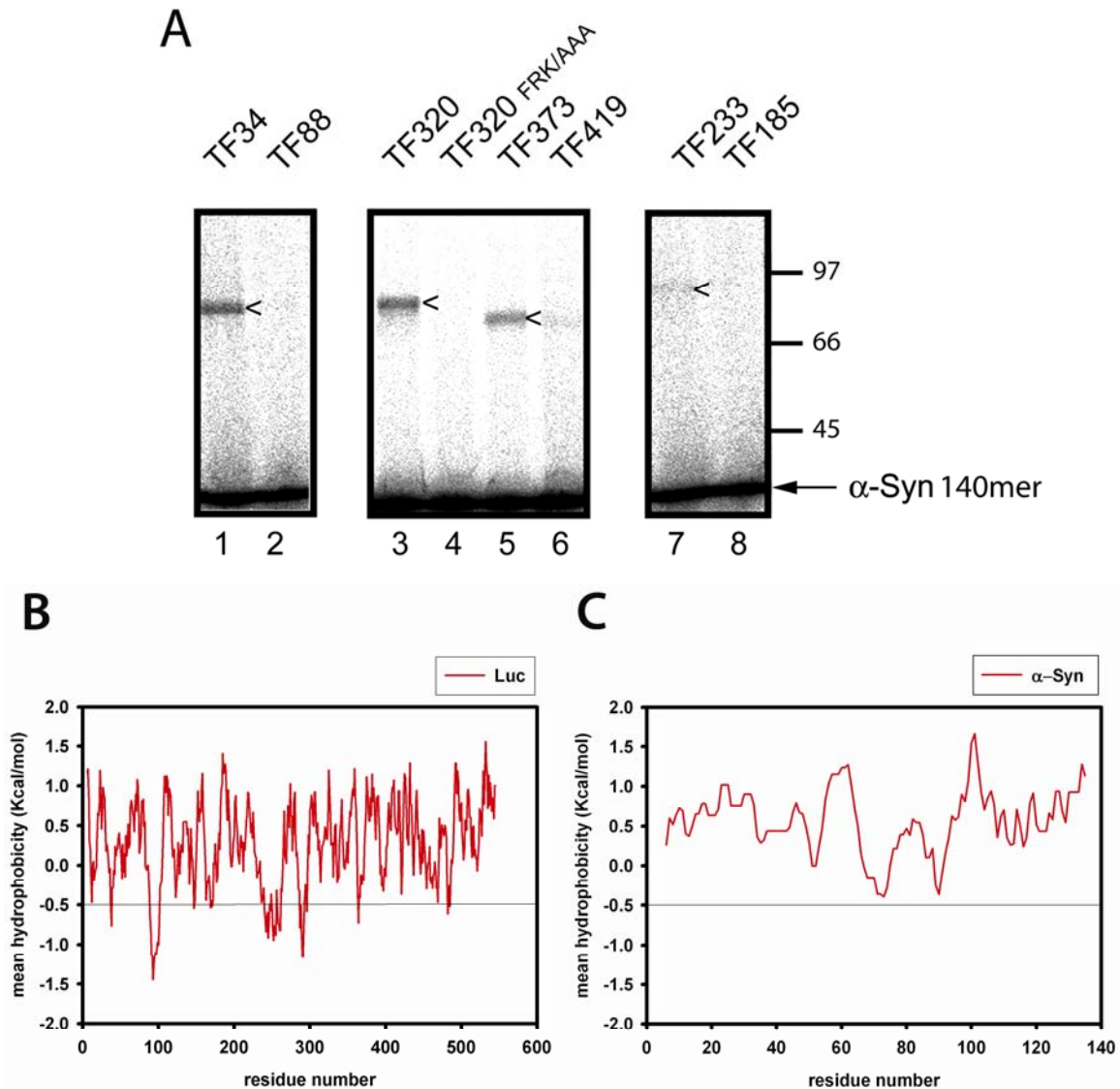


**Figure 22: Site-specific photocrosslinking of pBpa-TF to  $\alpha$ -Syn-RNCs and hydrophobicity analysis of the nascent chain substrates**

(A). *In vitro* translation of  $^{35}$ S-methionine labeled  $\alpha$ -Syn 140mer in the PURE system in the presence of the indicated pBpa-TF. The samples were crosslinked under UV light for 15 min. Hydrolyzed nascent chains are indicated by black arrows. Open arrows indicate photoadducts between pBpa-TF and nascent chains. Analysis of mean hydrophobicity of Luc (B) and  $\alpha$ -Syn (C). Using a window of 11 residues the mean hydrophobicity of each sequence was calculated according to the previously published method (Kaiser et al., 2006). If a sequence of maximum 5 consecutive residues have a mean hydrophobicity of  $< -0.5$  kcal/mol, they are predicted to bind to TF with high probability. Luc has three such regions to mediate increased TF binding while  $\alpha$ -Syn has no such regions.

To directly compare the crosslinking efficiency of Luc and  $\alpha$ -Syn nascent chains to the C-terminal domain and the PPIase domain, TF320 and TF233 were crosslinked to either Luc 125mer or  $\alpha$ -Syn 140mer nascent chains. TF320 and TF233 crosslinked to Luc 125mer with similar efficiency (Figure 23, lanes 1 and 2). TF320 crosslinked less efficiently to  $\alpha$ -Syn 140mer than to Luc 125mer while the crosslinking efficiency of TF233 to  $\alpha$ -Syn 140mer was reduced substantially (Figure 23, lanes 3 and 4). This would be consistent with the absence of strong hydrophobic patches in  $\alpha$ -Syn nascent chains (Figure 22 C), which might mediate the nascent chain's interaction with the PPIase domain.

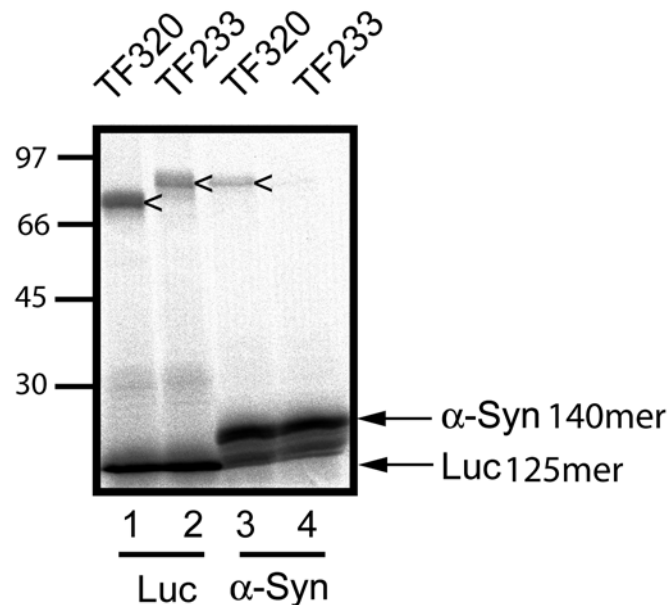


**Figure 23: Comparison of crosslinking efficiency between TF320 and TF233 to Luc and  $\alpha$ -Syn-RNCs**

*In vitro* translations of  $^{35}\text{S}$ -methionine labeled Luc 125mer (lanes 1 and 2) or  $\alpha$ -Syn 140mer (lanes 3 and 4) in the PURE system in the presence of either 1  $\mu\text{M}$  TF320 (lanes 1 and 3) or 1  $\mu\text{M}$  TF233 (lanes 2 and 4). Samples were irradiated with UV light for 15 min. Black arrows indicate hydrolyzed nascent chains and open arrows indicate crosslinked nascent chains.

#### IV.1.2.6 Nature of PPIase domain-nascent chain interactions

The PPIase domain displayed length and position-dependent crosslinks to Luc nascent chains and also differential crosslinking efficiency between Luc and  $\alpha$ -Syn nascent chains (Figures 21, 22 and 23). Although the PPIase domain interacted with the nascent chains during translation, it was not clear whether the interaction involves enzymatic activity of this domain. Interestingly, mutation of residue F233 in the PPIase domain, which was crosslinked to nascent chains, has been shown to cause a marked reduction in prolyl isomerisation activity *in vitro* (Tradler et al., 1997). To test the PPIase activity of TF labeled with *pBpa* at residue 233, refolding of reduced carboxymethylated RNase T1 (RCM-RNase T1) was analyzed. Two native disulfide bonds are broken in this form of RNase T1 and remain unfolded in the absence of NaCl (Mucke and Schmid, 1992). RCM-RNase T1 is converted into its folded and active form in the presence of NaCl. Slow *cis-trans* isomerisation of the Try38-Pro39 prolyl bond is the rate-limiting step of RCM-RNase T1 refolding, which is accelerated in the presence of PPI in a concentration dependent manner (Scholz et al., 1997; Schonbrunner et al., 1991) (Figure 24).

Refolding of RCM-RNase T1 in 0.1 M Tris-HCl, pH 8.0 was initiated by a 30-fold dilution into 2.0 M NaCl in the same buffer in the presence of 1  $\mu$ M WT TF, TF233, TF320, NC TF or in the absence of TF. TF320 was utilized as control to demonstrate that the presence of *pBpa* did not affect the ability of TF in the refolding reaction. Folding was monitored by the increase in intrinsic tryptophan fluorescence of RCM-RNase T1 as it approaches its natively folded structure. 1  $\mu$ M WT TF was able to accelerate the rate  $\sim$  30 fold compared to spontaneous refolding (Figure 24 A and B). The rate of refolding by TF233 was  $\sim$  10 fold slower compared to WT TF (Figure 24 A and B), indicating its markedly reduced PPIase activity. TF320 was as active as WT TF in the refolding reaction, suggesting that the presence of the *pBpa per se* does not hinder its PPIase activity (Figure 24 A).

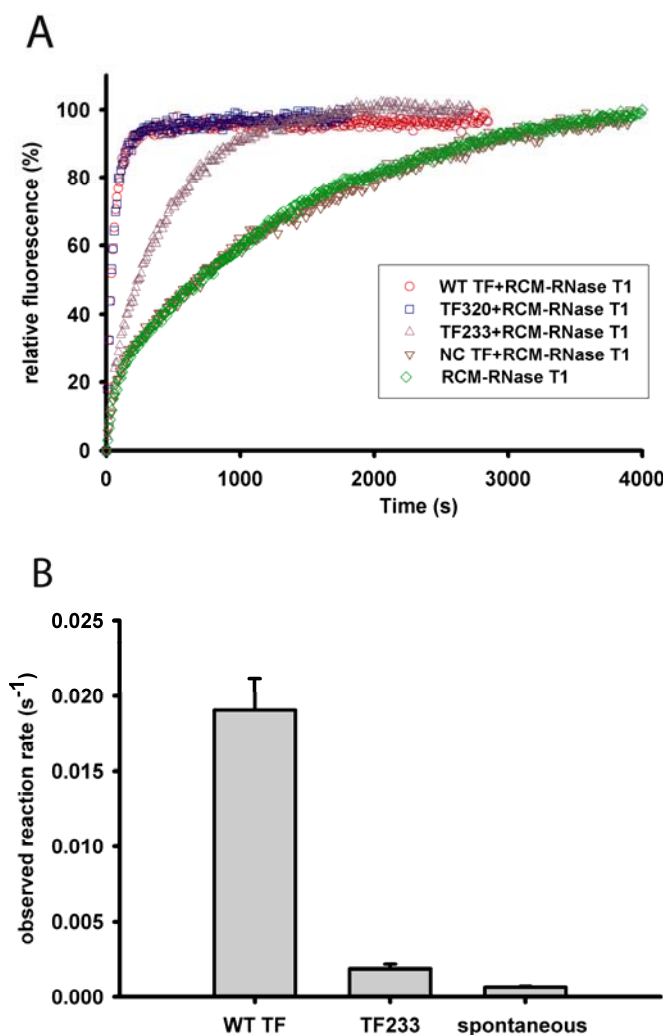


**Figure 24: Refolding of RCM-RNase T1**

(A). Refolding kinetics of 1  $\mu$ M RCM-RNase T1 in 2.0 M NaCl, 0.1 M Tris-HCl pH 8.0 and 1  $\mu$ M WT TF, TF233, TF320, NC TF or in the absence of TF. The refolding was carried out at 15  $^{\circ}$ C. The change in fluorescence at 320 nm was monitored after excitation at 268 nm. (B). Representation of the rates of RCM-RNase T1 refolding in the presence of TF variants.

#### IV.1.3 Identification of the TF dimer interface by photocrosslinking

Non-ribosome bound TF forms dimers with the  $k_D$  of  $\sim 2$   $\mu$ M but only the monomeric form binds to the ribosome (Patzelt et al., 2002). The monomer-dimer equilibrium follows rapid kinetics with a  $t_{1/2}$  value of  $\sim 1$  s, as determined by intermolecular FRET (Kaiser et al., 2006). In the same study it was shown that the TF dimer

equilibrium is shifted to the monomer upon addition of ribosomes. Model building based on inter-molecular FRET data indicated that the substrate binding site of TF may be buried in the dimeric form suggesting the inability of dimeric TF to bind to the ribosome associated nascent chains (Kaiser et al., 2006).

Photocrosslinking of *pBpa*-TF was performed with the aim of examining the positions in TF that are at the dimer interface. *pBpa*-TF variants at a final concentration of 5  $\mu$ M, favoring dimer formation, were exposed to UV light to induce crosslinks between the labeled proteins and their dimer partner.

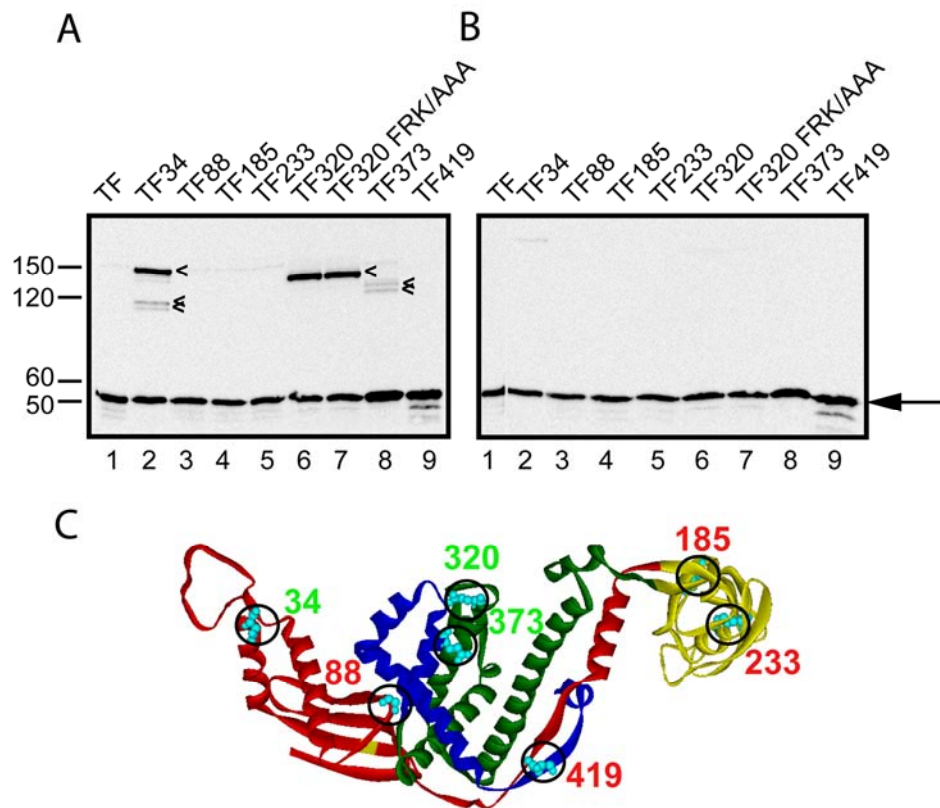


**Figure 25: Identification of TF dimer interface**

*pBpa*-TF at a final concentration of 5  $\mu$ M with the sites labeled as indicated were crosslinked with UV. Samples were subjected to western blotting against the C-terminal Myc tag. (A). Samples crosslinked under UV light for 15 min. (B). Samples not irradiated. (C). TF domain structure colored as in Figure 12 with the probe positions indicated. Residues marked in green indicate photoadduct formation and residues in red indicate sites that did not result in photoadduct formation.

Light and probe-dependent crosslinks appeared with positions 34, 320 and 373 in the N- and C-terminal domains (Figure 25 A, lanes 2, 6 and 8). Inter-molecular crosslinks with position 320 appeared also in the FRK/AAA mutant (Figure 25 A, lane 7). No detectable crosslinks were observed with positions 88, 233, 185 or 419. Two photoadducts appeared with TF34. This could be due to the flexibility of this region that might be adjacent to different sites of its dimer partner. As a result, dimers crosslinked at different sites would migrate with different mobilities on SDS-PAGE. Interestingly some of the sites involved in the dimer interface were also the sites which crosslinked to the nascent chains (TF34, TF320 and TF373 (Figures 19 and 20)). The above observation confirms that the substrate binding site of at least one subunit in the dimer is at the dimer interface.

In summary, the crosslinking experiments revealed that all the three domains of TF were in close proximity to luciferase nascent chains during translation. All the nascent chains tested interacted with the N- and the C-terminal domains while the PPIase domain displayed length dependent interactions. Luc nascent chains as short as 60 residues crosslinked to the PPIase domain.  $\alpha$ -Syn nascent chains, which are less hydrophobic than Luc crosslinked less efficiently to the PPIase domain compared to the N- and the C-terminal domains. The phenomenon of both length and hydrophobicity dependent interactions of PPIase domain with the nascent chains might be because it acts as a secondary site for binding nascent chains dependent on their conformation and hydrophobicity. The interaction of PPIase domain with the nascent chains was also independent of the PPIase activity. The substrate binding-site of at least one subunit in the dimer was found to be at the dimer interface based on crosslinking experiments. This explains the inability of the dimeric TF to interact with the ribosome-nascent chain complexes. The burial of substrate binding sites in the dimeric TF could be also a mechanism by which TF do not interact with other cellular proteins and as a result, confined as a ribosome-associated chaperone.

## IV.2 Trigger factor-nascent chain interactions monitored by real-time fluorescence measurements

As mentioned earlier, TF interactions with the ribosomes have been extensively studied and TF was shown to dissociate from the ribosomes with a  $t_{1/2}$  value of  $\sim 10$ - $12$  s. Data from intra-molecular FRET experiments showed that TF undergoes a conformational change upon binding to the ribosomes and this conformational change is stabilized by the presence of a nascent chain. The  $t_{1/2}$  value of the conformational relaxation from this state upon dissociation of TF from the ribosome was found to be dependent on the presence of hydrophobic amino acid residues in the nascent chains and was as high as  $\sim 35$  s. This phenomenon suggested prolonged interaction of TF with nascent chains (Kaiser et al., 2006) but, a direct experimental set-up to address TF interactions and dissociation from the nascent chains was still lacking. Hence in this study, a fluorescence-based approach to examine TF-nascent chain interactions directly and in real-time was employed. Fluorescence spectroscopy can be used to monitor biomolecular interactions in real-time by recording time-dependent changes in fluorescence signals and this is possible during the course of a translation reaction (Kaiser et al., 2006). To attain this, TF must be labeled with a fluorescent probe that has the ability to alter its fluorescence intensity in a hydrophobic environment characteristic of a non-native, nascent polypeptide. *N*-((2-(iodoacetoxy)ethyl)-*N*-methyl)amino-7-nitrobenz-2-oxa-1,3-diazole, an ester derivative of IANBD (NBD) was utilized for this purpose. NBD as a fluorescent probe is highly sensitive to changes in the environment of the fluorophore. It has been successfully used in previous studies mostly involving trafficking of proteins across biomembranes, because the fluorescence intensity of NBD increases appreciably when it encounters a more hydrophobic environment (Flanagan et al., 2003; Ramachandran et al., 2002; Ramachandran and Schmid, 2008). Initially, position 326 in arm 1 of the C-terminal domain of TF was chosen as a site for NBD (TF326-NBD) incorporation, because in previous crosslinking experiments *p*Bpa-TF incorporated in the arm 1 (TF320) yielded photoadducts with the nascent chains tested (Figure 20).

Luciferase (Luc) was used as a substrate for TF326-NBD to monitor TF-nascent chain interactions in real-time, as previously described in Section IV.1.2 Various cysteine mutants of TF were purified as mentioned earlier (see Materials and Methods). NBD was coupled to the single cysteine residue in TF. The E326C mutation was also introduced in the TF FRK/AAA version to serve as a control for the ribosome-dependence of TF-nascent chain interactions.

## **IV.2.1 TF interactions with RNCs**

### **IV.2.1.1 Characterization of TF labeled with NBD**

TF326-NBD was chosen specifically to monitor TF-nascent chain interactions. To confirm that the presence of the NBD moiety at position 326 does not alter its fluorescence intensity upon interaction with the ribosomes, 1  $\mu\text{M}$  of TF326-NBD was incubated with 1  $\mu\text{M}$  of purified ribosomes and emission scans were recorded. TF326-NBD showed no detectable changes in the emission maxima in the presence of ribosomes, indicating that NBD coupled at position 326 does not monitor TF's interaction with the ribosomes during non-translating conditions (Figure 26 B). As a positive control, 1  $\mu\text{M}$  TFB (TF R14C BADAN) was incubated with 1  $\mu\text{M}$  ribosomes to report TF binding to the ribosomes (Maier et al., 2003). The fluorescence of TFB decreases in the presence of ribosomes, indicative of ribosome binding (Figure 26 A).



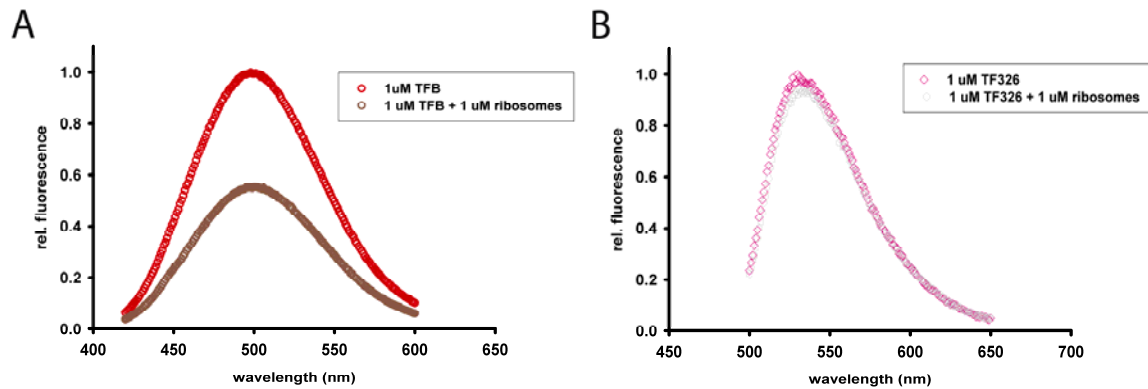


**Figure 26: Fluorescence emission spectra of TF R14C BADAN (TFB), TF326-NBD in the presence of ribosomes**

The labeled proteins were incubated with ribosomes for 10 min at 30 °C to attain equilibrium. Emission spectra of 1  $\mu$ M of TFB (A) or TF326-NBD (B) were recorded alone or in the presence of 1  $\mu$ M ribosomes at 30 °C. TFB was excited at 397 nm and TF326-NBD was excited at 472 nm. The fluorescence emission of the labeled proteins in the absence of ribosomes was normalized to one.

Additionally co-sedimentation analyses of the labeled proteins with the purified ribosomes were performed to demonstrate their ribosome binding (Figure 27). Stoichiometric amounts of the labeled proteins were observed in the pellet fraction when present along with the ribosomes (Figure 27 A, lanes 7 to 10, B, lanes 1 to 6), indicative of ribosome binding compared to when the proteins were present in the absence of ribosomes (Figure 27 A, lanes 1 to 4, C, 1 to 6).

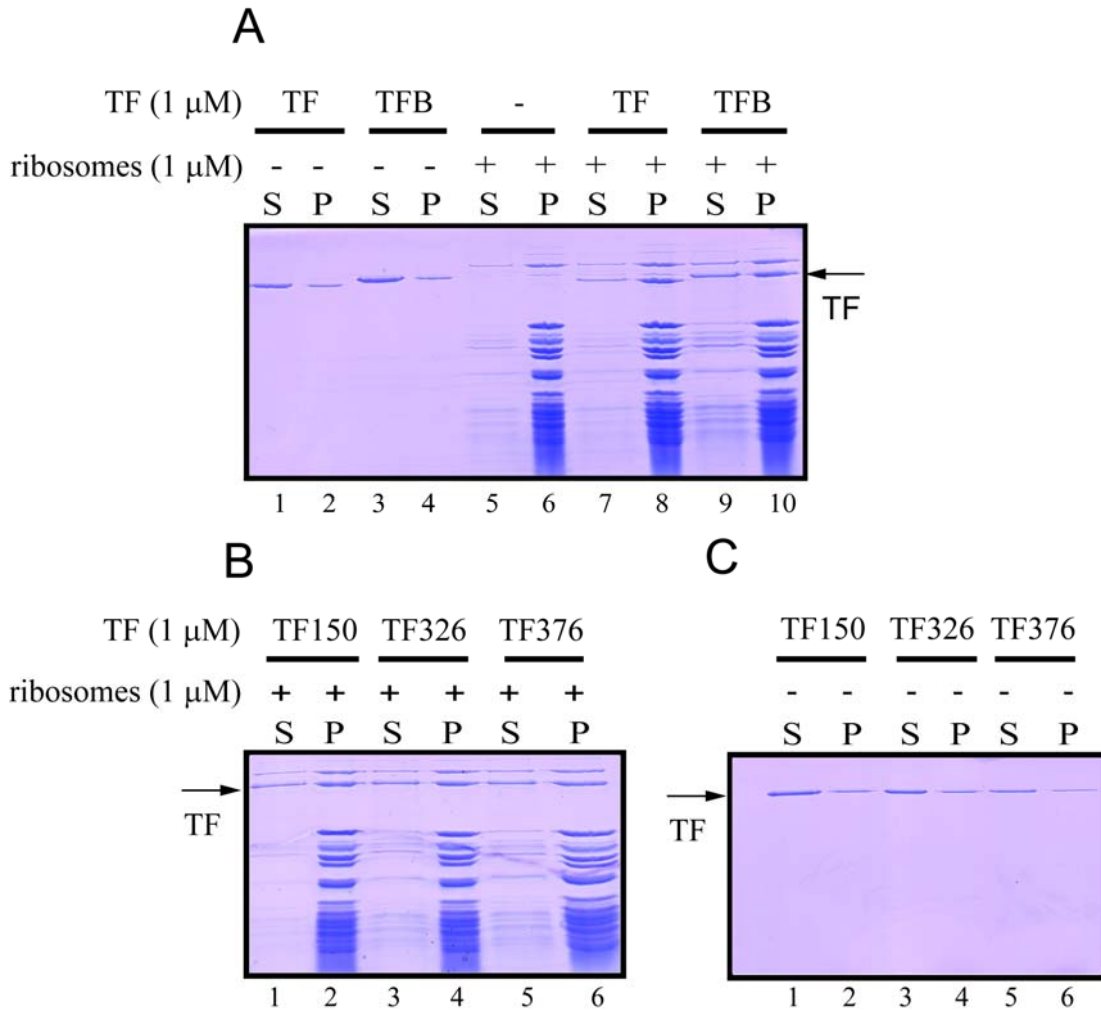


**Figure 27: Co-sedimentation of WT TF and labeled TF proteins along with non-translating ribosomes**

1  $\mu$ M of WT TF or labeled TF proteins as indicated were incubated with equimolar concentrations of ribosomes for 10 min at 30 °C. The ribosome associated pellet fraction (P) was separated from the non-ribosome associated fraction (S) by centrifugation at 100,000 rpm for 45 min through a 0.5 M sucrose cushion and loaded on SDS-PAGE, (A), lanes 7 to 10 and (B), lanes 3 and 4. As a control, the same procedure was performed in the absence of ribosomes, (A), lanes 1 to 4 and (C), lanes 3 and 4. The black arrows indicate the position of TF. Similar co-sedimentation analyses were performed with other TFNBD proteins and shown in this figure, which will be discussed in detail later in this section.

To confirm that the presence of the NBD moiety does not change TF's ability to chaperone nascent chains, translation of Luc was carried out in the presence of TF326-NBD. Luc was translated in the presence of  $^{35}\text{S}$ -methionine and either 5  $\mu\text{M}$  WT TF or 5  $\mu\text{M}$  TF326-NBD. The activity of Luc synthesized was measured after 50 min of translation by chemiluminescence in the luminometer. Specific activity of Luc was calculated as mentioned earlier (see Materials and Methods) (Figure 28).

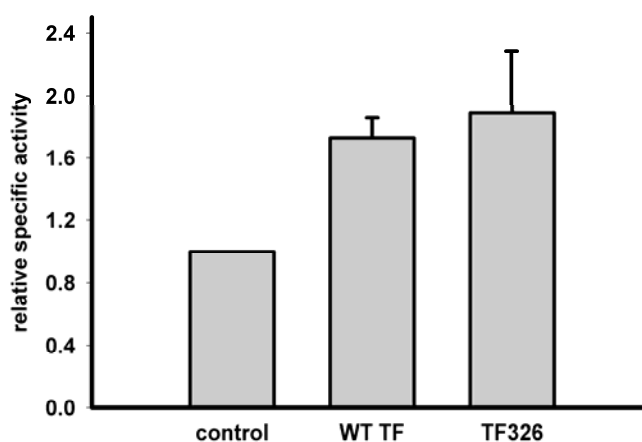


**Figure 28: Chaperone activity of TF326-NBD**

Luc was translated in the PURE system in the presence of  $^{35}\text{S}$ -methionine and either 5  $\mu\text{M}$  of WT TF or TF326-NBD. Luc activity was measured in the luminometer after  $\sim 50$  min of translation and the amount of Luc protein synthesized was quantified by autoradiography. The specific activity was calculated by dividing the Luc activity by the amount of protein made. The Luc specific activity in a control reaction without any added TF was to 1.

As seen in Figure 28, the presence of TF326-NBD increased the specific activity of Luc by a factor of  $\sim 2$  fold, which is similar to the effect of WT TF as reported earlier (Agashe et al., 2004). This confirms that TF326-NBD is as active as WT TF in chaperoning nascent chains.

#### IV.2.1.2 Recruitment of TF to RNCs

To monitor the kinetics of TF interactions with RNCs, translation of Luc nascent chains was performed in the PURE system in the presence of 250 nM TF326-NBD. In all experiments involving NBD, the samples were excited at 472 nm and emission was

monitored at 536 nm. The PURE system was reconstituted with TF326-NBD in a prewarmed cuvette at 30 °C and incubated for ~ 2-3 min until a stable fluorescence signal was observed. Translation was initiated by the addition of DNA at a final concentration of 10 ng/μl and TF326-NBD emission at 536 nm was followed over time as translation proceeded. In a parallel reaction, translation was carried out in the presence of <sup>35</sup>S-methionine and aliquots were taken at regular intervals for SDS-PAGE and subsequent autoradiography to document the profile of the nascent chain synthesis (Figure 29, bottom panel). To document that the recruitment of TF to translating ribosomes is indeed due to translation, a similar experiment was performed in the absence of DNA.

To confirm that the interaction of TF326-NBD with the RNCs is dependent on TF binding to the ribosomes, experiments were performed with the ribosome binding deficient version of TF. TF FRK/AAA326 was added to the PURE system and translation was initiated with the addition of Luc DNA. The emission of TF FRK/AAA326 was likewise monitored as translation proceeded (Figure 29 top panel).

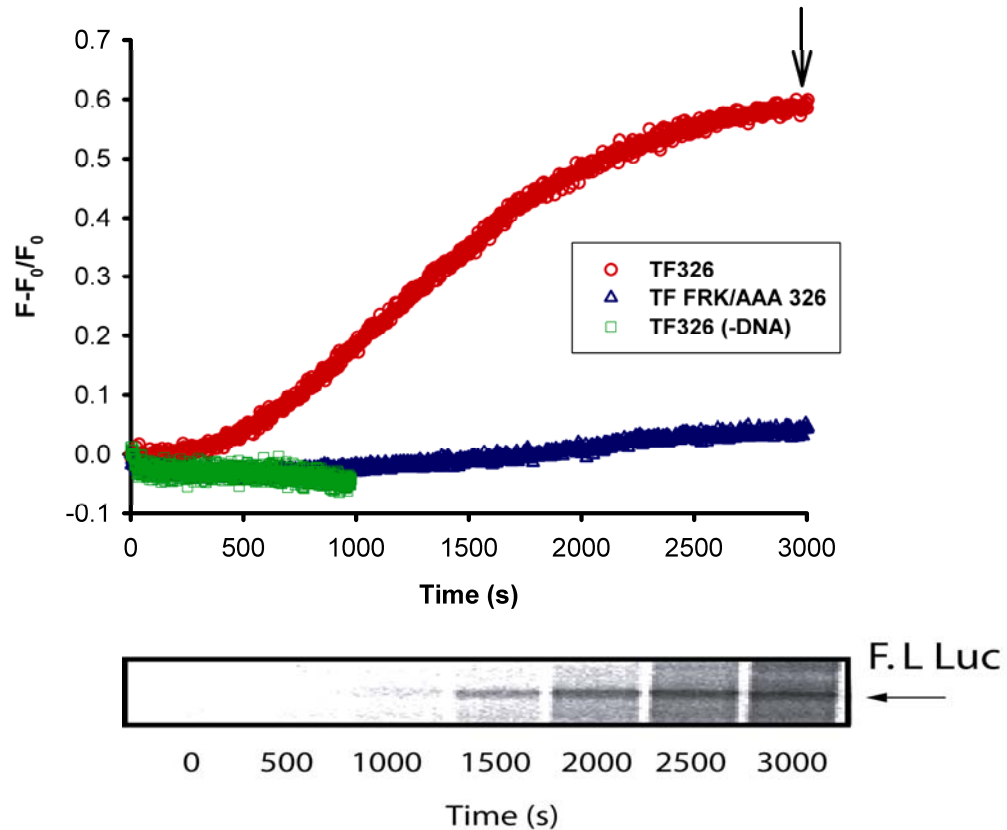


**Figure 29: TF326-NBD recruitment to Luc-RNCs monitored in real-time**

Top panel-The PURE system was supplemented with either 250 nM TF326-NBD (red) or TF FRK/AAA 326 (blue). Translation was initiated with the addition of Luc DNA and the fluorescence of TF326-NBD was monitored in real-time. The fluorescence change of TF326-NBD was also monitored in the absence of DNA (green). The change in fluorescence divided by the initial fluorescence ( $F-F_0/F_0$ ) was plotted against time. Bottom panel-the production of Luc protein was documented by  $^{35}\text{S}$ -methionine incorporation and autoradiography of the band corresponding to the full-length (F.L) protein synthesized. Saturation of TF326-NBD fluorescence occurred when protein synthesis was taking place at a steady state.

From the above experiments, it is evident that the observed fluorescence signal change of TF326-NBD over time is dependent on ribosome binding and also on translation (Figure 29). As mentioned earlier, NBD's fluorescence intensity increases in a more hydrophobic environment. Hence, the increase in fluorescence intensity of TF326-NBD during translation of Luc nascent chains would be due to the interaction of TF326-NBD with the more hydrophobic Luc nascent chains. To confirm this, interaction of

TF326-NBD with nascent chains that were less hydrophobic than Luc was tested. For this purpose, S7, the bacterial small ribosomal protein, and  $\alpha$ -Syn were chosen. Translation of S7 and  $\alpha$ -Syn nascent chains and fluorescence measurements were performed as below (Figure 30 A).

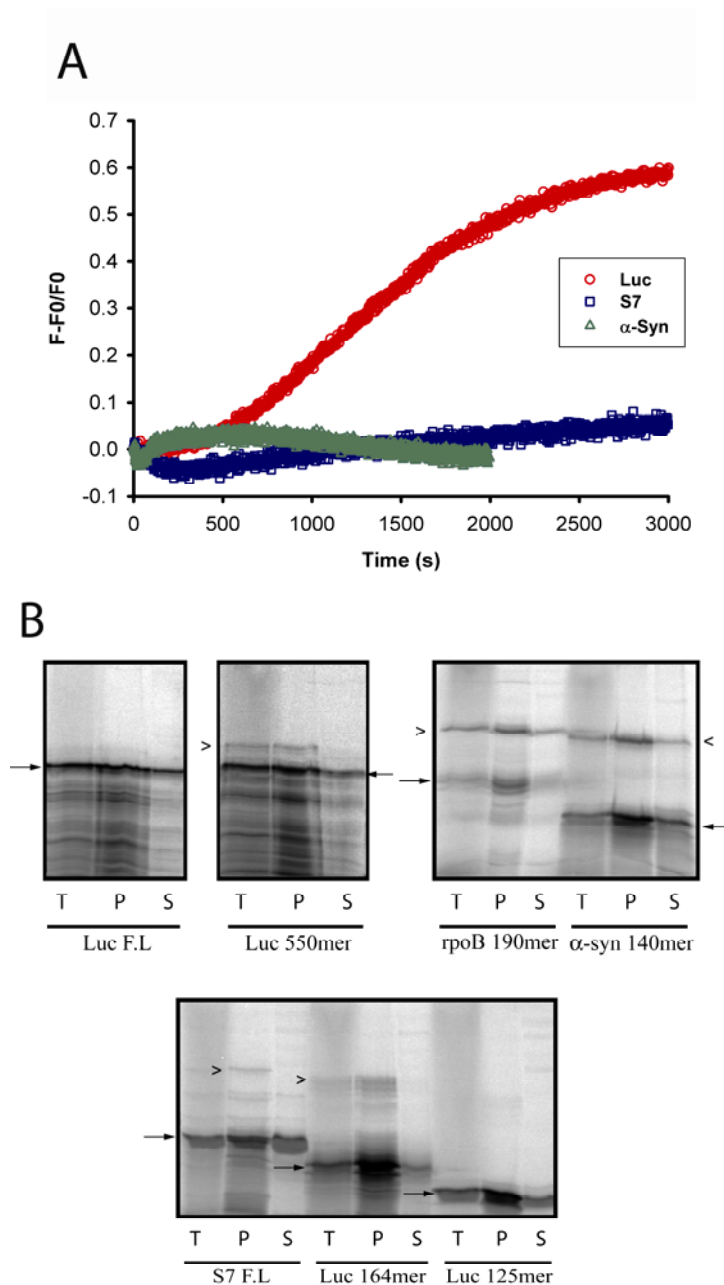


**Figure 30: TF326-NBD recruitment to S7-RNCs and  $\alpha$ -Syn-RNCs and translation of the nascent chain constructs**

(A). The PURE system was reconstituted with TF326-NBD and translation was initiated with the addition of either Luc (red), S7 (blue) or  $\alpha$ -Syn (green) DNA. The fluorescence of TF326-NBD was monitored in real-time as translation proceeded. The fluorescence of TF326-NBD reached a  $F-F_0/F_0$  value of  $\sim 0.6$  for Luc nascent chains and a value of  $< 0.05$  for S7 and  $\alpha$ -Syn nascent chains. (B). Translation of Luc, S7 and  $\alpha$ -Syn nascent chains in the presence of  $^{35}\text{S}$ -methionine in the PURE system. Translation was initiated by the addition of

either Luc, S7 or  $\alpha$ -Syn DNA in the reconstituted PURE system and proceeded for  $\sim 50$  min. The total (T) fraction was subjected to ultracentrifugation to separate the ribosome-associated pellet (P) and the supernatant fraction (S) (see Materials and Methods). Only 1/4<sup>th</sup> of the reaction was loaded representing the “Total” while the rest of the reaction was loaded for both the “Pellet” and “Supernatant” fractions. Black arrows indicate hydrolyzed nascent chains and open arrows indicate peptidyl-tRNA. Translation profiles of other nascent chains- Luc 550mer, Luc 164mer, Luc 125mer and rpoB 190mer used elsewhere in the study are also shown.

As shown in Figure 30 A, during translation of S7 or  $\alpha$ -Syn nascent chains, TF326-NBD did not undergo an appreciable fluorescence change compared to Luc nascent chains, although S7 and  $\alpha$ -Syn chains were translated as efficiently as Luc chains under the experimental conditions (Figure 30 B). Hydrophobicity analysis of S7 and  $\alpha$ -Syn proteins revealed that both lack strong hydrophobic patches present in Luc nascent chains, which are predicted to mediate TF’s interaction with nascent chains (Figure 31 A, 22 B and C) (Kaiser et al., 2006). The lack of these hydrophobic patches would explain the reduced interaction of TF326-NBD with S7 and  $\alpha$ -Syn.



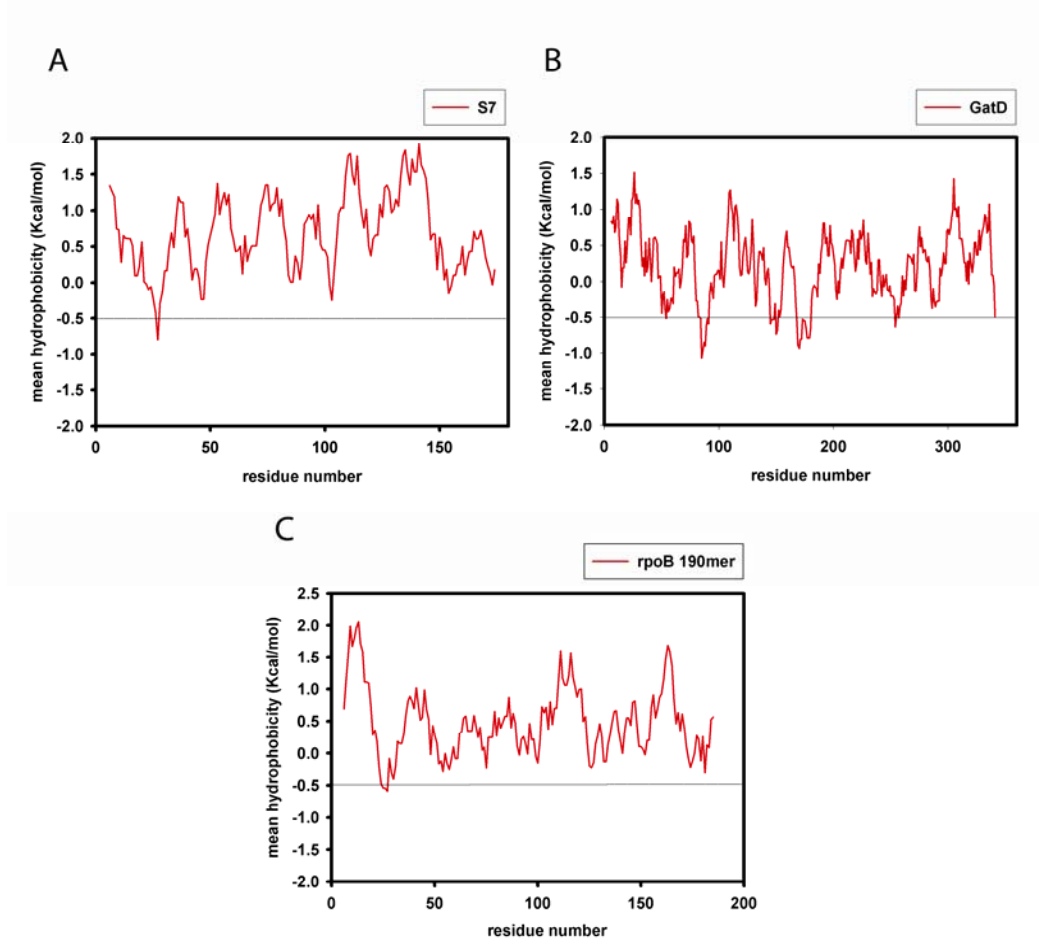


**Figure 31: Hydrophobicity analysis of S7 and other nascent chain substrates**

(A). The mean hydrophobicity of S7 using a window of 11 residues was calculated as described in Fig 22. S7 lacks significant hydrophobic regions predicted to mediate its interaction with TF which are otherwise present in Luc. Hydrophobicity analysis of other nascent chain substrates which appear later in the study-GatD (B) and rpoB 190mer (C) were also performed in a similar manner.

#### IV.2.1.3 Recruitment of additional TF molecules towards elongating nascent chains

It has been suggested that additional TF molecules can be recruited to RNCs during translation dependent on the size and hydrophobicity of the nascent chains (Agashe et al., 2004). The recruitment of multiple TF molecules to elongating chains could be a mechanism by which TF prevents nascent chain aggregation and misfolding in

a highly crowded environment. Luc is a multidomain protein, which was predicted to recruit additional TF molecules to the ribosomes during its translation (Agashe et al., 2004). In Luc there are three hydrophobic patches above the threshold level that might mediate interaction with TF (Figure 22B). The first hydrophobic patch is positioned in between 90-100 residues from the N-terminus followed by the second patch between 230-240 residues and the last between 280-290 residues (Figure 22 B). The presence of these multiple hydrophobic patches allowed us to investigate the recruitment of additional TF molecules during translation of Luc nascent chains. Luc chains of 77, 164, 520, 550 or full-length were synthesized and the interaction of TF326-NBD with these nascent chains was recorded (Figure 32).

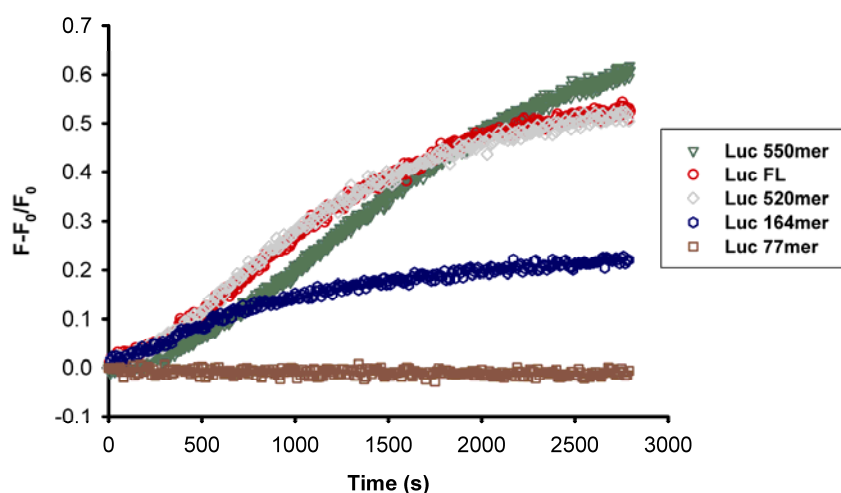


**Figure 32: TF recruitment during Luc nascent chain elongation**

The PURE system was reconstituted with TF326-NBD and translation was initiated with the addition of Luc 77mer (brown), Luc 164mer (blue), Luc 520mer (grey), Luc 550mer (green) or Luc F.L DNA (red). The change in TF326-NBD fluorescence was monitored as translation proceeded. TF326-NBD when present during translation of Luc 77mer showed no detectable fluorescence change and in the case of Luc 164mer showed an intermediate change. During translation of Luc 520mer, 550mer or F.L, TF326-NBD underwent a similar fluorescence change greater than that observed with Luc 164mer.

As shown in Figure 32, TF326-NBD when present during translation of Luc 77mer showed a negligible fluorescence change. This would be consistent with the absence of hydrophobic patches in the Luc 77mer. An intermediate fluorescence change corresponding to a  $F-F_0/F_0$  of  $\sim 0.22$  was observed after translation of Luc 164mer, which could be due to the exposure of the first hydrophobic patch outside the ribosomal exit tunnel. Translation of either Luc 520mer, Luc 550mer or F.L nascent chains resulted in a much greater fluorescence change with a  $F-F_0/F_0$  of  $\sim 0.5-0.6$  concomitant with the exposure of all the hydrophobic patches in the full-length protein outside the ribosomal exit tunnel.

#### **IV.2.2 Kinetics of TF dissociation from RNCs**

Since TF326-NBD offered the advantage of monitoring TF's interaction with the nascent chains in real-time, the kinetics of its dissociation from the nascent chains was next investigated. The dissociation of TF326-NBD was followed upon addition of excess unlabeled WT TF at a final concentration of 20  $\mu\text{M}$  once saturation of TF326-NBD binding to the RNCs had occurred. After the addition of unlabeled TF, the  $t_{1/2}$  value at which TF326-NBD dissociated from the RNCs was calculated from the rate of the dissociation reaction (Equations 3 and 4, see Materials and Methods). To confirm that the displacement of TF326-NBD with the unlabeled TF is dependent on ribosome binding, a similar competition experiment was performed with the addition of excess unlabeled FRK/AAA mutant of TF (Figure 33 A).

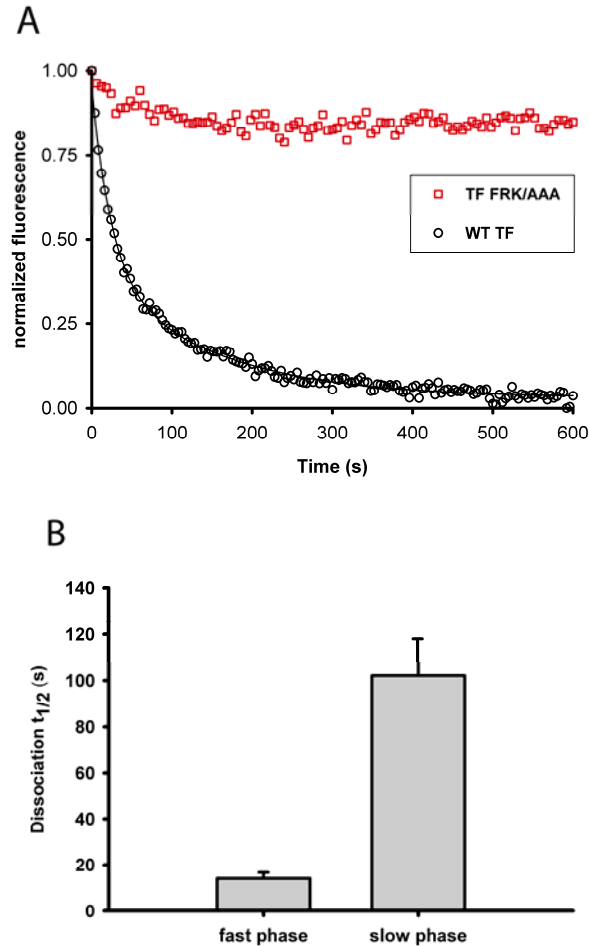


**Figure 33: Dissociation of TF326-NBD from Luc-RNCs with excess unlabeled TF**

(A). Excess unlabeled TF was added to the PURE system translating Luc nascent chains in the presence of TF326-NBD after saturation of its fluorescence had occurred (black). TF326-NBD dissociation from the nascent chains was best fitted to a five parameter double exponential function (black line). No remarkable competition was observed with TF FRK/AAA as the competitor (red). The change in amplitude of TF326-NBD fluorescence was normalized to unity. (B).  $t_{1/2}$  values for TF326-NBD dissociation from Luc-RNCs.

The best fit of the data from the dissociation experiments was to a double exponential function and not to a single exponential function. This suggests the presence of two processes occurring during the dissociation reaction. The first phase is fast with a

$t_{1/2}$  value of  $14 \pm 2$  s and the second phase is slow with a  $t_{1/2}$  value of  $102 \pm 16$  s (Figure 33 B).

To investigate nascent chain dependent changes in the dissociation process, GatD was used as another substrate of TF as it has hydrophobic patches shown to mediate TF-nascent chain interactions (Figure 31 B). The relaxation of TF to its compact state, presumably reflecting nascent chain dissociation, was shown to occur with a  $t_{1/2}$  value of  $\sim 26$  s from GatD-RNCs (Kaiser et al., 2006). TF326-NBD interaction with GatD-RNCs was monitored in real-time and its dissociation from GatD-RNCs was carried out (Figure 34).

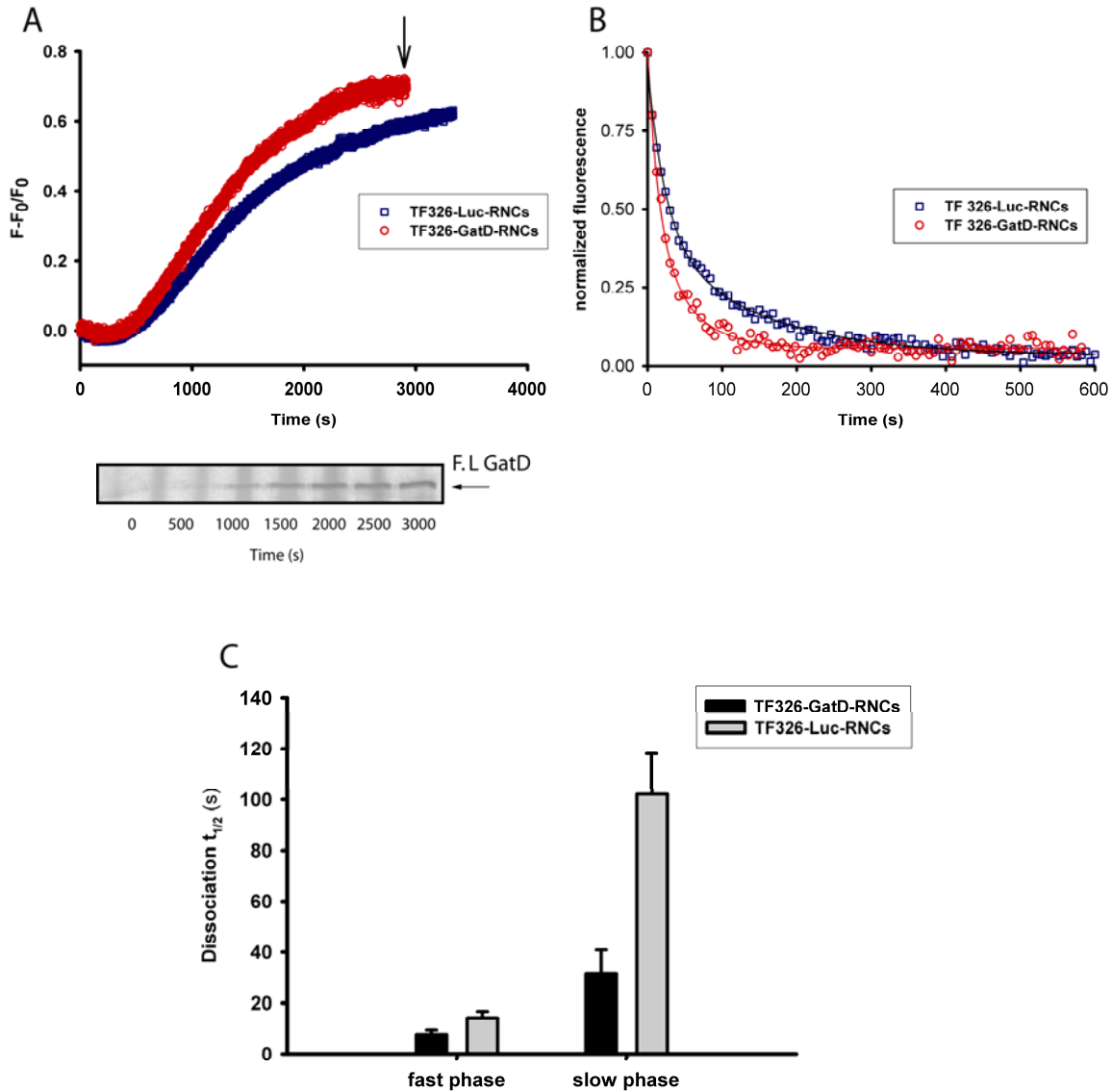


**Figure 34: Dissociation of TF326-NBD from Luc- and GatD-RNCs with excess unlabeled TF**

(A). Excess unlabeled TF was added to the PURE system, which had translated either Luc (blue) or GatD (red) nascent chains in the presence of TF326-NBD once its fluorescence saturation has occurred. (B). As observed with Luc-RNCs, TF326-NBD dissociation from GatD-RNCs was best fitted to a double exponential function (blue and red lines respectively). The change in amplitude was normalized to unity. (C).  $t_{1/2}$  values for TF326-NBD dissociation from GatD-RNCs (black bars) and Luc-RNCs (grey bars).

TF326-NBD underwent a similar fluorescence change during translation of GatD nascent chains as was observed in the case of Luc nascent chains (Figure 34 A). The dissociation of TF326-NBD from GatD-RNCs also followed biexponential kinetics as observed with Luc-RNCs (Figure 34 B). However, the kinetic phases of dissociation obtained during TF326-NBD dissociation from GatD-RNCs were faster than those obtained from Luc-RNCs. Both the fast phase ( $14 \pm 2$  s and  $7.5 \pm 1.5$  s from Luc and GatD-RNCs respectively) and the slow phase ( $102 \pm 16$  s and  $31.5 \pm 9$  s from Luc and GatD-RNCs respectively) varied considerably between the Luc and GatD-RNCs (Figure 34 C).

During the dissociation of TF326-NBD from both Luc- and GatD-RNCs, the amplitudes corresponding to both the phases were similar to each other. The amplitudes corresponding to both the fast and slow phases during the dissociation of TF326-NBD from Luc-RNCs were  $47.3 \pm 6.3$  % and  $42.5 \pm 4$  % respectively. In the case of TF326-NBD dissociation from GatD-RNCs the amplitudes for the fast and slow phases were  $46.6 \pm 9$  % and  $42.3 \pm 8.5$  % respectively (Figure 36).

To gain a better understanding regarding the biphasic nature of TF dissociation from these nascent chains, an additional site in TF was chosen for labeling with NBD. S376 in the tip of arm 2 was utilized for monitoring its interaction with the nascent chains (TF376-NBD). Similar competition experiments were performed to study the dissociation of TF376-NBD from Luc- and GatD-RNCs.

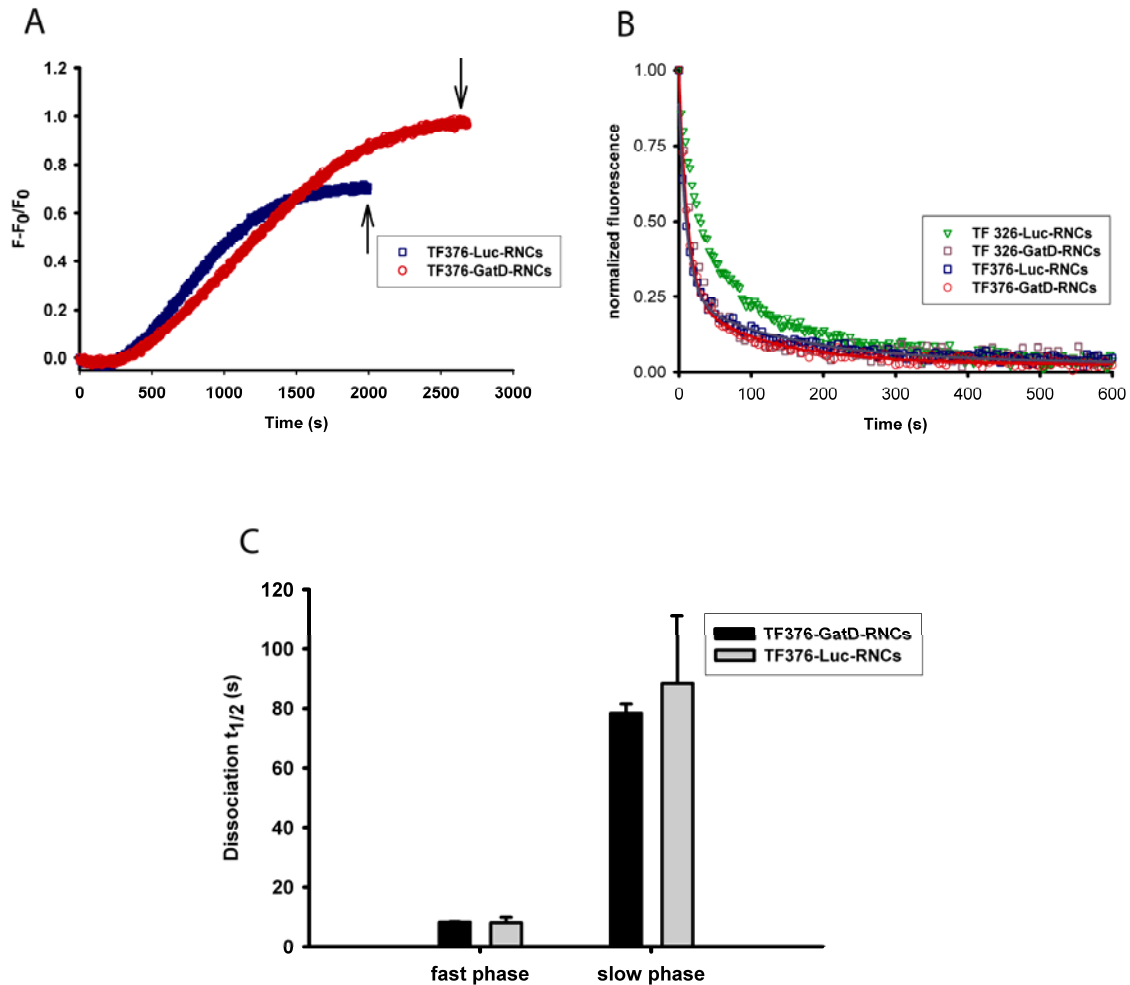


**Figure 35: Dissociation of TF376-NBD from Luc- and GatD-RNCs with excess unlabeled TF**

(A). Excess unlabeled TF was added to the PURE system, which had translated either Luc (blue) or GatD nascent chains (red) in the presence of TF376-NBD. (B). As observed with TF326-NBD, dissociation of TF376-NBD from both Luc- and GatD-RNCs had a biphasic nature (blue and red lines respectively). The change in amplitude was normalized to unity. (C).  $t_{1/2}$  values for TF376-NBD dissociation from GatD-RNCs (black bars) and Luc-RNCs (grey bars).

TF376-NBD showed a fluorescence change corresponding to  $F-F_0/F_0$  of 0.7 and 1.0 during translation of Luc and GatD nascent chains, respectively (Figure 35 A). The dissociation of TF376-NBD from Luc- and GatD-RNCs also followed biexponential



kinetics as observed with TF326-NBD (Figure 35 B). Both the first  $t_{1/2}$  value ( $8 \pm 2$  s and  $8.2 \pm 0.15$  s from Luc- and GatD-RNCs respectively) and the second  $t_{1/2}$  value ( $88.5 \pm 22.5$  s and  $78.5 \pm 3$  s from Luc- and GatD-RNCs respectively) did not vary considerably during TF376-NBD dissociation from both the RNCs (Figure 35 C). This was different from what was observed with TF326-NBD for which both the kinetics phases varied between the Luc and GatD chains.

The striking difference between TF326-NBD and TF376-NBD is the rate of the slow phase during their dissociation from GatD-RNCs which occurred with a  $t_{1/2}$  value of  $31.5 \pm 9$  s and  $78.5 \pm 3$  s respectively. The fractional amplitudes which correspond to this phase were  $42.3 \pm 8.5$  % and  $23.7 \pm 1.2$  % respectively. The reason for the difference in the rate of the slow phase between TF326-NBD and TF376-NBD dissociation from GatD-RNCs could be because an increasing population of TF376-NBD dissociated from GatD-RNCs faster ( $71.5 \pm 1.5$  %) compared to TF326-NBD ( $46.6 \pm 9$  %) (Figure 36).

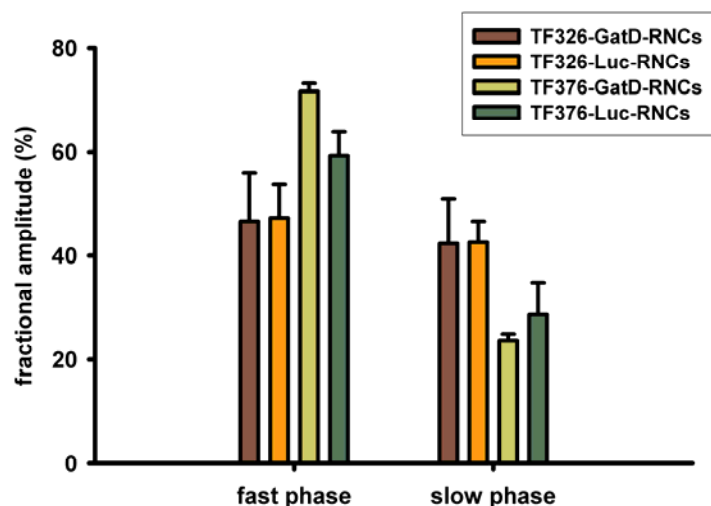


**Figure 36: Fractional amplitudes corresponding to both the  $t_{1/2}$  values during dissociation of TF326-NBD or TF376-NBD from Luc- and GatD-RNCs**

The fractional amplitudes corresponding to both the fast and the slow phases during the dissociation of TF326-NBD from GatD-RNCs and Luc-RNCs (brown and orange respectively) and TF376-NBD from GatD-RNCs and Luc-RNCs (light green and dark green respectively).

Two possible explanations may be offered for the biphasic nature of the dissociation reactions. The first might be that one of the rates represents TF326-NBD or TF376-NBD dissociating from regions other than the nascent chain. Inspection of the structural model of TF by Ferbitz and colleagues (Figure 8) (Ferbitz et al., 2004), suggests that the closest distance from the ribosomal surface to the tip of both the arms (where the NBD is attached) is  $\sim 10 \text{ \AA}$ , but a direct contact between the arms and the ribosome was not observed. An interaction of the arms with the ribosomal surface due to the flexible nature of TF (Yao et al., 2008) during translation might also cause a fluorescence change, which could give rise to one of the processes observed during the dissociation of TF326-NBD and TF376-NBD from the nascent chains. Currently, the first possibility is explored before the second.

To confirm this hypothesis, translation of the rpoB 190mer nascent chains was performed in the presence of TFB, TF326-NBD or TF376-NBD. The rpoB 190mer nascent chains lack the hydrophobic patches predicted to have high affinity for TF binding compared to Luc and GatD (Figure 31 C). During translation of rpoB 190mer, TFB underwent a fluorescence change and reached a level corresponding to  $\sim 65\%$ , indicative of increased ribosome binding (Figure 37). However, TF326-NBD and TF376-NBD showed a negligible fluorescence change during rpoB 190mer translation (Figure 37), indicating their weak affinity towards rpoB 190mer nascent chains. If the initial fast phase observed during the dissociation of both TF326-NBD and TF376-NBD were due to TF release from the ribosomes, it should also be present during the translation of rpoB 190mer nascent chains as TFB was recruited to rpoB 190mer-RNCs. Since no fluorescence change of TF326-NBD and TF376-NBD was observed during the translation of rpoB 190mer nascent chains, the initial fast phase observed during their dissociation from Luc- and GatD-RNCs is unlikely to be due to their release from the ribosomes.

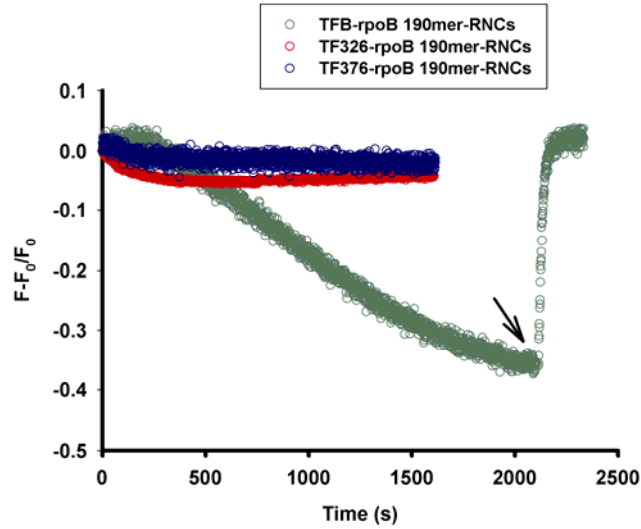


**Figure 37: Recruitment of TFB, TF326-NBD and TF376-NBD towards *rpoB* 190mer-RNCs**

Translation of *rpoB* 190mer-RNCs in the presence of TFB (green), TF326-NBD (red) or TF376-NBD (blue). TFB showed a decrease in fluorescence indicative of ribosome binding, but TF326-NBD and TF376-NBD underwent only negligible fluorescence changes. The black arrow indicates the time when unlabeled TF was added as a competitor.

The second possible explanation for the fast dissociation phase could involve the flexibility of the C-terminal domain of TF. Recent NMR measurements on the C-terminal domain of *E. coli* TF have shown that it exists in multiple conformations in solution (Yao et al., 2008) other than those observed in the crystal structure (Ferbitz et al., 2004). The biphasic nature observed during the dissociation of TF326-NBD and TF376-NBD from the nascent chains could thus be due to different conformational populations of TF bound to the nascent chain, which might dissociate at different rates.

To gain further insight into TF dissociation from the nascent chains, a position in TF other than the C-terminal domain was chosen for labeling with NBD. T150, which is at the interface between the C-terminal domain and the PPIase domain was selected for this purpose. The fluorescence intensity of TF376-NBD and TF150-NBD was not altered in the presence of ribosomes, as was observed with TF326-NBD (Figure 38 A), and also the labeled proteins also retained the chaperone activity similar to the WT TF (Figure 38 B).

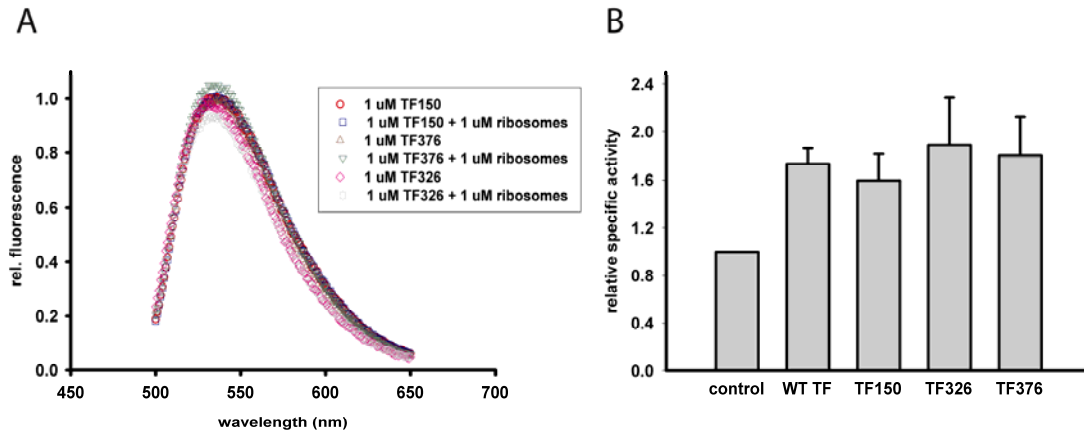


**Figure 38: Ribosome binding and chaperone activity of TF376-NBD and TF150-NBD**

(A). Emission spectra of 1  $\mu\text{M}$  of the labeled TF proteins alone or in the presence of 1  $\mu\text{M}$  ribosomes were recorded (see Materials and Methods) (B). Luc was translated in the PURE system in the presence of  $^{35}\text{S}$ -methionine and 5  $\mu\text{M}$  of WT TF, TF150-NBD, TF326-NBD or TF376-NBD and specific activity of Luc was calculated.

TF150-NBD showed a fluorescence change corresponding to an  $F-F_0/F_0$  of 0.25 during translation of Luc and GatD nascent chains (Figure 39 A). The  $F-F_0/F_0$  value observed in this case is not as high as observed with TF326-NBD and TF376-NBD. This would be consistent with the interpretation that the PPIase domain is a secondary site for nascent chain binding. Alternatively, TF150-NBD could be in a less hydrophobic environment than TF326-NBD or TF376-NBD when TF is bound to the nascent chains.

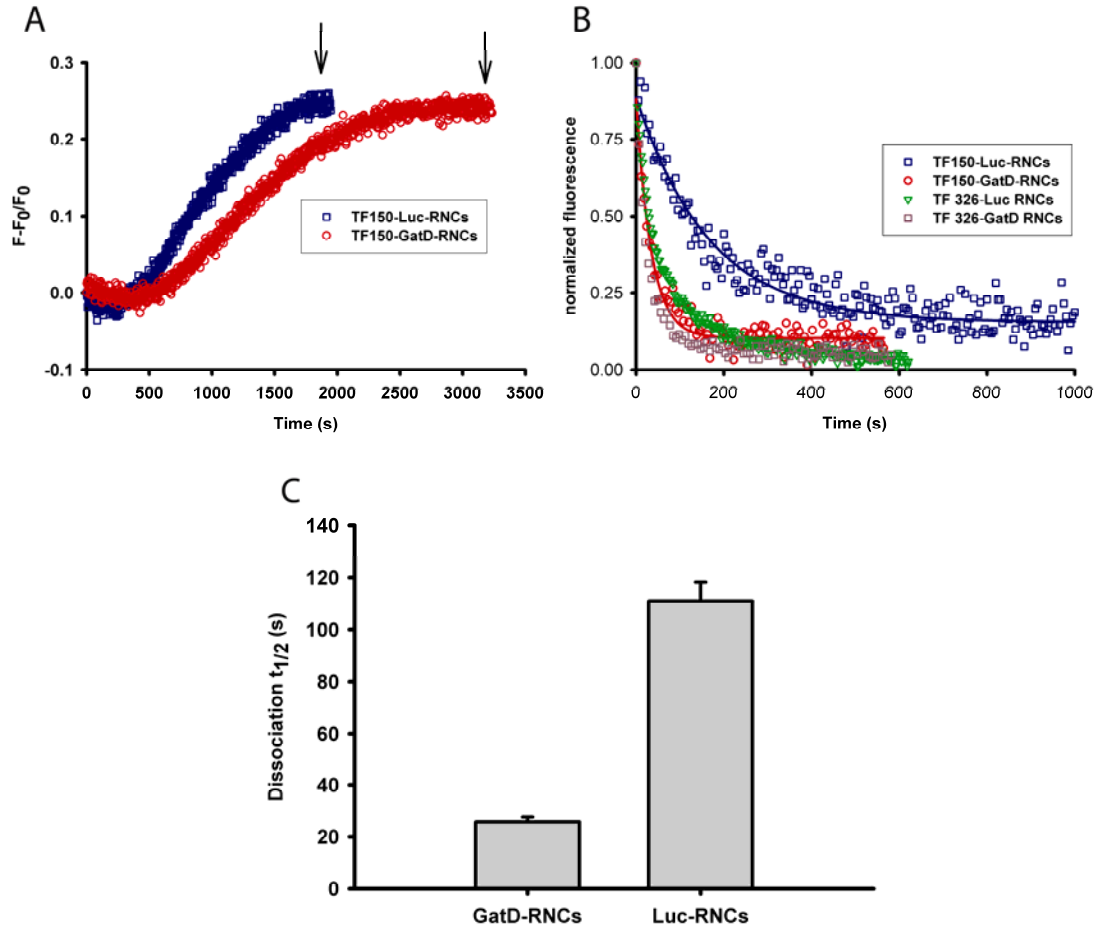


**Figure 39: Dissociation of TF150-NBD from Luc- and GatD-RNCs with excess unlabeled TF**

(A). Excess unlabeled TF was added to the PURE system, which had translated Luc (blue) or GatD (red) nascent chains in the presence of TF150-NBD after saturation of TF150-NBD fluorescence had occurred. (B). The dissociation of TF150-NBD from both Luc- and GatD-RNCs was fit to a single exponential function (blue and red lines respectively). The change in amplitude was normalized to unity. C.  $t_{1/2}$  values for TF150-NBD dissociation from GatD- and Luc-RNCs.

The dissociation of TF150-NBD from both the RNCs occurred with a single phase (Figure 39 B) corresponding to a  $t_{1/2}$  value of  $111 \pm 7$  s and  $25 \pm 2$  s from Luc- and GatD-RNCs, respectively (Figure 39 C). Thus the initial fast phase observed during the dissociation of TF326-NBD and TF376-NBD from both the RNCs is absent in the case of TF150-NBD. Since the fast phase is not observed in the case of TF150-NBD, it could be

possible that in the case of TF labeled with NBD in the C-terminal domain, the fast phase represents the dissociation of multiple conformations of TF from the nascent chain due to the flexible nature of the C-terminal domain. The  $t_{1/2}$  value of dissociation of TF150-NBD from both the RNCs, which is greater than the dissociation of TFB from these RNCs ( $t_{1/2}$  value  $14.5 \pm 0.5$  s and  $14.5 \pm 1.5$  s from Luc- and GatD-RNCs, respectively) (Figure 40 A, B), would imply that TF stays associated with the nascent chains after its dissociation from the ribosomes.

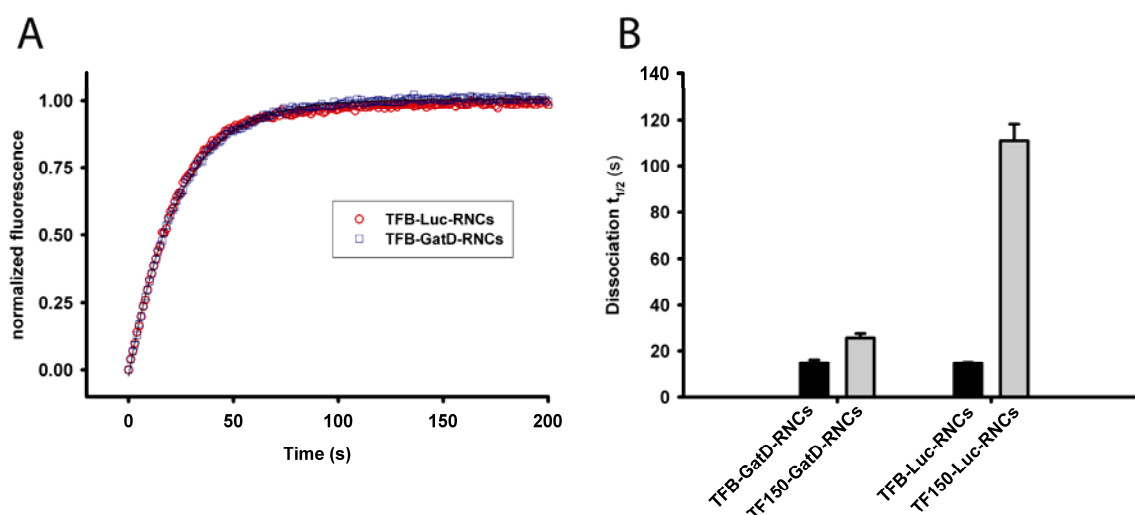


**Figure 40: Dissociation of TFB from Luc- and GatD-RNCs**

(A). Dissociation of TFB from Luc- (red) or GatD-RNCs (blue) was achieved by the addition of excess unlabeled TF to the PURE system translating either Luc or GatD nascent chains. The dissociation of TFB from Luc- and GatD-RNCs was fit to single exponential function and occurred with a  $t_{1/2}$  value of  $14.5 \pm 0.5$  s and  $14.5 \pm 1.5$  s respectively. The change in amplitude of TFB fluorescence was normalized to unity. (B). Comparison of the  $t_{1/2}$  values of TFB (black bars) and TF150-NBD dissociation (grey bars) from Luc- and GatD-RNCs.

The difference in the rate of TF150-NBD dissociation from both the RNCs could be attributed to the greater number of hydrophobic regions of Luc compared to GatD nascent chains. A higher  $t_{1/2}$  value observed in the case of Luc-RNCs could be correlated to the more hydrophobic nature of Luc than the GatD nascent chains (Figures 22 B and 31 B).

## V Discussion

During translation nascent polypeptides emerge from ribosomes in a vectorial fashion into the highly crowded environment of the cytosol in which they are prone to aggregate (Feldman and Frydman, 2000; Hartl and Hayer-Hartl, 2002; Young et al., 2004). All kingdoms of life have therefore evolved ribosome associated chaperones (Ito, 2005), which bind to and prevent aggregation of the elongating polypeptide chains. TF is such a ribosome-associated chaperone present in eubacteria that interacts with the 50S ribosomal subunit through the L23 and L29 proteins (Kramer et al., 2002). The goal of the experiments performed in this thesis was to identify the regions on TF that interact with the nascent chains. Additionally the interactions of TF with nascent chains were also studied in real-time to learn more about the mechanism of TF-assisted *de novo* folding.

Experiments to identify the domains of TF adjacent to the nascent chain as it emerges from the ribosome utilized a site-specific photocrosslinking approach with a photoactivable probe specifically attached to TF. All translation experiments were done in the reconstituted PURE system. We determined that the N-, C- and the PPIase domains of TF were all adjacent to Luc nascent chains even when the nascent chain was only 60 residues in length. The length dependence of nascent chain interactions with the domains of TF was also examined and it was observed that the PPIase domain interacted with short nascent chains and long nascent chains, but not with intermediate chain lengths tested. We propose that the PPIase domain might act as a secondary binding site. Additionally the N- and the C-terminal domains were observed to crosslink in the non-ribosome bound TF dimer.

Initial kinetic experiments to examine TF-ribosome interactions were performed in our laboratory (Kaiser et al., 2006). However, experiments to directly measure TF-nascent chain interactions had been lacking. Sites on TF were chosen for labeling with fluorescent probes in order to monitor its interaction with nascent chains, based on the observations from the photocrosslinking experiments. The association of NBD labeled TF with the nascent chains was investigated and found to be dependent on the hydrophobic regions of the nascent chain. The kinetics of TF dissociation from Luc and GatD nascent chains was examined and was found to be slower compared to the

dissociation of TF from the ribosomes. The process of dissociation from the nascent chains had two reaction phases in some cases, depending on the location of the fluorescent probe.

In the following sections the results observed during this study will be discussed in detail.

## V.1 Interaction of the domains of TF with nascent chains

In this study, all the domains of TF were shown to be in close proximity with the nascent chains by photocrosslinking, dependant on the length and properties of nascent chains. TF carrying the crosslinker at position 34 in the N-domain (TF34) crosslinked with all the nascent chains tested (Figure 19). Crosslinking of TF34 to the nascent chains, which is located close to the TF sequence for ribosome binding, confirms that the nascent chains are adjacent to regions of TF close to the ribosomal exit tunnel, as was predicted (Kramer et al., 2002). Moreover, the N-terminal domain has been shown to adopt a different conformation upon ribosome binding, exposing a hydrophobic cavity providing a binding area for the nascent chain (Figure 10) (Baram et al., 2005). Hence the interactions with the N-terminal domain could play a role in preventing aggregation of the nascent chains by shielding exposed hydrophobic sites. Another site in the N-terminal domain, TF88, failed to crosslink with the nascent chains (Figure 19), although it was surface exposed on the inside of the binding crevice (Figure 12). Absence of TF88 crosslinking may be explained if the nascent chains were maintained in a linear conformation across the top of the crevice. However, a negative crosslinking result may also have technical reasons and should not be over interpreted.

The central chaperone domain of TF crosslinked with all the nascent chains tested. This C-terminal domain is composed of two distinct arm-like structures, the arm 1 and arm 2. It was calculated that the C-terminal domain exposes  $\sim 3500 \text{ \AA}^2$  of surface area between the arms, providing space for a protein domain as large as 14 kDa (Ferbitz et al., 2004). TF labeled with *p*Bpa at residues 320 and 373, in the arm 1 and arm 2, respectively, crosslinked with all the nascent chains tested, implying that both the arms are in close proximity to the nascent chains (Figure 20). Nascent chains as short as 60



residues, which would expose only  $\sim 20$ - $25$  residues outside the exit tunnel were also adjacent to both the arms. Nascent chains were predicted to interact with the hydrophobic crevice formed by the N- and C-terminal domains as they exit the ribosomal tunnel (Ferbitz et al., 2004). To test this hypothesis, controls were performed with probes placed on the back of the TF crevice. TF118 and TF419 yielded no detectable crosslinks to the nascent chains tested, supporting the view that the nascent chains interact only with the highly hydrophobic crevice and not with the back of the molecule (Figure 20).

The PPIase domain also crosslinked with the nascent chains and displayed length dependant interactions (Figure 21). Interestingly, the PPIase domain crosslinked with Luc nascent chains as short as 60 residues. Based on the crystal structure of *E. coli* TF (Ferbitz et al., 2004), the distance between position 34, close to the exit tunnel, and position 233 in the PPIase domain is 87 Å. This would be the minimum distance as TF adopts a more open conformation upon ribosome binding (Kaiser et al., 2006). The length of the ribosomal exit tunnel is  $\sim 100$  Å (Ban et al., 2000). Hence a nascent chain of 60 residues would need to be maintained in a linear conformation (210 Å) to crosslink to the probe at position 233. The crosslinking of Luc 60mer with TF34 in the N-terminal domain, with both the arms in the C-terminal domain and to position 233 in the PPIase domain indicates that at least a portion of Luc nascent chains interact with both the arms and remain in a rather extended conformation until they reach the PPIase domain. This argument is further strengthened by the absence of crosslinking of TF88 with the nascent chains that lies in the interior of the hydrophobic crevice. Interaction in an extended state could be in agreement with the observation that TF delays the folding of Luc relative to its translation (Agashe et al., 2004).

Both the probe positions in the PPIase domain, TF185 and TF233, failed to crosslink to Luc 77mer even though TF233 crosslinked to Luc 164mer (Figure 21). The crosslinking of probes in the PPIase domain with Luc 60mer and 164mer but not with Luc 77mer suggests that the nascent chains move relative to TF. A plausible explanation for the observed length dependence of interactions with the PPIase domain is that the PPIase domain may function as an auxiliary binding site only for some nascent chains, a phenomenon that may be dependent on the conformation of the nascent chain.

Interestingly, the PPIase domain's interaction with the nascent chains did not involve its peptidyl prolyl isomerisation function. One of the probe sites in the PPIase domain, F233, was previously shown to have markedly reduced PPIase activity when mutated to a tyrosine residue (Tradler et al., 1997). To show that TF233 also had reduced PPIase activity, refolding of RCM-RNase T1 was conducted with TF233. The rate-limiting step in the refolding of this protein is the slow prolyl isomerisation of Pro39, which is accelerated in the presence of an active PPI. The rate of refolding in the presence of TF233 was ~ 10 fold slower compared to the presence of WT TF (Figure 24), confirming that the PPIase domain interactions with the nascent chains do not involve its prolyl isomerisation activity.

## V.2 Differential interaction of TF with nascent chains

To investigate whether the domains of TF interact in a similar manner with different types of nascent chains,  $\alpha$ -Synuclein ( $\alpha$ -Syn) was used as another model substrate. Although  $\alpha$ -Syn nascent chains were in close proximity to TF during translation, they were not shielded by TF from protease digestion (Tomic et al., 2006).  $\alpha$ -Syn nascent chains were generated in the PURE system (Figure 30 B) and photocrosslinking was performed with all the *pBpa*-TF variants available.  $\alpha$ -Syn nascent chains expose only little hydrophobicity when compared to Luc nascent chains (Figure 22 B and C). Although TF34, TF320 and TF373 crosslinked to  $\alpha$ -Syn nascent chains of 140 residues, TF233 showed much weaker crosslinking compared to the other positions (Figures 22 A and 23). This would be consistent with the view that the PPIase domain acts as an additional binding site for some nascent chains that expose significant hydrophobic surfaces (Kaiser et al., 2006).

## V.3 Dimerization interface of TF

TF binds to the ribosomes as a monomer but also exists in free solution as a dimer (Patzelt et al., 2002). The excess of TF (50  $\mu$ M) *in vivo*, compared to the ribosomes (30  $\mu$ M) (Lill et al., 1988), suggests that there exists a considerable population of dimeric TF in the cytosol. Addition of ribosomes stabilizes the monomeric form of TF (Kaiser et al.,

2006), emphasizing that the dimeric form does not interact with the ribosomes. Patzelt and colleagues have reported by non-specific glutaraldehyde crosslinking that the N- and C-terminal domains are at the dimer interface (Patzelt et al., 2002). Model building based on inter-molecular FRET data suggested that the arms of the C-terminal domain are at the dimer interface, with the monomers positioned perpendicular to each other (Kaiser et al., 2006). The *pBpa*-TF offered the advantage of identifying specific aspects of the dimer interface by crosslinking the labeled proteins in solution in the absence of ribosomes. Crosslinking was performed at TF concentrations favoring dimer formation.

Crosslinking with the purified proteins revealed that TF34, TF320, TF320 FRK/AAA and TF373 yielded inter-molecular crosslinks (Figure 25). Interestingly, the sites involved in the dimer formation were sites which also crosslinked to the nascent chains (TF34, TF320 and TF373) (Figures 19 and 20). Thus, based on this approach, the proposed substrate-binding site of at least one of the monomers is at the dimer interface. A “crevice to crevice” model in which both the substrate binding sites are at the dimer interface is supported by the assumption that TF419 is not at the dimer interface, based on the negative crosslinking obtained with TF419 under conditions in which TF dimers are populated (Figure 25).

## **V.4 TF-nascent chain interactions monitored by real-time fluorescence experiments**

Structural studies on *E. coli* TF and modeling based on the co-crystal structure of the TF ribosome binding domain and the 50S ribosomal subunit of *H. marismortui* have suggested that the hydrophobic crevice formed by the arms of the C-terminal domain in its ribosome bound form might accommodate a domain upto 14 kDa in size (Ferbitz et al., 2004). This model suggests that TF provides space for the nascent chains to fold immediately after they exit the tunnel. However, the co-crystal structure of the homologous complex of *D. radiodurans* 50S ribosomal subunit and 100 of the 112 residues comprising the ribosome-binding domain of TF revealed that a bacterial specific extension in ribosomal protein L24, absent in archaeobacteria, might occupy the “molecular cradle” proposed by Ferbitz and colleagues (Figure 9) (Schlunzen et al.,

2005). This suggests that any significant folding of small domains might not occur in the crevice formed by the C-terminal domain as was predicted by Ferbitz and colleagues.

Earlier reports based on the high affinity of TF for ribosomes (Maier et al., 2003) and its low affinity for short oligopeptides (Maier et al., 2001) suggested that TF might remain bound to the ribosomes till a major fraction of the nascent chains have been synthesized. However, this might not reflect TF's interaction with the nascent chains during translation. TF's interaction with the ribosomes during translation has been documented kinetically and TF was found to dissociate from the ribosomes with a  $t_{1/2}$  value of  $\sim 10$ -12 s. Importantly the dissociation was found to be independent of the translation status of the ribosomes (Kaiser et al., 2006). However, a recent study employing purified RNCs revealed that the nascent chain might act as a timer for TF dissociation from the ribosome (Rutkowska et al., 2007). Purified RNCs rather than translating ribosomes were utilized in these experiments with the aim of studying the interaction of TF with defined homogeneous population of ribosome-associated nascent chains. However, whether, these experiments reflect the dynamics of TF interaction with translating ribosomes remain to be seen.

Intra-molecular FRET experiments have shown that TF attains a more open conformation upon binding to the ribosomes and that this conformational change is stabilized during translation. The  $t_{1/2}$  value for relaxation from this conformational change (molecular compaction) was  $\sim 35$  s during translation of Luc nascent chains, presumably owing to a strong interaction of TF with hydrophobic regions in Luc nascent chains (Kaiser et al., 2006). Based on TF-ribosome dissociation and TF's molecular compaction data, it was concluded that TF's interactions with the nascent chains persist even after TF has dissociated from the ribosomes. To test this proposal, we sought to set up a system to directly measure TF-nascent chain interactions.

A fluorescent probe with the ability to undergo a change in its fluorescence intensity upon binding to the nascent chains was used in these experiments. IANBD (NBD) was used because it undergoes an appreciable fluorescence change in a hydrophobic environment. Initially, TF was labeled with NBD in arm 1 of the C-terminal domain (E326), because arm 1 was found to be in close proximity to the nascent chains (Figure 20). TF326-NBD, when present during translation of Luc nascent chains showed

substantial increase in fluorescence intensity but not during translation of S7 and  $\alpha$ -Syn nascent chains (Figure 30 A). This is consistent with the expectation that NBD would undergo a fluorescence increase in a hydrophobic environment, such as that of Luc nascent chains, but not with a less hydrophobic environment of S7 and  $\alpha$ -Syn nascent chains, even though it may be adjacent to them.

Recruitment of additional TF molecules towards elongating nascent chains would be a mechanism by which TF might prevent aggregation of nascent chains. Earlier experiments from our laboratory have suggested that more than one TF molecule might be associated with a nascent chain depending on its size and hydrophobicity (Agashe et al., 2004). Luc nascent chains have three hydrophobic patches that are predicted to have high affinity for TF binding (Kaiser et al., 2006). Luc F.L, Luc 550mer and Luc 520mer nascent chains have all of their hydrophobic regions exposed outside of the exit tunnel, Luc 164mer has only one such hydrophobic segment exposed. The pronounced increase in TF326-NBD fluorescence during translation of Luc F.L, Luc 550mer or Luc 520mer compared to Luc 164mer (Figure 32) might be due to the recruitment of additional TF molecules towards elongating nascent chains. The increase in fluorescence intensity is not due to the translation efficiency because Luc 164mer was translated as efficiently as the longer nascent chains (Figure 30 B). Alternatively, the increase in fluorescence intensity might also be due to a single TF326-NBD in a more hydrophobic environment contributed by the longer nascent chain in the absence of additional TF molecules.

## **V.5 Kinetic characterization of TF dissociation from nascent chains**

To examine the kinetics of TF dissociation from nascent chains, dissociation of TF326-NBD from Luc-RNCs was measured upon addition of excess unlabeled TF. Interestingly, the dissociation was found to have biphasic kinetics. The initial phase was fast and occurred with a  $t_{1/2}$  value  $14 \pm 2$  s. The second phase was slow and had a  $t_{1/2}$  value of  $102 \pm 16$  s (Figure 33). Similar displacement experiments performed with GatD-RNCs also yielded a biphasic nature of dissociation, although both the phases were faster compared to TF326-NBD dissociation from Luc-RNCs (Figure 34). Since the respective

phases differed between the dissociation from Luc- and GatD-RNCs, this prompted us to investigate which of the two phases actually represents TF dissociation from the nascent chains.

To address this, another position in the C-terminal domain was chosen (TF376-NBD) and similar dissociation experiments were performed. Interestingly the dissociation of TF376-NBD from both the RNCs was also determined to be biphasic (Figure 35). In contrast to TF326-NBD, for TF376-NBD dissociation the respective half-times did not vary between the two RNCs.

A closer look at the structural model built with full-length TF on the 50S ribosomal subunit revealed that the closest approach of both arms of the C-terminal domain to the ribosomal surface is 10 Å (Figure 8) (Ferbitz et al., 2004). According to the authors, a direct contact between the arms and the ribosomal surface was not observed. To confirm whether the arms of the C-terminal domain interact with the ribosomal surface during translation and give rise to one of the phases observed during the dissociation process, translation of rpoB 190mer nascent chains in the presence of TFB, TF326-NBD and TF376-NBD was performed. During translation of rpoB 190mer nascent chains, which expose very little hydrophobicity (Figure 31 C), TF326-NBD and TF376-NBD underwent only a negligible change in fluorescence, although TFB showed a considerable fluorescence decrease, indicative of TFB binding to rpoB 190mer-RNCs (Figure 37). If the first phase observed during the dissociation of TF326-NBD and TF376-NBD from either Luc- or GatD- RNCs was due to their release from the ribosomes, it should also be observed in the case of rpoB 190mer-RNCs, since TFB bound to rpoB 190mer-RNCs. This suggests that the observed phases do not report TF326-NBD or TF376-NBD dissociation from the ribosomes.

A possible reason for the biphasic nature during dissociation could be due to the flexibility of the C-terminal domain. In a recent NMR study, it was shown that the C-terminal domain exists in multiple conformations in solution (Yao et al., 2008) and may differ from the conformation observed in the crystal structure (Ferbitz et al., 2004). As a result, if the nascent chain-bound C-terminal domain exists in multiple conformations due to its flexible nature, it might dissociate from the nascent chains at different rates depending on the stability of the various conformations.

To obtain further insights into TF dissociation from the nascent chains, a position in the PPIase domain (TF150-NBD) was chosen for analysis. TF150-NBD showed an intermediate fluorescence change during translation of Luc and GatD nascent chains (Figure 39), compared to TF326-NBD and TF376-NBD, consistent with the fact that the PPIase domain acts as a secondary site for nascent chain binding. Interestingly, the dissociation of TF150-NBD from both these RNCs occurred with a single phase. This suggests that the process of TF dissociation from the nascent chains is more accurately monitored with this probe position. The dissociation of TF150-NBD from Luc- and GatD-RNCs occurred with a  $t_{1/2}$  value of  $111 \pm 7$  s and  $25 \pm 2$  s, respectively (Figure 39). The  $t_{1/2}$  values of TF150-NBD dissociation from both these RNCs are higher than the  $t_{1/2}$  values of TFB dissociation ( $t_{1/2}$  value  $14.5 \pm 0.5$  s and  $14.5 \pm 1.5$  s from Luc- and GatD-RNCs, respectively) (Figure 40). This implies that TF-nascent chain interactions persist even after TF had dissociated from the ribosomes.

The rate of TF150-NBD dissociation, which is slower from Luc-RNCs than GatD-RNCs, could be attributed to the more hydrophobic nature of Luc nascent chains compared to GatD (Figures 22 B and 31 B). Therefore the duration of TF interaction with the nascent chains could be dictated by the degree of hydrophobicity per individual region or the number of hydrophobic regions per nascent chain. The dissociation of TF150-NBD from GatD-RNCs, which occurs with a  $t_{1/2}$  value of  $25 \pm 2$  s, matches closely with the rate of molecular compaction of TF from GatD-RNCs ( $t_{1/2}$  value  $\sim 24$  s) (Kaiser et al., 2006). But interestingly, TF150-NBD dissociation from Luc-RNCs ( $t_{1/2}$  value of  $111 \pm 7$  s) occurs with a slower rate compared to the rate of molecular compaction of TF from Luc-RNCs ( $t_{1/2}$  value of  $\sim 35$  s), indicating that TF interaction with more hydrophobic nascent chains persist even after its molecular compaction has occurred.

## V.6 Overview of TF-nascent chain interactions

In this study the interactions of TF with nascent chains have been analyzed by site-specific photocrosslinking and real-time fluorescence experiments. Data from photocrosslinking experiments demonstrate that all the domains of TF are adjacent to the

nascent chains during translation. Interestingly, a portion of Luc nascent chains was maintained in a linear conformation until the chain reached the PPIase domain. This interaction may serve to prevent the formation of any premature structure or off-pathway aggregation. The N- and C-terminal domains of TF interacted with all the nascent chains tested but the PPIase domain displayed a length dependent interaction. Nascent chains less hydrophobic than Luc interacted less efficiently with the PPIase domain. The above observations along with the previously published data suggest that the PPIase domain acts as a secondary binding site for nascent chains, the primary site being the NC domain (Kaiser et al., 2006; Tomic et al., 2006). Photocrosslinking of purified *pBpa*-TF revealed that the nascent chain binding sites are at the dimer interface. This would be a regulatory mechanism by which the monomeric TF interacts with the ribosome-nascent chain complexes and the extra-ribosomal dimeric TF loses its ability to interact with the substrates. This mechanism might prevent any non-specific interaction of TF with already synthesized cellular proteins; confining its role in folding assistance to the ribosome.

TF dissociates from the ribosomes with a  $t_{1/2}$  value of  $\sim 10$ - $12$  s and this was found to be independent of the translation status of the ribosomes (Kaiser et al., 2006). The dissociation of TF from the nascent chains in this study was found to have a biphasic nature, suggesting the simultaneous occurrence of the two processes. This behavior might be due to the presence of different conformations of the C-terminal domain in solution (Yao et al., 2008). The flexibility of the C-domain might be important in accommodating nascent chains with diverse properties during translation. With a probe placed in the PPIase domain, the process of TF dissociation from nascent chains was accurately monitored. The dissociation occurred with a  $t_{1/2}$  value of  $111 \pm 7$  s and  $25 \pm 2$  s from Luc- and GatD-RNCs, respectively. Taken together, the kinetics of TF dissociation from ribosomes (Kaiser et al., 2006) and from nascent chains confirm that the interactions of TF with the nascent chains persist even after TF has dissociated from the ribosomes. The exact duration of interaction might be dictated by the extent of a nascent chain's hydrophobicity.

The prolonged association of TF with the nascent chains after its departure from the ribosome might provide an opportunity for additional TF molecules to be recruited towards elongating, aggregation prone-nascent chains during translation (Agashe et al.,



2004). Burial of hydrophobic regions in the nascent chains during the process of folding results in the displacement of TF (Kaiser et al., 2006). It will be interesting to investigate whether the multiple TF molecules present in larger nascent chain are released in a step-wise or sequential manner as folding towards the native state is initiated.

## VI References

- Agashe, V.R., Guha, S., Chang, H.C., Genevoux, P., Hayer-Hartl, M., Stemp, M., Georgopoulos, C., Hartl, F.U., and Barral, J.M. (2004). Function of trigger factor and DnaK in multidomain protein folding: increase in yield at the expense of folding speed. *Cell* 117, 199-209.
- Anfinsen, C.B. (1972). The formation and stabilization of protein structure. *The Biochemical journal* 128, 737-749.
- Anfinsen, C.B. (1973). Principles that govern the folding of protein chains. *Science (New York, NY)* 181, 223-230.
- Ban, N., Nissen, P., Hansen, J., Moore, P.B., and Steitz, T.A. (2000). The complete atomic structure of the large ribosomal subunit at 2.4 Å resolution. *Science (New York, NY)* 289, 905-920.
- Baram, D., Pyetan, E., Sittner, A., Auerbach-Nevo, T., Bashan, A., and Yonath, A. (2005). Structure of trigger factor binding domain in biologically homologous complex with eubacterial ribosome reveals its chaperone action. *Proceedings of the National Academy of Sciences of the United States of America* 102, 12017-12022.
- Barral, J.M., Broadley, S.A., Schaffar, G., and Hartl, F.U. (2004). Roles of molecular chaperones in protein misfolding diseases. *Seminars in cell & developmental biology* 15, 17-29.
- Beck, K., Wu, L.F., Brunner, J., and Muller, M. (2000). Discrimination between SRP- and SecA/SecB-dependent substrates involves selective recognition of nascent chains by SRP and trigger factor. *The EMBO journal* 19, 134-143.
- Behrends, C., Langer, C.A., Boteva, R., Bottcher, U.M., Stemp, M.J., Schaffar, G., Rao, B.V., Giese, A., Kretzschmar, H., Siegers, K., et al. (2006). Chaperonin TRiC promotes the assembly of polyQ expansion proteins into nontoxic oligomers. *Molecular cell* 23, 887-897.
- Blobel, G., and Sabatini, D.D. (1970). Controlled proteolysis of nascent polypeptides in rat liver cell fractions. I. Location of the polypeptides within ribosomes. *The Journal of cell biology* 45, 130-145.
- Bradford, M.M. (1976). A rapid and sensitive method for the quantitation of microgram quantities of protein utilizing the principle of protein-dye binding. *Analytical biochemistry* 72, 248-254.
- Brehmer, D., Gassler, C., Rist, W., Mayer, M.P., and Bukau, B. (2004). Influence of GrpE on DnaK-substrate interactions. *The Journal of biological chemistry* 279, 27957-27964.

- Brinker, A., Pfeifer, G., Kerner, M.J., Naylor, D.J., Hartl, F.U., and Hayer-Hartl, M. (2001). Dual function of protein confinement in chaperonin-assisted protein folding. *Cell* 107, 223-233.
- Buskiewicz, I., Deuerling, E., Gu, S.Q., Jockel, J., Rodnina, M.V., Bukau, B., and Wintermeyer, W. (2004). Trigger factor binds to ribosome-signal-recognition particle (SRP) complexes and is excluded by binding of the SRP receptor. *Proceedings of the National Academy of Sciences of the United States of America* 101, 7902-7906.
- Camasses, A., Bogdanova, A., Shevchenko, A., and Zachariae, W. (2003). The CCT chaperonin promotes activation of the anaphase-promoting complex through the generation of functional Cdc20. *Molecular cell* 12, 87-100.
- Chan, H.Y., Warrick, J.M., Gray-Board, G.L., Paulson, H.L., and Bonini, N.M. (2000). Mechanisms of chaperone suppression of polyglutamine disease: selectivity, synergy and modulation of protein solubility in *Drosophila*. *Human molecular genetics* 9, 2811-2820.
- Chin, J.W., Martin, A.B., King, D.S., Wang, L., and Schultz, P.G. (2002). Addition of a photocrosslinking amino acid to the genetic code of *Escherichiacoli*. *Proceedings of the National Academy of Sciences of the United States of America* 99, 11020-11024.
- Chin, J.W., and Schultz, P.G. (2002). In vivo photocrosslinking with unnatural amino Acid mutagenesis. *Chembiochem* 3, 1135-1137.
- Clark, P.L. (2004). Protein folding in the cell: reshaping the folding funnel. *Trends in biochemical sciences* 29, 527-534.
- Crooke, E., Brundage, L., Rice, M., and Wickner, W. (1988a). ProOmpA spontaneously folds in a membrane assembly competent state which trigger factor stabilizes. *The EMBO journal* 7, 1831-1835.
- Crooke, E., Guthrie, B., Lecker, S., Lill, R., and Wickner, W. (1988b). ProOmpA is stabilized for membrane translocation by either purified *E. coli* trigger factor or canine signal recognition particle. *Cell* 54, 1003-1011.
- Crooke, E., and Wickner, W. (1987). Trigger factor: a soluble protein that folds pro-OmpA into a membrane-assembly-competent form. *Proceedings of the National Academy of Sciences of the United States of America* 84, 5216-5220.
- Daggett, V., and Fersht, A.R. (2003). Is there a unifying mechanism for protein folding? *Trends in biochemical sciences* 28, 18-25.
- de Gier, J.W., Mansournia, P., Valent, Q.A., Phillips, G.J., Luirink, J., and von Heijne, G. (1996). Assembly of a cytoplasmic membrane protein in *Escherichia coli* is dependent on the signal recognition particle. *FEBS letters* 399, 307-309.

- Deuerling, E., Patzelt, H., Vorderwulbecke, S., Rauch, T., Kramer, G., Schaffitzel, E., Mogk, A., Schulze-Specking, A., Langen, H., and Bukau, B. (2003). Trigger Factor and DnaK possess overlapping substrate pools and binding specificities. *Molecular microbiology* 47, 1317-1328.
- Deuerling, E., Schulze-Specking, A., Tomoyasu, T., Mogk, A., and Bukau, B. (1999). Trigger factor and DnaK cooperate in folding of newly synthesized proteins. *Nature* 400, 693-696.
- Ditzel, L., Lowe, J., Stock, D., Stetter, K.O., Huber, H., Huber, R., and Steinbacher, S. (1998). Crystal structure of the thermosome, the archaeal chaperonin and homolog of CCT. *Cell* 93, 125-138.
- Dorman, G., and Prestwich, G.D. (1994). Benzophenone photophores in biochemistry. *Biochemistry* 33, 5661-5673.
- Feldman, D.E., and Frydman, J. (2000). Protein folding in vivo: the importance of molecular chaperones. *Current opinion in structural biology* 10, 26-33.
- Feldman, D.E., Thulasiraman, V., Ferreyra, R.G., and Frydman, J. (1999). Formation of the VHL-elongin BC tumor suppressor complex is mediated by the chaperonin TRiC. *Molecular cell* 4, 1051-1061.
- Ferbitz, L., Maier, T., Patzelt, H., Bukau, B., Deuerling, E., and Ban, N. (2004). Trigger factor in complex with the ribosome forms a molecular cradle for nascent proteins. *Nature* 431, 590-596.
- Ferguson, N., and Fersht, A.R. (2003). Early events in protein folding. *Current opinion in structural biology* 13, 75-81.
- Flanagan, J.J., Chen, J.C., Miao, Y., Shao, Y., Lin, J., Bock, P.E., and Johnson, A.E. (2003). Signal recognition particle binds to ribosome-bound signal sequences with fluorescence-detected subnanomolar affinity that does not diminish as the nascent chain lengthens. *The Journal of biological chemistry* 278, 18628-18637.
- Gautschi, M., Lilie, H., Funfschilling, U., Mun, A., Ross, S., Lithgow, T., Rucknagel, P., and Rospert, S. (2001). RAC, a stable ribosome-associated complex in yeast formed by the DnaK-DnaJ homologs Ssz1p and zuotin. *Proceedings of the National Academy of Sciences of the United States of America* 98, 3762-3767.
- Gautschi, M., Mun, A., Ross, S., and Rospert, S. (2002). A functional chaperone triad on the yeast ribosome. *Proceedings of the National Academy of Sciences of the United States of America* 99, 4209-4214.
- Genevaux, P., Keppel, F., Schwager, F., Langendijk-Genevaux, P.S., Hartl, F.U., and Georgopoulos, C. (2004). In vivo analysis of the overlapping functions of DnaK and trigger factor. *EMBO reports* 5, 195-200.

- Gill, S.C., and von Hippel, P.H. (1989). Calculation of protein extinction coefficients from amino acid sequence data. *Analytical biochemistry* 182, 319-326.
- Guthrie, B., and Wickner, W. (1990). Trigger factor depletion or overproduction causes defective cell division but does not block protein export. *Journal of bacteriology* 172, 5555-5562.
- Halic, M., Blau, M., Becker, T., Mielke, T., Pool, M.R., Wild, K., Sinning, I., and Beckmann, R. (2006). Following the signal sequence from ribosomal tunnel exit to signal recognition particle. *Nature* 444, 507-511.
- Harrison, C. (2003). GrpE, a nucleotide exchange factor for DnaK. *Cell stress & chaperones* 8, 218-224.
- Harrison, C.J., Hayer-Hartl, M., Di Liberto, M., Hartl, F., and Kuriyan, J. (1997). Crystal structure of the nucleotide exchange factor GrpE bound to the ATPase domain of the molecular chaperone DnaK. *Science (New York, NY)* 276, 431-435.
- Hartl, F.U., and Hayer-Hartl, M. (2002). Molecular chaperones in the cytosol: from nascent chain to folded protein. *Science (New York, NY)* 295, 1852-1858.
- Hesterkamp, T., and Bukau, B. (1996). Identification of the prolyl isomerase domain of *Escherichia coli* trigger factor. *FEBS letters* 385, 67-71.
- Hesterkamp, T., Deuerling, E., and Bukau, B. (1997). The amino-terminal 118 amino acids of *Escherichia coli* trigger factor constitute a domain that is necessary and sufficient for binding to ribosomes. *The Journal of biological chemistry* 272, 21865-21871.
- Ho, Y., Gruhler, A., Heilbut, A., Bader, G.D., Moore, L., Adams, S.L., Millar, A., Taylor, P., Bennett, K., Boutilier, K., et al. (2002). Systematic identification of protein complexes in *Saccharomyces cerevisiae* by mass spectrometry. *Nature* 415, 180-183.
- Hoffmann, A., Merz, F., Rutkowska, A., Zachmann-Brand, B., Deuerling, E., and Bukau, B. (2006). Trigger factor forms a protective shield for nascent polypeptides at the ribosome. *The Journal of biological chemistry* 281, 6539-6545.
- Huang, G.C., Li, Z.Y., Zhou, J.M., and Fischer, G. (2000). Assisted folding of D-glyceraldehyde-3-phosphate dehydrogenase by trigger factor. *Protein Sci* 9, 1254-1261.
- Ito, K. (2005). Ribosome-based protein folding systems are structurally divergent but functionally universal across biological kingdoms. *Molecular microbiology* 57, 313-317.
- Jakob, U., Lilie, H., Meyer, I., and Buchner, J. (1995). Transient interaction of Hsp90 with early unfolding intermediates of citrate synthase. Implications for heat shock in vivo. *The Journal of biological chemistry* 270, 7288-7294.

- Kaiser, C.M., Chang, H.C., Agashe, V.R., Lakshminpathy, S.K., Etchells, S.A., Hayer-Hartl, M., Hartl, F.U., and Barral, J.M. (2006). Real-time observation of trigger factor function on translating ribosomes. *Nature* 444, 455-460.
- Kauer, J.C., Erickson-Viitanen, S., Wolfe, H.R., Jr., and DeGrado, W.F. (1986). p-Benzoyl-L-phenylalanine, a new photoreactive amino acid. Photolabeling of calmodulin with a synthetic calmodulin-binding peptide. *The Journal of biological chemistry* 261, 10695-10700.
- Kauzmann, W. (1959). Some factors in the interpretation of protein denaturation. *Advances in protein chemistry* 14, 1-63.
- Keiler, K.C., Waller, P.R., and Sauer, R.T. (1996). Role of a peptide tagging system in degradation of proteins synthesized from damaged messenger RNA. *Science (New York, NY)* 271, 990-993.
- Kim, P.S., and Baldwin, R.L. (1982). Specific intermediates in the folding reactions of small proteins and the mechanism of protein folding. *Annual review of biochemistry* 51, 459-489.
- Kim, P.S., and Baldwin, R.L. (1990). Intermediates in the folding reactions of small proteins. *Annual review of biochemistry* 59, 631-660.
- Kramer, G., Patzelt, H., Rauch, T., Kurz, T.A., Vorderwulbecke, S., Bukau, B., and Deuerling, E. (2004a). Trigger factor peptidyl-prolyl cis/trans isomerase activity is not essential for the folding of cytosolic proteins in *Escherichia coli*. *The Journal of biological chemistry* 279, 14165-14170.
- Kramer, G., Rauch, T., Rist, W., Vorderwulbecke, S., Patzelt, H., Schulze-Specking, A., Ban, N., Deuerling, E., and Bukau, B. (2002). L23 protein functions as a chaperone docking site on the ribosome. *Nature* 419, 171-174.
- Kramer, G., Rutkowska, A., Wegrzyn, R.D., Patzelt, H., Kurz, T.A., Merz, F., Rauch, T., Vorderwulbecke, S., Deuerling, E., and Bukau, B. (2004b). Functional dissection of *Escherichia coli* trigger factor: unraveling the function of individual domains. *Journal of bacteriology* 186, 3777-3784.
- Laemmli, U.K. (1970). Cleavage of structural proteins during the assembly of the head of bacteriophage T4. *Nature* 227, 680-685.
- Lakowicz, J. (1999). *Principles of Fluorescence Spectroscopy*. New York, Kluwer Academic and Plenum Publishers.
- Langer, T., Lu, C., Echols, H., Flanagan, J., Hayer, M.K., and Hartl, F.U. (1992). Successive action of DnaK, DnaJ and GroEL along the pathway of chaperone-mediated protein folding. *Nature* 356, 683-689.

- Leroux, M.R., Fandrich, M., Klunker, D., Siegers, K., Lupas, A.N., Brown, J.R., Schiebel, E., Dobson, C.M., and Hartl, F.U. (1999). MtGimC, a novel archaeal chaperone related to the eukaryotic chaperonin cofactor GimC/prefoldin. *The EMBO journal* 18, 6730-6743.
- Levinthal, C., Signer, E.R., and Fetherolf, K. (1962). Reactivation and hybridization of reduced alkaline phosphatase. *Proceedings of the National Academy of Sciences of the United States of America* 48, 1230-1237.
- Lill, R., Crooke, E., Guthrie, B., and Wickner, W. (1988). The "trigger factor cycle" includes ribosomes, presecretory proteins, and the plasma membrane. *Cell* 54, 1013-1018.
- Liu, C.P., Perrett, S., and Zhou, J.M. (2005). Dimeric trigger factor stably binds folding-competent intermediates and cooperates with the DnaK-DnaJ-GrpE chaperone system to allow refolding. *The Journal of biological chemistry* 280, 13315-13320.
- Ludlam, A.V., Moore, B.A., and Xu, Z. (2004). The crystal structure of ribosomal chaperone trigger factor from *Vibrio cholerae*. *Proceedings of the National Academy of Sciences of the United States of America* 101, 13436-13441.
- Luirink, J., and Sinning, I. (2004). SRP-mediated protein targeting: structure and function revisited. *Biochim Biophys Acta.* 11;1694(1-3):17-35
- Macfarlane, J., and Muller, M. (1995). The functional integration of a polytopic membrane protein of *Escherichia coli* is dependent on the bacterial signal-recognition particle. *European journal of biochemistry / FEBS* 233, 766-771.
- Maier, R., Eckert, B., Scholz, C., Lilie, H., and Schmid, F.X. (2003). Interaction of trigger factor with the ribosome. *Journal of molecular biology* 326, 585-592.
- Maier, R., Scholz, C., and Schmid, F.X. (2001). Dynamic association of trigger factor with protein substrates. *Journal of molecular biology* 314, 1181-1190.
- Malkin, L.I., and Rich, A. (1967). Partial resistance of nascent polypeptide chains to proteolytic digestion due to ribosomal shielding. *Journal of molecular biology* 26, 329-346.
- Mathews, M. B., N. Sonenberg and J. W. B. Hershey (2000). Origins and principles of translational control. *Translational control of gene expression*. N. Sonenberg, J. W. B. Hershey and M. B. Mathews. Cold Spring Harbor, New York, Cold Spring Harbor Laboratory Press: 1-31.
- Matsuura, T., Yanagida, H., Ushioda, J., Urabe, I., and Yomo, T. (2007). Nascent chain, mRNA, and ribosome complexes generated by a pure translation system. *Biochemical and biophysical research communications* 352, 372-377.

- Mayhew, M., da Silva, A.C., Martin, J., Erdjument-Bromage, H., Tempst, P., and Hartl, F.U. (1996). Protein folding in the central cavity of the GroEL-GroES chaperonin complex. *Nature* 379, 420-426.
- Merz, F., Hoffmann, A., Rutkowska, A., Zachmann-Brand, B., Bukau, B., and Deuerling, E. (2006). The C-terminal domain of Escherichia coli trigger factor represents the central module of its chaperone activity. *The Journal of biological chemistry* 281, 31963-31971.
- Mucke, M., and Schmid, F.X. (1992). Enzymatic catalysis of prolyl isomerization in an unfolding protein. *Biochemistry* 31, 7848-7854.
- Nathan, D.F., Vos, M.H., and Lindquist, S. (1997). In vivo functions of the Saccharomyces cerevisiae Hsp90 chaperone. *Proceedings of the National Academy of Sciences of the United States of America* 94, 12949-12956.
- Nissen, P., Hansen, J., Ban, N., Moore, P.B., and Steitz, T.A. (2000). The structural basis of ribosome activity in peptide bond synthesis. *Science (New York, NY)* 289, 920-930.
- Onuchic, J.N. (1997). Contacting the protein folding funnel with NMR. *Proceedings of the National Academy of Sciences of the United States of America* 94, 7129-7131.
- Patzelt, H., Kramer, G., Rauch, T., Schonfeld, H.J., Bukau, B., and Deuerling, E. (2002). Three-state equilibrium of Escherichia coli trigger factor. *Biological chemistry* 383, 1611-1619.
- Patzelt, H., Rudiger, S., Brehmer, D., Kramer, G., Vorderwulbecke, S., Schaffitzel, E., Waitz, A., Hesterkamp, T., Dong, L., Schneider-Mergener, J., et al. (2001). Binding specificity of Escherichia coli trigger factor. *Proceedings of the National Academy of Sciences of the United States of America* 98, 14244-14249.
- Pellecchia, M., Montgomery, D.L., Stevens, S.Y., Vander Kooi, C.W., Feng, H.P., Gierasch, L.M., and Zudierweg, E.R. (2000). Structural insights into substrate binding by the molecular chaperone DnaK. *Nature structural biology* 7, 298-303.
- Pfund, C., Lopez-Hoyo, N., Ziegelhoffer, T., Schilke, B.A., Lopez-Buesa, P., Walter, W.A., Wiedmann, M., and Craig, E.A. (1998). The molecular chaperone Ssb from Saccharomyces cerevisiae is a component of the ribosome-nascent chain complex. *The EMBO journal* 17, 3981-3989.
- Pierpaoli, E.V., Sandmeier, E., Baici, A., Schonfeld, H.J., Gisler, S., and Christen, P. (1997). The power stroke of the DnaK/DnaJ/GrpE molecular chaperone system. *Journal of molecular biology* 269, 757-768.
- Pool, M.R., Stumm, J., Fulga, T.A., Sinning, I., and Dobberstein, B. (2002). Distinct modes of signal recognition particle interaction with the ribosome. *Science (New York, NY)* 297, 1345-1348.



- Prodromou, C., Siligardi, G., O'Brien, R., Woolfson, D.N., Regan, L., Panaretou, B., Ladbury, J.E., Piper, P.W., and Pearl, L.H. (1999). Regulation of Hsp90 ATPase activity by tetratricopeptide repeat (TPR)-domain co-chaperones. *The EMBO journal* 18, 754-762.
- Ramachandran, G.N., and Sasisekharan, V. (1968). Conformation of polypeptides and proteins. *Advances in protein chemistry* 23, 283-438.
- Ramachandran, R., Heuck, A.P., Tweten, R.K., and Johnson, A.E. (2002). Structural insights into the membrane-anchoring mechanism of a cholesterol-dependent cytolysin. *Nature structural biology* 9, 823-827.
- Ramachandran, R., and Schmid, S.L. (2008). Real-time detection reveals that effectors couple dynamin's GTP-dependent conformational changes to the membrane. *The EMBO journal* 27, 27-37.
- Ranson, N.A., Clare, D.K., Farr, G.W., Houldershaw, D., Horwich, A.L., and Saibil, H.R. (2006). Allosteric signaling of ATP hydrolysis in GroEL-GroES complexes. *Nature structural & molecular biology* 13, 147-152.
- Ranson, N.A., Farr, G.W., Roseman, A.M., Gowen, B., Fenton, W.A., Horwich, A.L., and Saibil, H.R. (2001). ATP-bound states of GroEL captured by cryo-electron microscopy. *Cell* 107, 869-879.
- Rospert, S., Dubaquié, Y., and Gautschi, M. (2002). Nascent-polypeptide-associated complex. *Cell Mol Life Sci* 59, 1632-1639.
- Rudiger, S., Germeroth, L., Schneider-Mergener, J., and Bukau, B. (1997). Substrate specificity of the DnaK chaperone determined by screening cellulose-bound peptide libraries. *The EMBO journal* 16, 1501-1507.
- Rudiger, S., Schneider-Mergener, J., and Bukau, B. (2001). Its substrate specificity characterizes the DnaJ co-chaperone as a scanning factor for the DnaK chaperone. *The EMBO journal* 20, 1042-1050.
- Rutkowska, A., Mayer, M.P., Hoffmann, A., Merz, F., Zachmann-Brand, B., Schaffitzel, C., Ban, N., Deuerling, E., and Bukau, B. (2007). Dynamics of trigger factor interaction with translating ribosomes. *The Journal of biological chemistry*.
- Rye, H.S., Burston, S.G., Fenton, W.A., Beechem, J.M., Xu, Z., Sigler, P.B., and Horwich, A.L. (1997). Distinct actions of cis and trans ATP within the double ring of the chaperonin GroEL. *Nature* 388, 792-798.
- Sabatini, D.D., and Blobel, G. (1970). Controlled proteolysis of nascent polypeptides in rat liver cell fractions. II. Location of the polypeptides in rough microsomes. *The Journal of cell biology* 45, 146-157.

- Schaffar, G., Breuer, P., Boteva, R., Behrends, C., Tzvetkov, N., Strippel, N., Sakahira, H., Siegers, K., Hayer-Hartl, M., and Hartl, F.U. (2004). Cellular toxicity of polyglutamine expansion proteins: mechanism of transcription factor deactivation. *Molecular cell* 15, 95-105.
- Scheufler, C., Brinker, A., Bourenkov, G., Pegoraro, S., Moroder, L., Bartunik, H., Hartl, F.U., Moarefi, I. (2000). Structure of TPR domain-peptide complexes: critical elements in the assembly of the Hsp70-Hsp90 multichaperone machine. *Cell*. 14;101(2):199-210.
- Schlunzen, F., Wilson, D.N., Tian, P., Harms, J.M., McInnes, S.J., Hansen, H.A., Albrecht, R., Buerger, J., Wilbanks, S.M., and Fucini, P. (2005). The binding mode of the trigger factor on the ribosome: implications for protein folding and SRP interaction. *Structure* 13, 1685-1694.
- Scholz, C., Stoller, G., Zarnt, T., Fischer, G., and Schmid, F.X. (1997). Cooperation of enzymatic and chaperone functions of trigger factor in the catalysis of protein folding. *The EMBO journal* 16, 54-58.
- Schonbrunner, E.R., Mayer, S., Tropschug, M., Fischer, G., Takahashi, N., and Schmid, F.X. (1991). Catalysis of protein folding by cyclophilins from different species. *The Journal of biological chemistry* 266, 3630-3635.
- Seluanov, A., and Bibi, E. (1997). FtsY, the prokaryotic signal recognition particle receptor homologue, is essential for biogenesis of membrane proteins. *The Journal of biological chemistry* 272, 2053-2055.
- Sha, B., Lee, S., and Cyr, D.M. (2000). The crystal structure of the peptide-binding fragment from the yeast Hsp40 protein Sis1. *Structure* 8, 799-807.
- Shimizu, Y., Inoue, A., Tomari, Y., Suzuki, T., Yokogawa, T., Nishikawa, K., and Ueda, T. (2001). Cell-free translation reconstituted with purified components. *Nature biotechnology* 19, 751-755.
- Shimizu, Y., Kanamori, T., and Ueda, T. (2005). Protein synthesis by pure translation systems. *Methods (San Diego, Calif)* 36, 299-304.
- Spreter, T., Pech, M., and Beatrix, B. (2005). The crystal structure of archaeal nascent polypeptide-associated complex (NAC) reveals a unique fold and the presence of a ubiquitin-associated domain. *The Journal of biological chemistry* 280, 15849-15854.
- Stoller, G., Rucknagel, K.P., Nierhaus, K.H., Schmid, F.X., Fischer, G., and Rahfeld, J.U. (1995). A ribosome-associated peptidyl-prolyl cis/trans isomerase identified as the trigger factor. *The EMBO journal* 14, 4939-4948.
- Taniuchi, H., and Anfinsen, C.B. (1969). An experimental approach to the study of the folding of staphylococcal nuclease. *The Journal of biological chemistry* 244, 3864-3875.

- Teter, S.A., Houry, W.A., Ang, D., Tradler, T., Rockabrand, D., Fischer, G., Blum, P., Georgopoulos, C., and Hartl, F.U. (1999). Polypeptide flux through bacterial Hsp70: DnaK cooperates with trigger factor in chaperoning nascent chains. *Cell* 97, 755-765.
- Theysen, H., Schuster, H.P., Packschies, L., Bukau, B., and Reinstein, J. (1996). The second step of ATP binding to DnaK induces peptide release. *Journal of molecular biology* 263, 657-670.
- Tomic, S., Johnson, A.E., Hartl, F.U., and Etchells, S.A. (2006). Exploring the capacity of trigger factor to function as a shield for ribosome bound polypeptide chains. *FEBS letters* 580, 72-76.
- Tradler, T., Stoller, G., Rucknagel, K.P., Schierhorn, A., Rahfeld, J.U., and Fischer, G. (1997). Comparative mutational analysis of peptidyl prolyl cis/trans isomerases: active sites of *Escherichia coli* trigger factor and human FKBP12. *FEBS letters* 407, 184-190.
- Ullers, R.S., Houben, E.N., Raine, A., ten Hagen-Jongman, C.M., Ehrenberg, M., Brunner, J., Oudega, B., Harms, N., and Luirink, J. (2003). Interplay of signal recognition particle and trigger factor at L23 near the nascent chain exit site on the *Escherichia coli* ribosome. *The Journal of cell biology* 161, 679-684.
- Vainberg, I.E., Lewis, S.A., Rommelaere, H., Ampe, C., Vandekerckhove, J., Klein, H.L., and Cowan, N.J. (1998). Prefoldin, a chaperone that delivers unfolded proteins to cytosolic chaperonin. *Cell* 93, 863-873.
- Valent, Q.A., de Gier, J.W., von Heijne, G., Kendall, D.A., ten Hagen-Jongman, C.M., Oudega, B., and Luirink, J. (1997). Nascent membrane and presecretory proteins synthesized in *Escherichia coli* associate with signal recognition particle and trigger factor. *Molecular microbiology* 25, 53-64.
- Warrick, J.M., Chan, H.Y., Gray-Board, G.L., Chai, Y., Paulson, H.L., and Bonini, N.M. (1999). Suppression of polyglutamine-mediated neurodegeneration in *Drosophila* by the molecular chaperone HSP70. *Nature genetics* 23, 425-428.
- Wegrzyn, R.D., Hofmann, D., Merz, F., Nikolay, R., Rauch, T., Graf, C., and Deuerling, E. (2006). A conserved motif is prerequisite for the interaction of NAC with ribosomal protein L23 and nascent chains. *The Journal of biological chemistry* 281, 2847-2857.
- Weissman, J.S., Hohl, C.M., Kovalenko, O., Kashi, Y., Chen, S., Braig, K., Saibil, H.R., Fenton, W.A., and Horwich, A.L. (1995). Mechanism of GroEL action: productive release of polypeptide from a sequestered position under GroES. *Cell* 83, 577-587.
- Weissman, J.S., Rye, H.S., Fenton, W.A., Beechem, J.M., and Horwich, A.L. (1996). Characterization of the active intermediate of a GroEL-GroES-mediated protein folding reaction. *Cell* 84, 481-490.

- Woolhead, C.A., McCormick, P.J., and Johnson, A.E. (2004). Nascent membrane and secretory proteins differ in FRET-detected folding far inside the ribosome and in their exposure to ribosomal proteins. *Cell* 116, 725-736.
- Xu, Z., Horwich, A.L., and Sigler, P.B. (1997). The crystal structure of the asymmetric GroEL-GroES-(ADP)<sub>7</sub> chaperonin complex. *Nature* 388, 741-750.
- Yao, Y., Bhabha, G., Kroon, G., Landes, M., and Dyson, H.J. (2008). Structure discrimination for the C-terminal domain of Escherichia coli trigger factor in solution. *Journal of biomolecular NMR* 40, 23-30.
- Young, J.C., Agashe, V.R., Siegers, K., and Hartl, F.U. (2004). Pathways of chaperone-mediated protein folding in the cytosol. *Nature reviews* 5, 781-791.
- Zeng, L.L., Yu, L., Li, Z.Y., Perrett, S., and Zhou, J.M. (2006). Effect of C-terminal truncation on the molecular chaperone function and dimerization of Escherichia coli trigger factor. *Biochimie* 88, 613-619.
- Zwanzig, R., Szabo, A., and Bagchi, B. (1992). Levinthal's paradox. *Proceedings of the National Academy of Sciences of the United States of America* 89, 20-22.

## VII Appendices

### VII.1 Abbreviations

aa	aminoacid
ADP	adenosine 5-diphosphate
Amp	ampicillin
APS	ammonium peroxodisulfate
ATP	adenosine 5'-triphosphate
BADAN	6-bromoacetyl-2-dimethyl-aminonaphthalene
BSA	albumin bovine serum
CDTA	trans 1,2-diaminocyclohexane- <i>N,N,N,N'</i> -tetraacetic acid
CIAP	Calf Intestinal Alkaline Phosphatase
DNA	deoxyribonucleic acid
DNase	desoxyribonuclease
DTT	dithiothreitol
E. coli	Escherichia coli
EDTA	ethylenediaminetetraacetic acid
FKBP	FK506 Binding Protein
FL	firefly luciferase
FRET	fluorescence resonance energy transfer
g	acceleration of gravity, 9.81 m/s <sup>2</sup>
GAPDH	glyceraldehyde 3-phosphate dehydrogenase
GatD	galactitol-1-phosphate 5-dehydrogenase
GTP	guanosine 5'-triphosphate
HEPES	4-(2-hydroxyethyl)-1-piperazineethanesulfonic acid
HRP	horseradish peroxidase
Hsp	heat shock protein
IANBD	<i>N</i> -((2-(iodoacetoxy)ethyl)- <i>N</i> -methyl)amino-7-nitrobenz-2-oxa-1,3-diazole
IPTG	isopropyl- $\beta$ -D-1-thiogalactopyranoside
Kan	kanamycin
LB	Luria Bertani

Luc	luciferase
mRNA	messenger RNA
NAC	nascent chain associated complex
NC	PPIase-deletion mutant of TF
NTA	nitrilo-triacetic acid
OAc	acetate
OD	optical density
PAGE	PolyAcrylamide Gel Electrophoresis
<i>p</i> Bpa	<i>para</i> -Benzoyl-L-phenylalanine
PBS	phosphate buffered saline
PCR	Polymerase Chain Reaction
PDB	Protein Data Bank. <a href="http://www.rcsb.org/pdb/">http://www.rcsb.org/pdb/</a>
PPIase	peptidyl prolyl isomerase
psi	Pound per square inch (6894.76 Pa)
RAC	ribosome associated complex
RIPA	Radioimmunoprecipitation assay
RNA	ribonucleic acid
RNase A	ribonuclease A
RPL	ribosomal protein of the large subunit
RPS	ribosomal protein of the small subunit
rRNA	ribosomal RNA
<i>S. cerevisiae</i>	<i>Saccharomyces cerevisiae</i>
SAP	shrimp alkaline phosphatase
SDS	sodiumdodecylsulfate
Tet	tetracycline
TCA	trichloroacetic acid
TCEP	tris-(2-carboxyethyl)phosphine
TEMED	N,N,N',N'-tetramethylethylenediamine
Tet	tetracycline
TEV	tobacco etch virus
TF	trigger factor

tig	gene encoding TF
TRiC	TCP1 Ring Complex
Tris-HCl	tris(hydroxymethyl)aminomethane hydrochloride
UV	ultraviolet
WT	wildtype

## VII.2 *Curriculum vitae*

**Name** Sathish Kumar Lakshmipathy  
**Birth date** 4<sup>th</sup> July 1980  
**Birth place** Cuddalore, Tamilnadu, India  
**Nationality** Indian

### **Dissertation**

March 2004-present Ph.D. dissertation under the supervision of Prof. Dr. F. Ulrich Hartl in the Department of Cellular Biochemistry, Max-Planck Institute of Biochemistry, Martinsried: Analysis of TF interactions with ribosome-nascent chain complexes - photocrosslinking and fluorescence spectroscopic approaches

### **Education**

2000-2002 Master of Science in Integrated Biology  
Master thesis under the supervision of Dr. Hussain Munavar in the School of Biological Sciences, Madurai Kamaraj University, Madurai, India: *Genetic characterization of PMJ420; A Ts<sup>+</sup> Rif<sup>R</sup> Derivative Of fitC4 Ts Mutant of Escherichia coli*

1997-2000 Bachelor of Science  
Department of Zoology, The American College, Madurai, India.

1995-1997 Higher Secondary School Leaving Certificate  
N.S.B. H. Secondary School, Theni, Tamilnadu, India

1990-1995 Secondary School Leaving Certificate  
N.S.B. H. Secondary School, Theni, Tamilnadu, India.

### **Experience**

2002-2004 Project Assistant under the supervision of Prof. Dr. Dipankar Chatterji, Molecular Biophysics Unit, Indian Institute of Science, Bangalore, India.